# 9.10 Mass Spectrometry: An Essential Tool for Trace Identification and Quantification

**Charles H. Hocart**, Australian National University, Canberra, ACT, Australia

## 9.10.1 Introduction

### 9.10.1.1 Overview

Mass spectrometry (MS) is an essential tool in the identification and quantification of natural products, primarily because of its speed, sensitivity, selectivity, and its versatility in analyzing solids, liquids, and gases. Indeed there are reports of viable viruses being collected after passage through a mass spectrometer.[1] MS has become an interdisciplinary methodology, impacting very many areas of science from physics, through chemistry, to biology.

The first mass spectrometer was constructed in the 1890s and was critical to the discovery of the electron by Sir Joseph John Thompson (winner of the Nobel Prize for Chemistry in 1906). Since then, MS has proven to be a technique of immense importance to scientific endeavors in a variety of fields, initially physics with the discovery of the electron and then stable isotopes and later, biology where it has been an essential tool for the high-throughput identification of proteins and their posttranslational modifications (PTMs). It is interesting to note that Thompson[2] observed in his book *Rays of Positive Electricity and Their Application to Chemical Analysis* that the new technique could be profitably used for chemical analysis. However, this potential was largely ignored until World War II when MS came to be used to monitor the cracking process in oil refineries and to separate $^{235}U$ and $^{238}U$ for use in the atomic bomb.

The last century has also seen considerable innovation and development of the technique and three further Nobel Prizes have been awarded for the discovery of isotopes of nonradioactive elements (1922, Francis Aston), development of new analyzers (1989, Wolfgang Paul – quadrupoles (Q's) and ion trap), and soft desorption ionization methods (2002, Koichi Tanaka and John B. Fenn – laser desorption ionization and electrospray ionization (ESI), respectively). MS continues to evolve and innovations in hardware and software are being driven by demands from medicine and biology for instruments with better mass accuracy, better mass resolution, increased dynamic range, faster data acquisition, and enhanced tandem MS capabilities. Samples of increasing complexity and diminishing size are being presented for analysis and entirely new fields of endeavor, such as proteomics and metabolomics, have been established, based on modern and continuing developments in MS. Those interested in the history of MS are referred to Grayson,[3] Griffiths,[4] and to Watson and Sparkman.[5]

Today, MS instruments are used in identifying and quantifying, for example, drugs, pollutants, products of chemical syntheses, planetary atmospheric components, biopolymers, and metabolites from microorganisms, plants, and animals. These analytes range in size from a few mass units (e.g., elemental gases) to hundreds of kilodaltons (kDa) (e.g., proteins and protein complexes) and cover a large range of polarities (e.g., hydrocarbons

to sulfated carbohydrates). In addition to the wide applicability, another attractive feature of mass spectrometric analyses is that they can potentially be performed with a large degree of specificity and sensitivity (e.g., zeptomolar concentrations – $10^{-21}$ mol $l^{-1}$). Thus these instruments are used by a multitude of research disciplines and regulatory authorities (e.g., drug testing in sport,[6,7] Olympic Games,[8] space exploration,[9] geological dating,[10] biological tissue imaging,[11] wine industry,[12] metabolomics,[13,14] proteomics,[15–17]).

Although mass spectrometers are of widespread utility, it is also important to understand their limitations. Particular instruments are usually designed and dedicated to a narrow range of tasks dictated by their linkage to specific modes of sample presentation (e.g., solids probe, liquid chromatograph, gas chromatograph, or a proton transfer reaction drift tube) and methods of ionization (e.g., electrospray or electron impact). A well-equipped MS laboratory will therefore contain a variety of instruments with different capabilities.

#### 9.10.1.2 Scope of the Present Work

MS is most commonly applied to problems of identification and quantification, particularly in the area of natural products chemistry. I hope in this brief chapter to give the nonspecialist chemist or biologist some basic background in MS and its capabilities so that they can sensibly engage with the MS specialist or MS literature in seeking solutions to their particular analytical problems. To this end, we will look specifically at the components of a mass spectrometer, the presentation of samples, the ionization processes available, and how the data generated from an analysis can be used for identification and quantification. Readers should also refer to complementary chapters in this volume on chromatography (chromatographically separated components of mixtures may be fed directly into the MS source for analysis) and proteomics (high-throughput technique for identification and quantification of large sets of proteins by MS (see Chapters 9.11–9.13).

In keeping with the philosophy of this series, only selective references to the literature have been made and wherever possible these have been review and tutorial style articles.

### 9.10.2 Components of a Mass Spectrometer

#### 9.10.2.1 The Mass Spectrometer – Overview

The mass spectrometer may be divided into a number of discrete components: a sample inlet, an ion source, one or more analyzers, a detector, and finally, a computer to both collect data and control the operational parameters of the instrument (**Figure 1**). In principle, gas-phase neutral molecules are ionized so that they may be separated by the electric and/or magnetic fields of the analyzer according to their mass ($m$) to charge ($z$) ratios ($m/z$). The ions are then detected and recorded as a mass spectrum, graphing the ion abundance against the $m/z$ ratio of the individual ions (**Figure 2**).

To enhance the passage of the ion stream, the ion source, analyzer region, and detector are held under vacuum. At atmospheric pressure (760 torr), there is a density of some $10^{19}$ molecules $ml^{-1}$, yielding a mean free path of $10^{-4}$ cm. However, in an evacuated region at $10^{-6}$ torr, the density drops to $10^{10}$ molecules $ml^{-1}$ and the mean free path is extended out to $10^{3}$ cm, increasing the probability that an ion will be able to physically traverse the instrument without collision with a residual gas molecule. This requirement for a maximal mean free path is particularly important for the beam-type instruments (magnetic sectors and multiple analyzer instruments) and for ion cyclotron resonance (ICR) cells. In the latter, ions may literally travel many kilometers over an observation period of 1 s.[18] In some respects, the linear and Q ion traps are the exception, in that although the analyzers are held within a vacuum system, the traps themselves contain a helium buffer gas, which is required to collisionally cool the trapped ions.

#### 9.10.2.2 Ion Source and Ionization Methods

Prior to analysis, the sample must be volatilized and ionized.[19] These processes can be separate or linked, depending on the nature of the sample and the ionization process being used. Samples may be presented for MS analysis in solid, liquid, or gaseous form and, furthermore, they may be a mixture of components. In the case of mixtures, separation is usually necessary for unambiguous identification or quantification because the

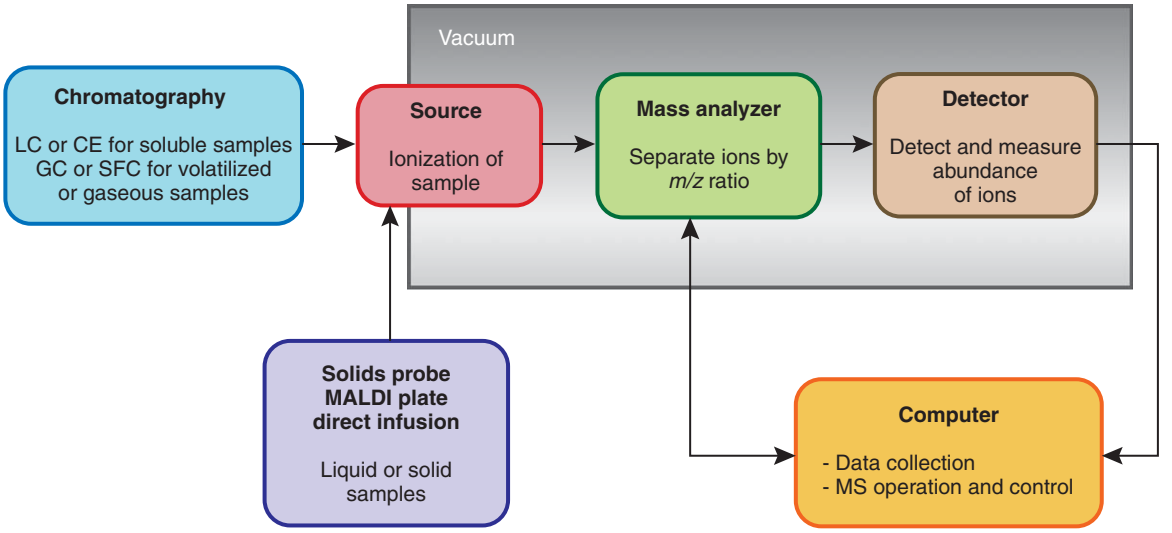


**Figure 1** Principle components of a mass spectrometer. For mass spectrometry (MS) analysis of a sample, the neutral analyte(s) must first be ionized, positively or negatively, to allow manipulation by the magnetic and/or electric fields in the MS analyzer. Ions are sorted according to their mass to charge ratio (*m/z*), which is then plotted against their intensity to generate a mass spectrum. The flight path of the ions is evacuated to maximize the mean free path of the ions and to reduce the possibility of unfavorable interactions with residual air molecules.

simultaneous presence of two or more components in the source region will result in an overlapping or mixed spectrum. Mixtures are therefore often separated by gas chromatography (GC) or capillary electrophoresis (CE) or supercritical fluid chromatography (SFC) or liquid chromatography (LC), with the eluted and separated components being supplied directly into the MS source.[20] These hyphenated approaches are known as GC/MS, CE/MS, SFC/MS and LC/MS, respectively.

If chromatography is not required, samples may be introduced directly into the ion source. In the case of gaseous samples, volatilization is of course unnecessary, and the sample can be introduced into the source using appropriate gas handling techniques. Nonpolar, thermally stable, low-molecular-weight solids and liquids can be placed in metal or glass crucibles (solids probe or direct insertion probe) or may be directly applied to a wire loop (direct exposure probe). The crucible or wire loop is then heated to thermally desorb or volatilize the sample. Some polar low-molecular-weight compounds may also be directly analyzed after being chemically derivatized[21–27] to mask the polar functional groups and thereby increase volatility (e.g., by alkylation or silylation) and improve thermal stability (Section 9.10.4.3.2). Otherwise, samples may be dissolved in an appropriate solvent and subject to either an atmospheric pressure ionization process or be laser desorbed from a solid matrix as described below.

#### *9.10.2.2.1 Electron ionization*

Electron ionization (EI), originally developed by Dempster,[28] is widely used in MS for relatively volatile samples that are thermally stable and have relatively low molecular weight. Samples are typically presented in the effluent from a GC or are volatilized from a solids probe inserted into the high vacuum source. Ionization is effected by interaction between the gas-phase analyte molecules and a stream of high-energy electrons (typically 70 eV) drawn from a filament. Ionization occurs by removal of an electron to form an odd-electron ion, $M^{+\cdot}$ (Equation (1)). EI generally creates a singly charged positive ion, and any doubly or triply charged ions are of very low abundance. EI is also a high-energy process and excess energy remaining after ionization can be dissipated by fragmentation (possibly with rearrangement) of covalent bonds in the molecular ion, to lose either a radical (e.g., $CH_3^{\cdot}$) (Equation (2)) or a neutral species (e.g., $H_2O$ or $CH_3OH$) (Equation (3)).

$$\text{Ionization}: \quad M + e^- \rightarrow M^{+\cdot} + 2e^- \tag{1}$$

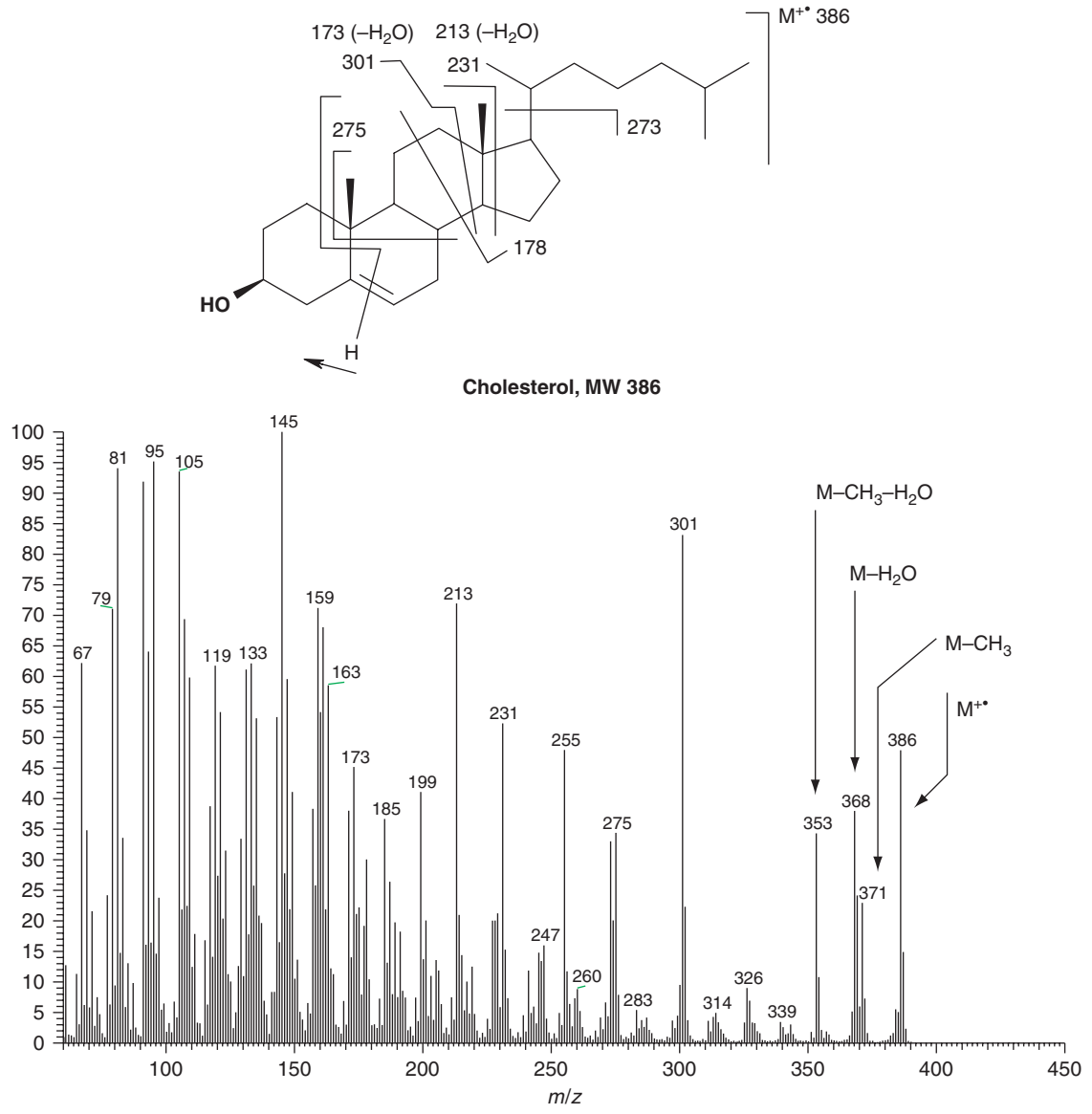


**Figure 2** Mass spectrum of cholesterol generated by electron ionization (EI). The EI mass spectrum of cholesterol is characterized by the presence of a molecular ion at *m/z* 386 and by extensive fragmentation and contains information on the steroid nucleus and side chain. There is no indication as to the position of the double bond in this spectrum but the 3-hydroxy-$\Delta^5$ structure can be identified after conversion to an ester.[29,30]

$$\text{Fragmentation}: \quad M^{+\cdot} \rightarrow [M-R]^{+} + R^{\cdot} \quad \text{radical loss} \tag{2}$$

$$M^{+\cdot} \rightarrow [M-R]^{+\cdot} + R \quad \text{neutral loss} \tag{3}$$

The fragmentation observed during EI is defined by the chemical structure of the analyte and the resulting highly reproducible pattern of fragmentation may be used for structural elucidation and identification of unknowns[5,31–34] (**Figures 2** and **3(a)**). This reproducibility has been exploited to develop user-generated and commercial libraries of spectra (some containing several hundred thousand spectra), which can be rapidly searched for comparable spectra. For some compounds, fragmentation may be so extensive that the molecular ion does not appear in the EI spectrum (e.g., **Figure 3(a)**). If this molecular

mass information is required, then the analyst will have to resort to one of the softer or less energetic ionization processes such as chemical ionization (CI, **Figures 3(b), 3(c), and 3(e)**) or ESI (**Figure 3(g)**) as outlined below.

The displaced electron is generally assumed to be the electron with the lowest ionization energy. In order of probability, this will be a nonbonding electron followed by a $\pi$ bond electron and then a $\sigma$ bond electron. Thus EI yields, in the first instance, a molecular ion which is a radical cation with an unpaired electron. In principle, any remaining energy will then be dissipated by bond cleavages that result in the formation of the most stable cation with a paired electron (even-electron ion). These even-electron ions may be formed by homolytic or heterolytic cleavages. This whole process happens very rapidly ($<10^{-8}$ s) and is the reason for the close similarity of EI spectra produced across all different instruments. It is important to remember that mass spectral reactions in the EI source are unimolecular. This is because the pressure in the EI source is too low for bimolecular (ion–molecule) reactions to occur.

#### *9.10.2.2.2 Chemical ionization (positive and negative) and electron capture ionization*

Like EI, CI is also typically applied to samples presented via a GC interface or volatilized from a solids probe. It is a less energetic or soft form of ionization and is designed to minimize fragmentation.[35–38] CI is usually carried out in a source similar to that used for EI except that a reagent gas, commonly methane, isobutane, or ammonia, is added at a pressure of 0.3–1 torr. The electron beam then interacts with the reagent gas to produce reagent ions (**Table 1**) and thermal electrons. The neutral analyte molecules are then ionized by ion–molecule reactions to produce positive and negative analyte ions (**Figures 3(b), 3(c), and 3(e)**). The thermal electrons are also available for electron capture by electrophilic analytes, yielding negative analyte ions.

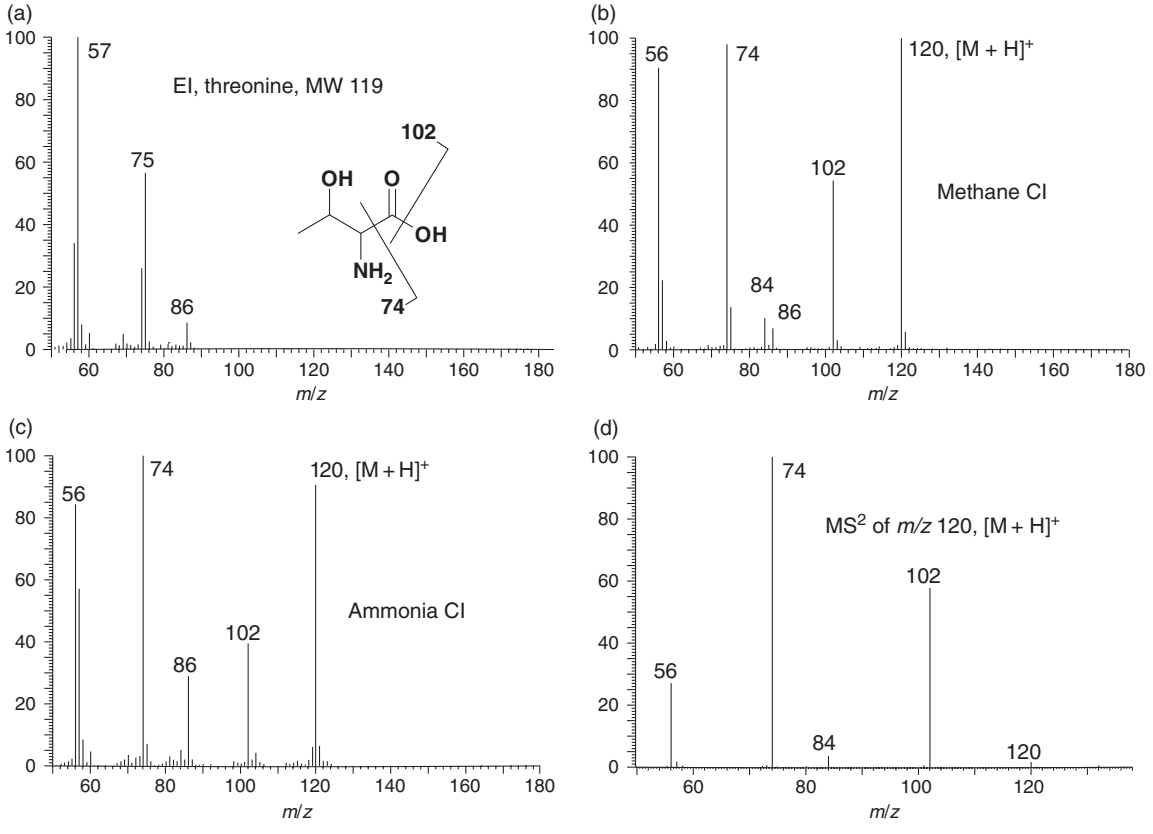


**Figure 3** (Continued)

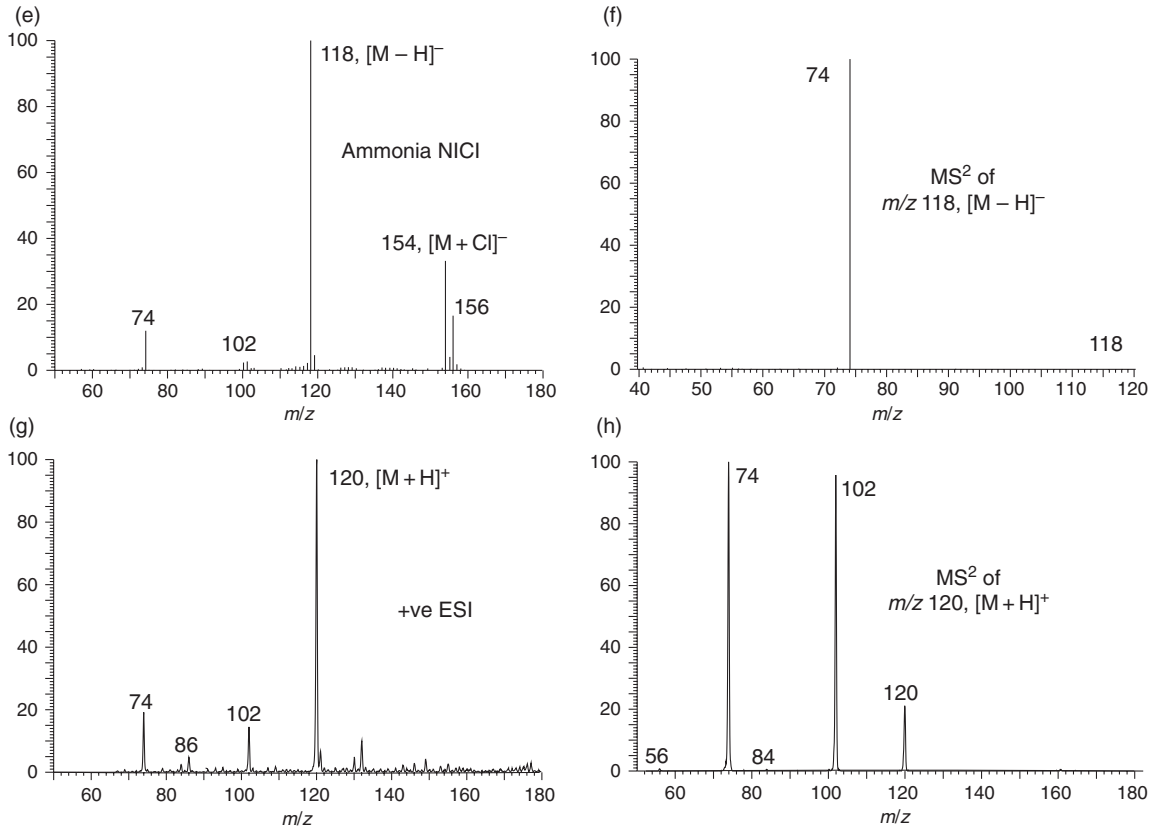


**Figure 3** Mass spectra of the amino acid threonine. (a) Electron ionization (EI) mass spectra generated at an ionization energy of 70 eV. No molecular ion is observed. For an interpretation of the EI fragmentation, see Bieman and McCloskey[39] and Junk and Svec.[40] (b) Chemical ionization (CI) spectra generated using methane as the reagent gas. A prominent $[M + H]^+$ ion is observed at *m/z* 120. A discussion of the CI fragmentation may be found in Milne *et al*.[41] and Solovev *et al*.[35] (c) CI spectra generated using ammonia as the reagent gas. The spectrum is very similar to that in (b). (d) Tandem $MS^2$ experiment selecting *m/z* 120 from the ammonia CI spectra. (e) Negative ion chemical ionization (NICI) spectra demonstrating proton abstraction $[M - H]^-$ *m/z* 118 and adduct formation with chlorine $[M + Cl]^-$ *m/z* 154 and 156. Threonine HCl was dissolved in 50% EtOH/water. (f) Tandem $MS^2$ of *m/z* 118, in the negative mode. (g) Electrospray ionization (ESI) spectra, again featuring a prominent $[M + H]^+$ ion at *m/z* 120. (h) Tandem $MS^2$ experiment of *m/z* 120 from the ESI spectra.

**Table 1** Common reagent and analyte ions in chemical ionization (CI)

| *Reagent gas* | *Major reagent ions* | *Product ions* |
|---|---|---|
| *Positive CI* | | |
| Methane, $CH_4$ | $CH_5^+$, $C_2H_5^+$, $C_3H_5^+$ | $[M + H]^+$, $[M + C_2H_5]^+$ |
| Isobutane, $C_4H_{10}$ | $C_4H_9^+$ | $[M + H]^+$, $[M + C_4H_9]^+$ |
| Ammonia, $NH_4$ | $NH_4^+$ | $[M + H]^+$, $[M + NH_4]^+$ |
| *Negative CI* | | |
| Chloroform | $Cl^-$ | $[M - H]^-$, $[M + Cl]^-$ |
| Ammonia | $NH_2^-$ | $[M - H]^-$, $[M + NH_2]^-$ |
| $N_2O/CH_4$(1:1) | $OH^-$ | $[M - H]^-$ |

It is important to remember that these reactions are all occurring simultaneously in the source and that either the positive or negative ions can be selectively extracted from the source into the mass analyzer by placing the appropriate voltages on the extracting and focusing lenses. In the case of Q analyzers (Section 9.10.2.3.3), the switching between positive and negative polarity can be accomplished very rapidly so that

positive and negative ions may be analyzed from a single GC peak. This technique is known as pulsed positive ion/negative ion CI (PPINICI).

In positive ion chemical ionization (PICI), the neutral analyte is most commonly ionized by proton transfer (Equation (4)) or adduct formation (Equations (5) and (6)).

When, for example, methane is used as a reagent gas, the $[M+1]^+$, $[M+29]^+$, and $[M+41]^+$ series of ions (Equations (4)–(6)) is good confirmation of the analyte molecular mass.

$$M + CH_5^+ \rightarrow [M+H]^+ + CH_4 \quad \text{proton transfer} \tag{4}$$

$$M + C_2H_5^+ \rightarrow [M+C_2H_5]^+ \quad \text{adduct formation} \tag{5}$$

$$M + C_3H_5^+ \rightarrow [M+C_3H_5]^+ \quad \text{adduct formation} \tag{6}$$

Less commonly, charge transfer (Equation (7)) and hydride abstraction (Equation (8)) may be observed.

$$M + CH_4^{+\cdot} \rightarrow M^{+\cdot} + CH_4 \quad \text{charge transfer} \tag{7}$$

$$M + C_2H_5^+ \rightarrow [M-H]^+ + C_2H_6 \quad \text{hydride abstraction} \tag{8}$$

Under CI conditions, negative reagent ions are also formed (**Table 1**) and these can effect analyte ionization by hydride abstraction (Equation (9)) or anion attachment (Equation (10)) (**Figure 3(e)**).

$$M + NH_2^- \rightarrow [M-H]^- + NH_3 \quad \text{hydride abstraction} \tag{9}$$

$$M + NH_2^- \rightarrow [M-NH_2]^- + NH_3 \quad \text{anion attachment} \tag{10}$$

As mentioned above, thermal electrons are also generated in the CI source, along with the reagent ions. These can be exploited for electron capture ionization (ECI), particularly in the case of molecules containing electrophilic moieties such as F, Cl, $NO_2$, and CN and this may confer advantages of increased sensitivity and selectivity for a particular analyte. These electron-capturing groups can of course be added into the target analyte by appropriate derivatization prior to analysis, to selectively enhance the possibility of electron capture.[21–27] It should be noted that this electron capture process is not, strictly speaking, negative CI as the analyte molecules are interacting with the thermal electrons and not the reagent ions derived from the CI gas.

There are three different mechanisms for ECI:

$$M + e^-(\sim 0.1\,eV) \rightarrow M^{-\cdot} \quad \text{resonance electron capture} \tag{11}$$

$$M + e^-(0-15\,eV) \rightarrow [M-A]^- + A^{\cdot} \quad \text{dissociative electron capture} \tag{12}$$

$$M + e^-(>10\,eV) \rightarrow [M-B]^- + B^+ + e^- \quad \text{ion pair formation} \tag{13}$$

The sensitivity of ECI analysis is generally two to three orders of magnitude greater than that of CI or EI analysis. Little fragmentation occurs during ECI, and this mode of ionization is generally employed for quantification of trace amounts of known compounds.

#### *9.10.2.2.3 Ionization by proton transfer reaction*

Recently, a variant of CI has been specifically developed to monitor in real time low concentrations of volatile organic compounds (VOCs).[42] VOCs are normally present in complex mixtures that could be separated by GC; however, these separations are relatively slow (15–60 min) and are not suitable for real-time monitoring. Proton transfer reaction mass spectrometry (PTR-MS) uses CI based on proton transfer from hydroxonium ions ($H_3O^+$). These hydroxonium ions are produced in an external glow discharge ion source operating in pure water vapor. The reagent ions are then passed into a drift tube that is continuously flushed with the ambient air containing the VOCs of interest. The $H_3O^+$ ion does not react with any of the common constituents of the atmosphere ($N_2$, $O_2$, Ar, or $CO_2$) as their proton affinities are lower than those of water. However, most VOCs have proton affinities higher than water (>166.5 kcal $mol^{-1}$), and so proton transfers to the VOCs occur exothermically as a consequence of ion–molecule reactions in the drift tube. For the most part, these proton transfers are nondissociative and the mass analyzer can monitor a single ion species for each individual VOC (Equation (14)).

$$H_3O^+ + M_{VOC} \rightarrow MH^+_{VOC} + H_2O \quad (14)$$

However, some dissociation to $[M-OH]^+$ (Equation (15)) or $[M-OR]^+$ (Equation (16)), depending on the chemical class of the analyte, can occur.

$$MH^+ \rightarrow [M-OH]^+ + H_2O \quad (15)$$

$$MH^+ \rightarrow [M-OR]^+ + ROH \quad (16)$$

Some further selectivity can be introduced into the process by using ammonia as the reagent gas ($NH_4^+$ reagent ions) so that proton transfers occur only with compounds with a proton affinity >204 kcal mol$^{-1}$.

A more sophisticated, though less common version of PTR-MS is selected ion flow tube mass spectrometry (SIFT-MS). In this technique, a mixture of reagent ions is generated in a gas discharge ion source and then a Q mass filter is used to select one reagent ion, which is then injected into an inert carrier gas (usually He), for reaction with the gaseous sample, which is also injected into the carrier gas. The products of the ion–molecule reactions are then analyzed by a second mass analyzer. Recently, a triple cell PTR Fourier transform ion cyclotron resonance MS (FTICR MS) has been built to encompass the whole process with the advantage of high mass resolution and accuracy to characterize the ion–molecule reaction products[43] (see also Section 9.10.2.3.8). This, however, is achieved at the cost of sensitivity (1 ppm compared with 0.1 ppb).

The most common reagent ions used in SIFT-MS are $H_3O^+$, $NO^+$, and $O_2^{+\cdot}$, and their reactions with many different classes of volatile organics have been well documented.[44] The $NO^+$ reagent ion can react with the VOCs, depending on their chemistry, in one or two of several different ways – charge transfer (Equation (17)), hydride ion transfer (Equation (18)), hydroxide ion transfer (Equation (19)), alkoxide ion transfer, and ion–molecule association (Equation (20)).

$$M + NO^+ \rightarrow M^{+\cdot} + NO^{\cdot} \quad (17)$$

$$M + NO^+ \rightarrow [M-H]^+ + HNO \quad (18)$$

$$M + NO^+ \rightarrow [M-OH]^+ + HNO_2 \quad (19)$$

$$M + NO^+ \rightarrow [M+NO]^+ \quad (20)$$

VOCs mostly react with $O_2^{+\cdot}$ via charge transfer (Equation (21)) or dissociative charge transfer (Equation (22)); however, this reagent ion has found most use in monitoring NO, $NO_2$, and $CS_2$ as $NO^+$, $NO_2^+$, and $CS_2^{+\cdot}$, respectively.

$$M + O_2^{+\cdot} \rightarrow M^{+\cdot} + O_2 \quad (21)$$

$$M + O_2^{+\cdot} \rightarrow [M-R]^+ + R^{\cdot} + O_2 \quad (22)$$

Reactions of different chemical classes with the $H_3O^+$, $NO^+$, and $O_2^{+\cdot}$ reagent ions may be found in Smith and Španěl.[44]

#### 9.10.2.2.4 Electrospray ionization

Electrospray is a process of transferring solution ions, typically large, nonvolatile polar molecules such as proteins, peptides, and carbohydrates, into the gas phase by ion desorption or ion evaporation.[45] Samples are supplied to the source directly via a syringe or, most commonly, as the eluent from an LC column. The liquid is passed through a metal needle held at high voltage (1–3 kV with respect to the sample cone or MS inlet) and sprayed into the ionization chamber at atmospheric pressure. A coaxial nebulizer gas may assist spray formation in the case of high solvent flow rates. As the charged droplets evaporate and shrink in size, the charge concentration in the droplets increases to the point where like-charge repulsion overcomes surface tension and the droplets explode to form microdroplets. The process is repeated and ultimately ions are ejected (desorbed) into the gas phase. These ions are then attracted into the off-axis or orthogonal sample inlet (counterelectrode) of the mass spectrometer. This off-axis geometry has the advantage of excluding neutral molecules and solvent clusters from the mass spectrometer.

ESI is a very 'soft' process, inducing little fragmentation, but in the case of molecules with a number of chargeable sites, a distribution of charge states is generated (**Figures 3(g) and 6**). The distribution and nature of the charges is very much a function of the sample solvent. In protic solvents such as water or mixtures of water and methanol or acetonitrile, sample ions will form a protonated, $[M + nH]^{n+}$, or deprotonated, $[M - nH]^{n-}$, series of multicharged ions. If alkali metals or ammonia is present in solution, then cationization will also be observed.

The number of charges that can be carried on an electrosprayed molecule depends on a number of factors including the size of the molecule, the tertiary structure (e.g., some charge-carrying sites – basic amino acids in +ve ESI – may be physically removed from exposure to the solvent at the center of a folded protein), the number of sites on which a charge may be localized (acidic and basic sites), and the nature of the solvent (pH and presence of salts). The effect of solvent pH on the abundance and distribution of the charges on myoglobin is illustrated in **Figure 4**.

The multicharging phenomenon means that ions of very large mass can be detected with conventional analyzers with mass ranges up to 3000 u. As a general rule, there will be one charge for every 8–10 amino acids (~1000 mass units). Thus, for example, a protein or protein complex of 200 000 Da can be readily analyzed if it can accommodate 100 charges. Hence,

$$\frac{200\,000\ \text{Da}}{100z} = 2000\ m/z$$

This distribution of charges, especially when there may be more than one molecular species, can represent a very confusing picture. This situation may be further compounded by the presence of additional ion series that can occur when protonation competes with cations such as sodium and potassium. However, it is possible to deconvolute the multiple charge states and to calculate the mass of the molecule in question, by application of simple algebra.

First, it is reasonable to assume when looking at the multicharged envelope of an unknown that adjacent peaks differ by one charge. For the most part, this will represent a proton, as the multicharged envelopes due to sodium and potassium tend to be much less abundant. In the myoglobin spectrum (**Figure 4**), two adjacent ions have been labeled $M_1$ (higher value) and $M_2$ (lower value) and these will carry $n_1$ and $n_2$ charges (protons), respectively.

Thus

$$n_2 = n_1 + 1 \tag{23}$$

Second, the observed $m/z$ values of each of the peaks can be written as

$$M_1 = \frac{M_r + n_1 H}{n_1} \tag{24}$$

where $M_r$ is the mass of the unknown, $n$ is the number of charges, $H$ is the mass of a proton, $M_1$ is the $m/z$ experimental value, and

$$M_2 = \frac{M_r + n_2 H}{n_2} = \frac{M_r + (n_1 + 1)H}{n_1 + 1} \tag{25}$$

The charge state, $n_1$, can then be calculated from

$$n_1 = \frac{M_2 - H}{M_1 - M_2} \tag{26}$$

The mass of the unknown, $M_r$, can then be determined from

$$M_r = n_1(M_1 - H) \tag{27}$$

Where the multicharged series is due to cationization, the mass of $H$ should be replaced by that of the cation (e.g., $Na^+$ or $K^+$). Fortunately, most modern ESI-MS data systems have computer-based deconvolution algorithms to automate this process (**Figure 4(c)**).

ESI is most commonly associated with the analysis of large biomolecules of medium to high polarity, and it is a major tool for proteomic analyses,[17] but it can also be used for the MS analysis of small molecules provided they contain basic groups (e.g., amino, amide) for positive ESI or acidic groups (e.g., carboxylic acid, hydroxyl) for negative ESI.

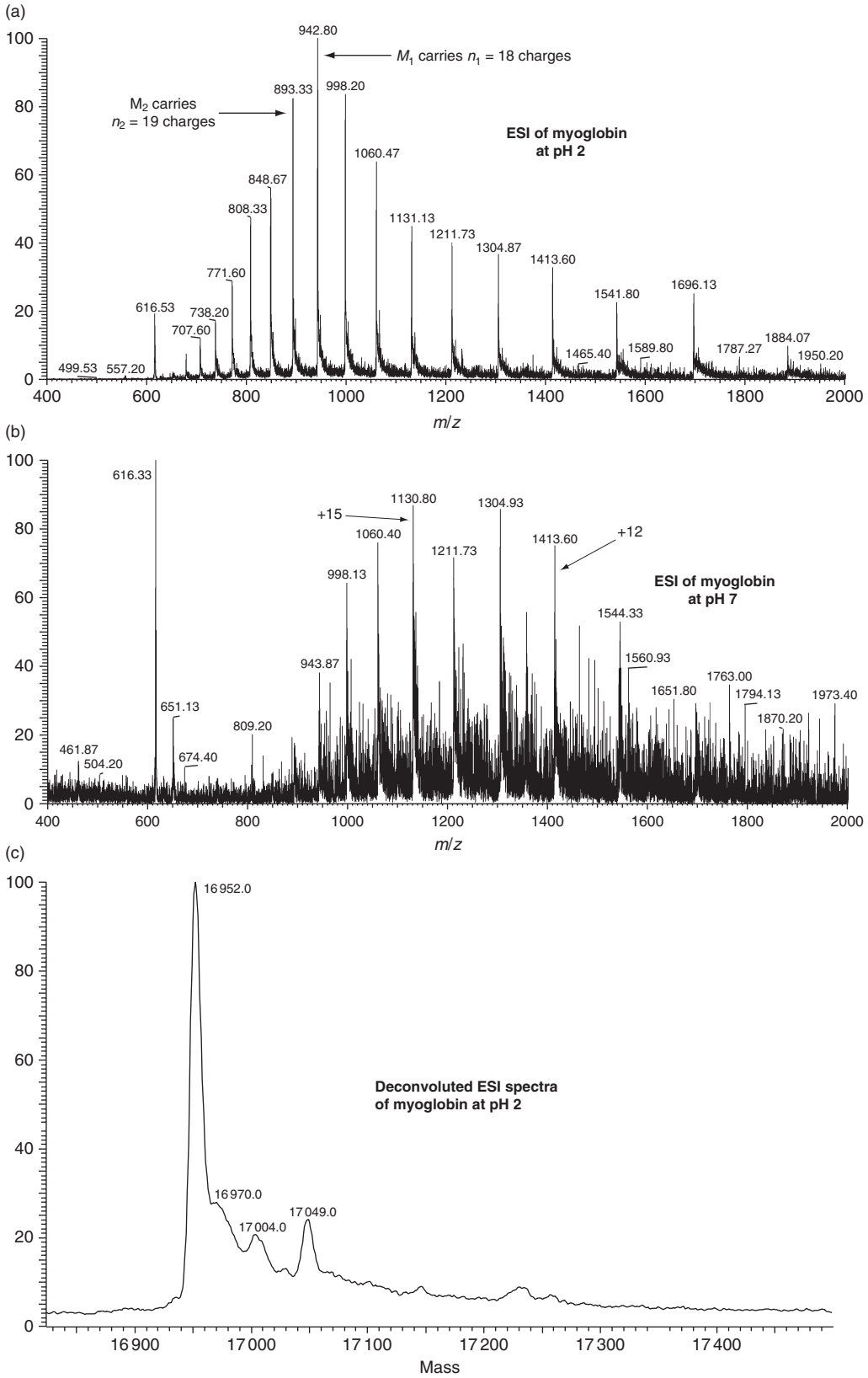


**Figure 4** ESI mass spectrum of horse heart myoglobin ($M_r$, 16 951.49 Da) illustrating the multiple charge phenomena. Note that protonation is most effective at acid pH (a) rather than neutral pH (b) significantly altering the abundance and distribution of charge on myoglobin. Determination of the charge state can be made from first principles, using adjacent pairs of ions, from Equation (26), and the mass of the protein from Equation (27). The average mass determined from using all the data is 16 952.0 Da (c).

One of the great advantages of ESI is that generally it is very successful without the added complications of derivatization. Derivatization is often carried out under harsh conditions and the risk of sample degradation or the formation of multiple derivatives is very real. Nevertheless, derivatization can be a useful adjunct to ESI and there are many reports of derivatization being used to improve the ionization efficiency (and hence the sensitivity of an assay) by increasing the hydrophobicity or adding a group with a fixed charge to the analyte (see the review by Zaikin and Halket[46]).

Although ESI can be performed at quite high flow rates (up to 1–2 ml $min^{-1}$), the trend has been to run at lower and lower flow rates. Low flow rates mean that the coaxial nebulizer gas and the heated drying gases are no longer required, simplifying the construction and operation of the source. However, the most attractive feature of low flow rates is the dramatic improvement in the ESI efficiency with nano-ESI (20–50 nl $min^{-1}$) producing smaller initial droplets (200 nm diameter compared with 1–2 μm, a 100–1000-fold reduction in volume) allowing a much greater proportion of the sample to pass into the gas phase and then into the MS analyzer. Consequently, smaller amounts of sample are required, allowing more sophisticated biological experiments to be attempted on smaller samples. The second advantage of using low flow rates in ESI is that the problem of ion suppression is reduced. Analytes and other components in the spray compete for charge so that analytes with the lowest ionization energy will be preferentially ionized at the expense, for example, of more abundant analytes with higher ionization energy. Therefore, when using ESI, caution should be exercised in extrapolating from the observed spectrum ion abundance to the concentration of the neutral analyte in solution.

#### *9.10.2.2.5 Atmospheric pressure chemical ionization*

The atmospheric pressure chemical ionization (APCI) source is similar in design to the ESI source but the process of ionization is quite different.[47] The liquid sample solution is sprayed through a heated nebulizer into the source at atmospheric pressure. A corona discharge acts to ionize the atmospheric gases and solvent molecules to generate a series of reagent ions, in a manner similar to CI. Ionization of the analyte molecules then occurs by ion–molecule reactions, with minimal fragmentation. In most cases, only singly charged ions are generated and these are then extracted out of the source into the MS analyzer.

Unlike ESI, APCI actively generates ions from neutrals, making small (up to 1000–2000 Da), low to medium polarity analytes amenable to MS analysis. However, APCI is not as readily adaptable to low flow conditions as ESI because it is reliant on a concentrated cloud of solvent molecules to generate the necessary reagent ions.

#### *9.10.2.2.6 Atmospheric pressure photoionization*

Atmospheric pressure photoionization (APPI) is a relatively new technique[48–51] but the source design is almost identical to that used for APCI except that the corona discharge needle is replaced by a krypton discharge lamp, which irradiates the hot vaporized plume from the heated nebulizer with photons (10 and 10.6 eV). The mechanism of direct photoionization is quite simple. Where the ionization energy of the molecule is less than the energy of the photon, absorption of a photon is followed by ejection of an electron to form the molecular radical ion $M^{+\cdot}$ (Equation (28)).

$$M + h\nu \rightarrow M^{+\cdot} + e^{-} \quad \text{direct APPI} \tag{28}$$

However, in an atmospheric pressure environment, the major ion observed is $[M+H]^{+}$, the result of ion–molecule reactions abstracting a proton from protic solvents to yield $[M+H]^{+\cdot}$ (Equation (29)).[50] Charge may also be lost by proton transfer or electron attachment.

$$M^{+\cdot} + S \rightarrow [M+H]^{+} + [S-H]^{\cdot} \tag{29}$$

It should be noted that direct photoionization is not a very efficient process due to the strong absorption by the nebulizing gases and the solvent. Ionization efficiencies may be significantly enhanced by the use of a dopant such as toluene or acetone or anisole, which is added in excess to the vaporized solvent plume.[50,51] These dopants can be photoionized (Equation (30)) and the resultant reagent ions are then available to ionize the analyte by ion–molecule reactions, resulting in proton transfer (Equation (31)) and charge exchange (Equation (32)).

$$D + h\nu \rightarrow D^{+\cdot} + e^{-} \quad \text{dopant APPI} \tag{30}$$

$$D^{+\cdot} + M \rightarrow [M + H]^{+} + [D - H]^{\cdot} \quad \text{proton transfer} \tag{31}$$

$$D^{+\cdot} + M \rightarrow M^{+\cdot} + D \quad \text{charge exchange} \tag{32}$$

All the reactions are dependent on the ionization energies and proton affinities of the analyte, solvent, and dopant. Thus there are three possibilities for ionization in the positive mode, direct photoionization, proton transfer, and charge exchange.

The APPI source is also an effective generator of thermal electrons and is thus well suited to the generation of negatively charged analyte ions by ECI. Thermal electrons are readily generated by the 10 eV photons striking a metal surface (3–5 eV electron binding energy) and as can be seen from Equations (28) and (30), a thermal electron is generated for every photoionization event.

The great advantage of APPI is that it can be used to ionize nonpolar classes of compounds such as alkanes, alkenes, and aromatics that are not ionized by ESI or APCI and it can be interfaced with normal-phase chromatography,[49,51] where the corona discharge (APCI) and the high-voltage discharge (ESI) present a potential explosion hazard.

The full potential of APPI, particularly in the context of combined APCI/APPI or ESI/APPI sources, has yet to be explored. The photoionization and fragmentation of peptides/proteins is not well characterized and may represent another method, along with electron caphere dissociation (ECD) (Section 9.10.3.2.3) and electron transfer dissociation (ETD) (Section 9.10.3.2.5), of generating sequence information.[51,52] Also, unlike APCI, photoionization can be applied to very low solvent flow rates (less than 5 $\mu l\,min^{-1}$) relying on the analyte interacting with a photon of sufficient energy, and not on the solvent as a charge carrier. This alleviates the ESI and APCI problem of ion suppression where some analytes are unable to compete for charge from the charge carriers.

#### 9.10.2.2.7 Matrix-assisted laser desorption ionization

Matrix-assisted laser desorption ionization (MALDI), like ESI, is capable of ionizing and launching very large molecules (e.g., polysaccharides, synthetic polymers, peptides, and proteins) into the gas phase and is a major analytical tool for high-throughput proteomic studies.[17,53] In many respects, MALDI is a complementary technique to ESI and both techniques are often applied to the same sample when determining protein identity. ESI produces macromolecular ions from solution, whereas MALDI produces them from the solid state.

In principle, the sample is cocrystallized with a matrix onto a stainless-steel target or a target with a hydrophilic spot surrounded by a hydrophobic surface designed to concentrate the sample into a small area.[54–57] The dried sample is then illuminated with a pulse of laser light (usually UV but also infrared (IR)) that is absorbed by the matrix chromophore. The photon energy is then transferred from the matrix to the embedded analyte which in turn is ionized and desorbed from the target. Singly charged ions, $[M + H]^{+}$, are typically produced and because this is another 'soft' ionization process, little fragmentation occurs. This makes for a relatively simple interpretation of the spectra; however, it must be noted that the lower end of the mass scale ($<\sim 800\ m/z$) is dominated by a plethora of intense matrix-derived ions. The lack of multiple charging of large analytes means that MS analyzers with an extended $m/z$ range, such as time-of-flight (ToF) (see below), must be used.

Successful MALDI analysis is dependent on a number of factors, not the least of which is selection of an appropriate matrix. The matrix must be soluble in solvents compatible with the analyte (usually an aqueous/organic solvent mixture) and it must be possible to cocrystallize the analyte and matrix onto the target. The matrix must also be vacuum stable and be able to absorb at the emission wavelength of the laser. In addition, it must be able to cause codesorption of the analyte and promote analyte ionization. See **Table 2** for a list of commonly used MALDI matrices.

Other important factors that need to be optimized for MALDI analysis include the molar ratio of analyte to matrix ($\sim 1{:}10^{4}$ is a good starting value) and the power or fluence (energy per unit area) of each laser shot. The best spectra, in terms of minimizing fragmentation and achieving the best resolution, are acquired at just above the laser fluence for ion formation. However, at low laser power, few ions are generated by a single laser pulse, so MALDI spectra are typically accumulated over tens or even hundreds of laser pulses. One of the drawbacks with MALDI is that the quality of the spectra generated is very dependent on good sample preparation and

**Table 2** Common UV absorbing MALDI matrices (nitrogen laser, $\lambda = 337$ nm) and their area of application

| *Matrix* | *Analyte* |
|---|---|
| Picolinic acid (PA) | DNA, RNA |
| 3-Hydroxypicolinic acid (HPA) | DNA, RNA |
| 3-Aminopicolinic acid (APA) | DNA, RNA |
| Dihydroxybenzoic acid (DHB) | Oligosaccharides |
| $\alpha$-Cyano-4-hydroxycinnamic acid ($\alpha$CHCA) | Peptides, lipids, oligonucleotides |
| Sinapinic acid (SA) | Proteins |
| 2-(4-hydroxyphenylazobenzoic acid (HABA) | Polymers |
| 2,4,6-Trihydroxyacetophenone (THAP) | Polymers, glycopeptides, oligonucleotides |
| 6,7-Dihydroxycoumarin | Lipids |

even then some parts of the sample surface, the so-called 'sweet spots', will generate better quality spectra than others. Practice and automated sample preparation, however, go some way in reducing this problem.

The sensitivity of the MALDI technique is generally comparable with that achieved by ESI but any advantage is offset, where automation is not available, by the work required in sample preparation and the difficulty of reproducibility. However, MALDI has a clear advantage over ESI in that targets holding a successful sample preparation can be stored and exploited repeatedly, at leisure. By comparison, ESI samples are nebulized and the sample consumed.

While MALDI is reputed to be relatively insensitive to contaminants (e.g., buffers, detergents, and salts), it must be said that the cleaner the sampler, the better the sensitivity and the better the coverage of analytes because ionization suppression is reduced.

A recent and exciting development of the MALDI technique has seen it adapted to molecular imaging of biological tissue sections (see discussion in Section 9.10.4.5).

#### *9.10.2.2.8 Secondary-ion mass spectrometry*

Secondary-ion mass spectrometry (SIMS) is an ionization technique that with the advent of ESI and MALDI had largely fallen out of favor with chemists and biologists. However, it has undergone something of a revival as its ability to chemically characterize a surface is now being applied to MS imaging of biological tissues (see Section 9.10.4.5). In this technique, a solid surface is bombarded with a continuous beam of highly focused, high-energy ions such as gold ($Au_3^+$), cesium ($Cs^+$), or bismuth ($Bi_3^+$) from a liquid metal ions gun (LMIG) or ions of Buckminster fullerene ($C_{60}^+$).[11,58–60] These ions penetrate the sample surface to a certain depth, depositing their energy through nuclear collisions and generating secondary ions (protonated or cationized) along the way. These secondary ions ($<\sim 500\ m/z$) are sputtered or emitted from the surface and are then directed to the entrance of the mass spectrometer for analysis.

#### *9.10.2.2.9 Ambient ionization methods*

Recently, a new family of ionization techniques that are distinguished by their ability to ionize analytes from surfaces under ambient conditions have been developed.[61] These methods are also characterized by the fact that no prior separation or extraction of the sample is required. Of these methods two have so far been well characterized, desorption electrospray ionization (DESI)[62] and direct analysis in real time (DART).[63]

DESI is closely related to ESI, with surface samples being ionized by a stream of charged solvent droplets to produce low-energy intact molecular ions. This technique has been successfully applied to a wide range of analytes (e.g., proteins, peptides, oligosaccharides, amino acids, terpenes, steroids, and lipids) that have been desorbed from a variety of surfaces, including paper, fabric, plastic, skin, and plant tissues. Ionization has also been demonstrated at up to 3 m away from the MS analyzer using an extended heated ion transfer capillary[64] and sensitivities down to attomole levels have also been reported.[62]

DART uses a glow discharge plasma to excite a heated stream of inert gas, usually nitrogen or helium, which is directed onto the surface to be analyzed. These excited state atoms and molecules have been shown to effect,

like DESI, low-energy ionization of a variety of analytes (e.g., chemical warfare agents, pharmaceuticals, explosives, peptides) from a range of different surfaces (currency, concrete, skin, plant tissue, fabric, and glass). Again, like DESI, excellent sensitivities have been reported.

### 9.10.2.3 Mass Analyzers

After sample ionization, the ions are passed to the mass analyzer(s) where they are separated according to their mass to charge ratio ($m/z$). This separation can be based on a number of different ion properties, including momentum (magnetic sectors), kinetic energy (electrostatic analyzer), path stability (linear Q's), resonance frequencies (Q ion traps, linear ion traps), orbital frequencies (ion cyclotrons), velocity (ToF), or axial frequency (Orbitrap), as ions transit or are contained by combinations of electric and/or magnetic fields. The principle of operation, compatibility with different ionization sources, mass accuracy, mass resolution, and utility for tandem MS experiments of these different analyzers will be briefly discussed. Other factors that can be used to compare the performance of mass analyzers include the mass range limit, scan speed, efficiency of ion transmission, mass accuracy, and mass resolution (**Table 3**). More prosaic considerations include, of course, cost and vendor support. A more in-depth discussion of this subject matter will be found in Gross,[33] McLuckey and Wells,[65] Tarantin,[66] and Wollnik.[67]

Finally, it is important to realize that there is no one analyzer that is superior to all others. The choice of analyzer, therefore, must be based on the information required from the particular type of sample, remembering that analyses based on different mass analyzers can provide complementary information.

#### *9.10.2.3.1 Resolution and accuracy*

No discussion of MS data or comparison of mass analyzers would be complete without including some definition of the data quality, particularly, the accuracy of the data and the resolving power at which they were obtained.

**Table 3** Common mass analyzers: their attributes and typical specifications

| *Mass analyzer* | *Measures* | *Upper mass* | *Resolving power* | *Accuracy (ppm)* | *Dynamic range*[a] | *Cost*[b] |
|---|---|---|---|---|---|---|
| E[c] | Kinetic energy | | | | | |
| B[c] | Momentum | | | | | |
| EB or BE[d] | | $10^4$ | $10^2$–$10^5$ | 1–5 | $10^9$ | ++++ |
| Q[c] | Path stability | $10^4$ | $10^2$–$10^4$ | 100 | $10^7$ | + |
| ToF[e] | Flight time | $>10^4$ | $>10^4$ | 5–50[f] | $10^2$–$10^4$ | +++ |
| QIT[g] | Resonance frequency | $>10^3$ | $10^3$–$10^4$ | 50–100 | $10^2$–$10^3$ | ++ |
| LIT[h] | Resonance frequency | $>10^3$ | $10^3$–$10^4$ | 100 | $10^2$–$10^4$ | +++ |
| FTICR[i] | Orbital frequency | $>10^4$ | $>10^6$ at $m/z$ 100 | <1 | $10^2$–$10^5$ | +++++ |
| Orbitrap[j] | Axial frequency | $>10^4$ | $6 \times 10^4$ at $m/z$ 400 | 2–5[k] | $10^3$–$10^4$ | ++++ |

[a] Linear dynamic range.
[b] + = low cost; +++++ = high cost.
[c] May be configured with other analyzers for tandem-in-space experiments (e.g., QqQ, QqLIT, QqToF, and QqFTICR).
[d] Double-focussing BE or EB analyzer may be configured with other analyzers for tandem-in-space experiments (e.g., EBE).
[e] ToF combined with reflectron may be configured with other analyzers for tandem-in-space experiments (e.g., ToF–ToF, QIT-ToF, and QqToF).
[f] 1–5 ppm with a lock mass.
[g] Trapping-type instrument capable of tandem-in-time experiments and can be linked to ToF analyzer (QIT-ToF).
[h] Trapping-type instrument capable of tandem-in-time experiments and can be linked to Q, FTICR, or Orbitrap analyzers (e.g., QqLIT-FTICR, and LIT-Orbitrap).
[i] Trapping-type instrument capable of tandem-in-time experiments and can be configured to analyze fragments generated externally (e.g., QqFTICR or LIT-FTICR).
[j] Trapping-type instrument configured to analyze fragments generated externally (e.g., LIT-Orbitrap).
[k] < 1 ppm with a lock mass.

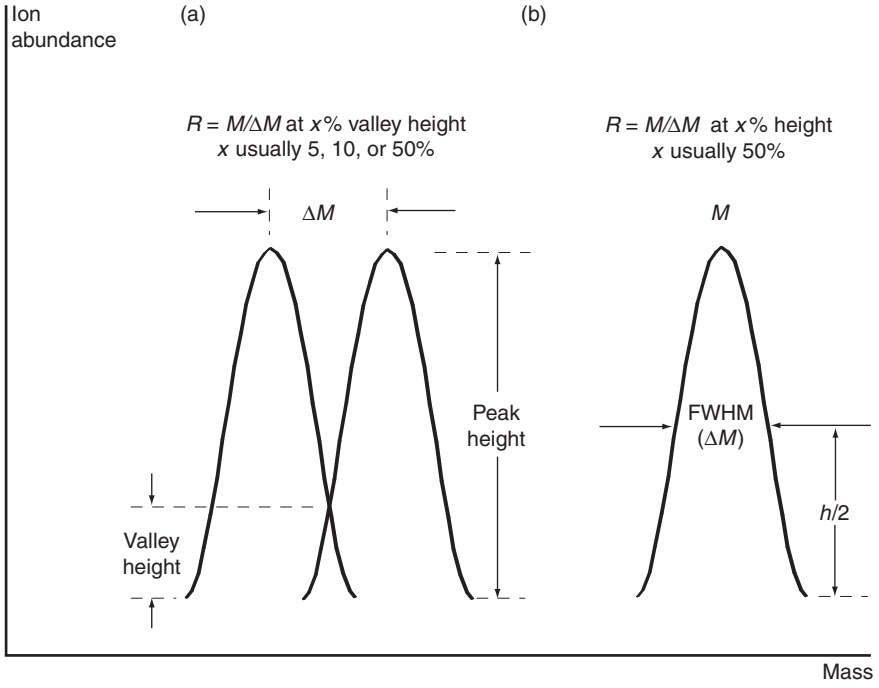


**Figure 5** There are two definitions of mass resolution. These are based on either two overlapping peaks of equal intensity separated by $\Delta M$ (a) or a single well-defined peak with $\Delta M$ defined as the full-width at half-maximum height (FWHM) (b).

There are two commonly used definitions for mass resolution ($R$). The first, used with magnetic sector instruments, is defined as the ability to separate two neighboring ions in a mass spectrum where $\Delta M_x$ is the difference in $m/z$ between the two peaks. The two peaks should be of equal size and similar shape and the degree of overlap ($x$) should be specified (**Figure 5(a)**). The latter is often specified as 10 or 50% of the valley height. $M$ is the average of the two masses.

$$R = \frac{M}{\Delta M_x} \tag{33}$$

A more convenient definition, commonly used with trapping and ToF analyzers, pertains to a single well-resolved peak where $\Delta M_x$ is the peak width at a specified height $x$, usually half-maximum height (full-width at half-maximum height, FWHM) (**Figure 5(b)**). It should be noted that this FWHM definition of resolution equates to about twice that calculated from the 10% valley definition.

Resolution can vary over the mass range and this should also be specified. For example, Q mass filters and ion traps are usually operated at 'unit mass resolution' ($\Delta M_x = 1$) constant over the whole mass range. Thus the peaks at 100 $m/z$ and 101 $m/z$ will be separated at a resolution of 100 and the peaks at 1000 $m/z$ and 1001 $m/z$ will be separated with a resolution of 1000.

Mass accuracy is the difference ($\Delta M$) between the measured accurate mass $M$ and the calculated exact mass. It can be stated as absolute units of mass (differences of so many millimass units, mmu, $10^{-3}$ u) or as a relative mass accuracy in parts per million.

$$\text{Relative mass accuracy} = \frac{\Delta M}{M} \times 10^6 \text{ ppm} \tag{34}$$

Mass accuracy is also closely bound up with mass resolution as failure to achieve sufficient resolution of the ion of interest, away from interfering isobaric ions, will seriously impinge on the attainable mass accuracy. An

appropriate level of mass accuracy and mass resolution in a mass spectrum can enable the determination of the elemental composition of the ions and can allow the analyst to distinguish, for example, glutamine from lysine ($\Delta M = 0.036$ u) and phenylalanine from oxidized methionine ($\Delta M = 0.033$ u) (see Section 9.10.4.3.3).

#### 9.10.2.3.2 Magnetic and electric

The use of magnetic and electric fields to separate ions was introduced by Thompson[2] in his parabola mass spectrometer. The many developments that followed on from this culminated in the modern 'double-focusing' mass spectrometer that is available today. In principle, ions may be deflected by magnetic ($B$, momentum analyzer) or electric fields ($E$, kinetic energy analyzer). An ion, extracted with accelerating voltage ($V$) from the ion source and introduced orthogonally into a magnetic field, will follow a circular trajectory the radius ($r$) of which will be dependent on the ion's $m/z$ value, its velocity $v$, and the magnetic field strength $B$.

The magnetic force $zvB$ will be balanced by the centrifugal force $mv^2/r$.

Thus
$$zvB = \frac{mv^2}{r} \quad \text{or} \quad \frac{mv}{z} = Br \tag{35}$$

Hence it can be seen that the magnetic sector separates ions according to their momentum to charge ratio.

If the velocity ($v$) of the ion as calculated from the kinetic energy ($E_k$) of the ion emerging from the source
$$E_k = zV = \frac{mv^2}{2} \tag{36}$$
is substituted into Equation (35), we derive
$$\frac{m}{z} = \frac{B^2 r^2}{2V} \tag{37}$$
from which it can be seen that changing the magnetic field ($B$) as a function of time will allow the successive passage of ions with varying $m/z$ values. Ions with the same $m/z$ value and the same kinetic energy will follow the same trajectory through the magnetic field. However, the process of ionization in the source results in ions being created with a small spread of kinetic energy. This energy dispersion then acts to limit the resolution achievable by the magnetic analyzer. This limitation can be countered by the addition of an electrostatic analyzer set to pass ions of a defined kinetic energy.

An ion entering an electrostatic field travels in a circular path of radius $r$ such that the centrifugal force is balanced by the electrostatic field strength ($E$).

For ions carrying $z$ charges
$$\frac{mv^2}{r} = zE \tag{38}$$

Substituting for the ion's kinetic energy (Equation (36))
$$r = \frac{2E_k}{zE} \tag{39}$$

It can be seen from Equation (39) that the ion path is independent of the mass and that the electric field is a kinetic energy analyzer. The combination of the magnetic sector's directional focusing and the electrostatic analyzer's energy focusing results in a dramatic increase in the overall mass resolution and accuracy of the instrument. However, high resolving power is achieved at the cost of sensitivity because ions are selected within an increasingly narrow spread of energy and direction, with the rest being discarded. This double focusing characteristic can be obtained with the magnetic and electric analyzers arranged in either of the so-called forward (EB) or reverse (BE) geometries.

These types of mass spectrometers are today rarely used for biological applications, primarily because of their expense, size, and the relatively slow scan speed, which is incompatible with the trend toward fast,

high-resolution LC and GC. The relatively low transmission efficiency also serves to limit the sensitivity of these instruments. The polarity of the magnetic field cannot be rapidly changed to perform, for example, PPNICI and rapid switching to selectively monitor a discrete number of ions (selected ion monitoring, SIM) is possible only over a narrow mass range. In addition, the high-voltage sources lend themselves to discharges when interfaced to liquid chromatographs or the relative high pressures in CI sources. The most important attribute of the double-focusing BE and EB instruments has been the acquisition of high mass accuracy and high mass resolution measurements; however, much of this demand is increasingly being met by ToF analyzers and by FTICR and Orbitrap instruments. Samples are usually introduced into these types of mass spectrometers by either a solids probe or GC.

#### *9.10.2.3.3 Quadrupole*

The Q mass filter consists of four parallel rods of circular or hyperbolic cross section (~10 cm long), extending in the $z$ direction (direction of the ion beam). A high-frequency oscillating electric field is created in the space between the rods by rapidly switching the voltages applied to the rods, with adjacent rods having opposite polarity. The voltages are made up of a DC component ($U$) and a radio frequency (RF) component ($V\cos\omega t$). The forces acting on ions within the central volume (radius $r$) of the rods are given by

$$F_x = ma_x = z(U + V\cos t)\frac{2x}{r^2} \tag{40}$$

$$F_y = ma_x = -z(U + V\cos t)\frac{2y}{r^2} \tag{41}$$

Ions are thus alternately attracted and repelled by the rod voltages as they pass through these quadrupolar fields along the central axis of the rods. The equations of motion are complex (Mathieu equations[33]), but in principle, only ions with a narrow range of $m/z$ values will be able to traverse the field for particular values of $U$ and $V$. Other ions will undergo unstable oscillations and be ejected. From these equations, it can be seen that mass and charge are the only factors describing the ion trajectories. Scanning of the mass spectrum is achieved by varying $U$ and $V$ while maintaining the ratio of $U/V$ constant. Q performance is dependent on the number of RF cycles experienced by the ion as it traverses the rods, so the accelerating voltage (and thus ion velocity) applied to ions entering the rods is limited to approximately 10–20 eV. These low accelerating voltages mean that Q analyzers can tolerate higher pressures than the high-voltage sources of magnetic analyzers and are more suited to interfacing with atmospheric pressure sources (e.g., ESI and APCI).

Q's are compact, robust, and inexpensive. They have high ion transmission properties and because scanning is achieved by sweeping electric potentials, the mass range can be rapidly scanned, so they are readily adapted to interfacing with fast chromatography. The ability to rapidly change electric potentials in the source means that it is possible to rapidly switch between analyzing positive and negative ions in alternate scans, something that is impossible with BE-or EB-type instruments, which would require a change in the direction of the magnetic field. The potentials on the Q rods can also be rapidly switched to allow the selective monitoring of a discrete number of ions (SIM). Most importantly, Q's are readily interfaced to a variety of ion sources and methods of ionization. However, the mass range is limited (2000–4000) and they are not generally capable of high mass resolution. The circular cross-section rods only approximate the required quadrupolar trapping fields and higher mass resolution can be achieved by the use of the more expensive hyperbolic rods.

Q's are also used in the so-called 'RF-only' mode (DC voltage set to zero) allowing transmission of ions with a wide range of $m/z$ values and characteristically focusing them into the central region between the rods. This latter property means that RF-only Q's have found wide use as ion guides or collision cells, to focus an ion beam or to improve the transmission of collision products. The amplitude of the RF voltage determines the low mass cutoff and, theoretically, all ions of $m/z$ greater than the low cutoff value are transmitted. However, there is some discrimination against ions of high mass. Hexapoles and octapoles are used in a similar manner but have better wide band pass characteristics. All these RF-only multipole devices are designated 'q' in the shorthand used to describe instrumental configurations. These RF-only multipoles are commonly found in hybrid mass spectrometers used for tandem MS (Section 9.10.3) serving as collision cells and to efficiently transport ions between differentially pumped regions of the instrument.

Q mass spectrometers may be found interfaced with most of the sample introduction and ionization methods described above with the exception of MALDI.

#### 9.10.2.3.4 Quadrupole 3D-ion trap

The quadrupole ion trap (QIT) is about the size of a small fist and consists of a ring electrode and two hyperbolic end electrodes (see March and Todd[68] for a detailed theory of operation and history of development). Like the linear ion trap (LIT, see below), the QIT operates at relatively high pressure ($10^{-3}$ torr) with a helium buffer gas that assists the ions to maintain a stable orbital frequency. The buffer gas also serves as the collision gas for collision-induced dissociation (CID) during MS/MS experiments.

Ions may be created inside the QIT or, more commonly, externally. An oscillating saddle field inside the trapping volume contains and focuses the ions into the center of the trap. From here the operator can scan the ions out of the trap to create a classic full mass spectral scan of the ions in the trap. Alternatively, a particular ion can be selected (isolated), collisionally fragmented and a scan of all the product ions generated ($MS^2$ scan). This whole process can be repeated with any one of these fragment ions ($MS^3$ scan) and as long as there are sufficient ions remaining in the trap to provide an adequate signal-to-noise ratio (S/N), the process can be repeated (**Figure 6**).

The number of ions that can be retained in the QIT, or indeed in any trapping-type instrument, is limited by space charging effects. Space charging occurs when the cloud of ions becomes sufficiently dense that coulombic repulsion between the like-charged ions starts to overcome the trapping potential, resulting in degraded mass resolution and accuracy. Limiting the number of ions in the trap at any one time normally controls this effect.

The QIT is compatible for use with the full range of methods for introducing solids, liquids, and gases – solids probe, GC, and LC – and with all the ionization methods described above including MALDI.

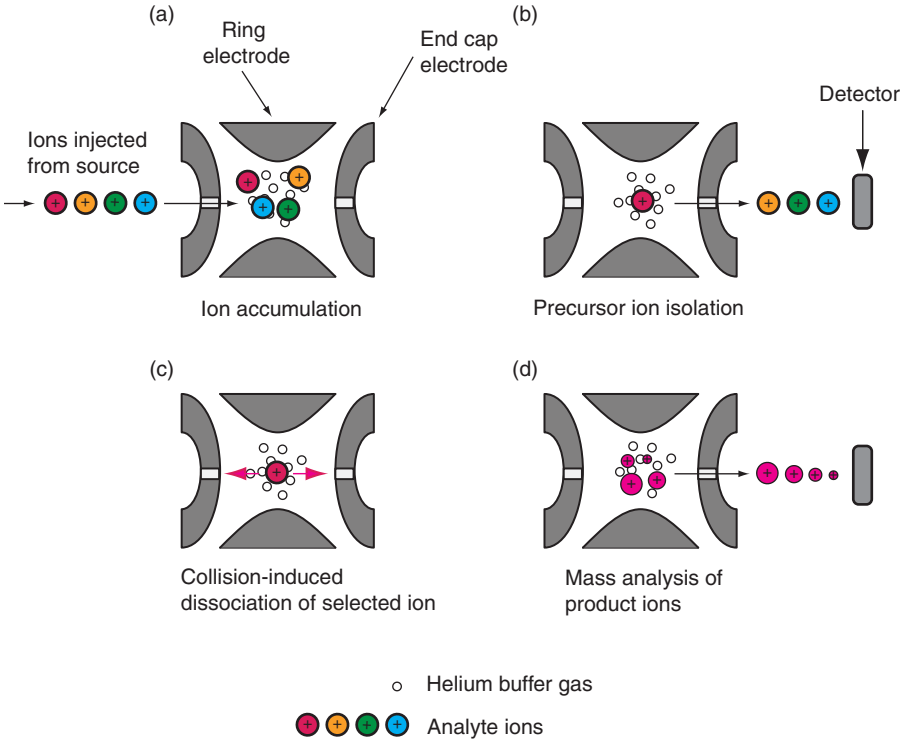


**Figure 6** Schematic of collision-induced dissociation (CID) in the quadrupole ion trap (QIT) ($MS^2$ experiment). In separate events, ions from the source are accumulated and trapped in the space at the center of the electrodes (a). Ions with a specified *m/z* value are retained in the trap and all others ejected (b). The specified ions are then collisionally fragmented by axial excitation between the two end caps (c). The resulting product ions are then sequentially ejected to generate the product ion spectrum (d). In an $MS^3$ experiment, one of these product ions may be selectively retained in the trap, excited, and fragmented.

#### 9.10.2.3.5 Linear 2D-ion trap

The two-dimensional linear ion trap (2D-LIT) is a logical development of the Q mass filter, described above, in that by the imposition of appropriate potentials at the entrance and exit of the Q's, ions with a range of $m/z$ values can be trapped within the axial quadrupolar field (see March and Todd[69] for a detailed theory of operation and history of development). In common with the QIT, the LIT operates at relatively high pressure ($10^{-3}$ torr) with a helium buffer gas. The buffer gas collisionally cools the ions and also acts as a collision gas for MS/MS experiments.[70,71]

The LIT has several advantages over the QIT. The larger volume means that more ions can be contained within the LIT before space charging becomes evident. This results in a greater dynamic range and improved sensitivity that can translate into lower detection limits for MS/MS analysis. Trapping efficiencies are also enhanced, as ions entering the trap have to overcome the trapping potential only on the front section. Once in the trap, the ions are collisionally cooled by interaction with the helium buffer gas and thereafter lack the energy to escape the trapping potential on the front section. Once in the trap, the ions are collisionally cooled by interaction with the helium buffer gas and thereafter lack the energy to escape the trapping potential on the front and back sections. This is in contrast to the QIT where there is only a narrow time window in which the amplitude and phase of the RF voltage are such that ions can pass through the end cap to enter the trap. This limits the trapping efficiency for the QIT to <5% compared to 29% for the LIT. At other phases and amplitudes, ions will have either too little or too much momentum so that the ions do not experience a sufficient number of collisions with the QIT buffer gas to be cooled and trapped.[70] In summary, the LIT has a significant sensitivity advantage over the QIT.

Using mass selective instability with resonance ejection, ions are scanned out of the trap through slits in the center of two opposite center section rods and focused onto two separate conversion dynodes. In the case of the QIT, where ions are scanned out of both end cap electrodes, the only place for a detector is behind the end cap opposite the ion entrance, so that only half of the ions scanned out of the trap are detected. Both the QIT and LIT operate at unit mass resolution with similar scan rates and both have the capacity to generate higher resolution spectra at slower scan rates.

In theory, the LIT should have the same universal utility as the QIT in terms of the types of samples and in being interfaced with GC or LC but to date only the LC interface is commercially available.

#### 9.10.2.3.6 Orbitrap

A new mass analyzer, the Orbitrap, is a modified development of the 'Knight-style' Kingdon trap.[68,72–73] The Orbitrap radially traps ions about a central spindle electrode that is contained by an outer barrel-like electrode maintained at a vacuum of more than $3 \times 10^{-10}$ torr. The $m/z$ values of the ions are then measured from the frequency of the ion's harmonic oscillations along the axis of the central electrode. These axial frequencies are independent of the energy and spatial spread of the ions and they are detected as a broadband image current of a time-domain signal that is converted to a mass spectrum by fast Fourier transform algorithms.[74]

The Orbitrap is available as a stand-alone instrument and as a hybrid consisting of a linear ion trap coupled to the Orbitrap via a C-trap, which is responsible for focusing and injecting ions tangentially into the Orbitrap (LTQ-Orbitrap).

The performance characteristics of this analyzer are quite remarkable with mass accuracies of <2 ppm at a resolving power of 60 000 using an external calibration[75] and of <1 ppm with internal calibration.[76] As such, it has attracted the attention of analysts and instrument developers alike. New features have included ETD (see Section 9.10.3.2.5) and options for higher energy collisions in the C-trap or in an additional octapole collision cell.[77]

#### 9.10.2.3.7 Time-of-flight

Conceptually, the ToF analyzer is very simple, in that ions of the same kinetic energy, $E_k$ (extracted from the ion source with accelerating voltage $V$), but differing $m/z$ values take different times $t$ to traverse a fixed distance $d$. Thus lighter ions travel the fastest and are detected before the heavier ones. For an ion of mass $m$, the electric charge $q$ is equal to the number $z$ of electron charges $e$ ($ez$).

$$E_k = ezV = \frac{mv^2}{2} \tag{42}$$

$$t = \frac{d}{v} \tag{43}$$

Substituting for velocity into Equation (43) yields

$$t^2 = \frac{m}{z} \quad \frac{d^2}{2Ve} \tag{44}$$

To measure the flight time, the ions must be accelerated from the source in discrete packets. The resolving power of this simple experimental setup, linear ToF, was not good and after some initial popularity, the technique languished. The resolution was limited by the fact that at the time when ions are accelerated out of the source, they are not neatly lined up at the starting line. Rather they are positioned throughout the source and have a range of different kinetic energies. For the ultimate resolution, ions of the same mass (isobaric ions) positioned anywhere within the ion source need to arrive simultaneously at the detector.[78,79]

When the laser-induced ion plume is formed, there is no immediate application of the source extraction field and the plume is allowed to expand as if in a field-free region. If we consider just a group of isobaric ions, the more energetic ions fly faster and reach further into the source region than less energetic ones. Then at a chosen time, one of the electrodes of the extraction region is appropriately pulsed with high voltage to create the extraction potential. The ions in the tailing end of the plume (the originally less energetic) find themselves in a higher potential than the rest, and eventually acquire slightly higher velocity, enough to catch up with the leading-end ions by the time they reach the detector position.

Variations in the longitudinal velocity of isobaric ions can also be corrected by the use of a reflectron. This is basically an electric field that initially slows the ions and then accelerates, or reflects, them back out toward the detector. The more energetic ions will penetrate deeper into the decelerating field than less energetic ions of the same $m/z$ value and experience a longer flight path and a longer flight time. The end result is that ions of a given $m/z$ value will arrive at the detector in a much narrower time span (time focusing). The combination of delayed extraction, to compensate for positional differences of the ions, the addition of one or more reflectrons in the flight path, to compensate for different ion kinetic energies, and fast digital electronics, can boost the mass resolution of the ToF analyzer to better than $10^4$ (FWHM).

At the start of the ToF renaissance, these analyzers were associated with MALDI sources as the discontinuous laser pulses are ideally suited to the pulsed nature of the ToF analyzer. However, continuous ion beams (e.g., EI and ESI) have also been coupled with ToF analyzers.[78] This has been achieved by locating the ToF analyzer orthogonal to the continuous ion beam axis. An orthogonal accelerating voltage is then applied to the beam and a discrete linear ion packet can then be pulsed into the ToF. During the time that the ions are moving in the drift region, and in the reflectron, the orthogonal acceleration volume is refilled by the continuous beam, hence the high, mass analyzer efficiency that is characteristic of ToF analyzers. For illustrative purposes, Guilhaus *et al.*[78] compared the approximate mass analyzer efficiency of a Q scanning over a 1000 u mass range and a ToF analyzer, with calculations of 0.025 and 25% maximum efficiencies, respectively. As Guilhaus *et al.*[78] have stated,

> In scanning instruments some of the mass range is detected all of the time while in TOF instruments all of the mass range is detected some of the time.

ToF analyzers are relatively small and of medium expense and so represent a good alternative to magnetic sector and Q analyzers, especially when their speed and sensitivity advantages are considered. Their mass accuracy and ease of calibration are also well established. ToF analyzers also have the highest practical mass range of all mass analyzers. However, the digitizer speed may place limitations on the instrumental dynamic range. The very fast acquisition rates that are achieved in ToF analyzers mean that they are also ideally suited

to analyze fast GC separations with the added benefit that the high acquisition rates mean that coeluting components are much more readily deconvoluted than when a slower analyzer such as a Q is used.

#### *9.10.2.3.8 Fourier transform ion cyclotron resonance*

The FTICR is a trapping-type instrument with the ICR cell being held within the field of a superconducting magnet.[18,33,80] The cell itself consists of three pairs of opposing plates in the form of a cube or a cylinder. Ions are injected into the cell along the axis of the magnetic field and are then electrostatically trapped within the cell by the trapping potential placed on the two trapping plates that are orthogonal to the direction of travel. These ions are then subjected to an excitation pulse from the excitation plates and they will then, under the direction of the Lorentz force, spiral out from the center of the cell into a circular orbit. As noted above (Section 9.10.2.3.2), ions introduced orthogonally into a magnetic field will, under the direction of the Lorentz force, follow a circular trajectory, the radius ($r$) of which will be dependent on the ion's $m/z$ value, its velocity $v$, and the magnetic field strength $B$.

The Lorentz force, $qvB$ ($q$, charge; $v$, velocity), can be equated to the centripetal force

$$\frac{mv^2}{r} = qvB \tag{45}$$

and the angular frequency ($\omega$) of the ions trapped in these circular orbits (cyclotron motion) is given by

$$\omega = \frac{v}{r} \tag{46}$$

so that substituting for $v$ from Equation (46) into Equation (45) yields

$$\begin{aligned} m\omega^2 r &= q\omega rB \\ \omega &= \frac{qB}{m} \end{aligned} \tag{47}$$

the cyclotron equation.

From Equation (47) it can be seen that while the ion cyclotron frequency ($\omega$) of an ion is a function of its mass, charge, and the magnetic field, it is independent of the ion's initial velocity.

The cyclotron orbits of thermal energy ions when they first enter the ICR cell are both too small and incoherent to be detected. However, if an excitation pulse is applied at the cyclotron frequency, the resonant ions will absorb energy and be brought into phase with the excitation pulse. They will have a larger orbital radius and the ion packets will orbit coherently. The ions may then be detected as an image current induced in the receiver plates. Additionally, this excitation pulse increases the kinetic energy of the trapped ions to the extent that fragmentation can be collisionally induced by ion–molecule reactions. Alternatively, the excitation pulse may be used to increase the cyclotron radius so that ions are ejected from the ICR cell.

Normally, many different ions will be present within the cell but they may all be excited by a rapid frequency sweep. The $m/z$ values of the ions present in the ICR cell, and their abundance, may then be extracted mathematically from the resultant complex image current using a Fourier transformation to generate the mass spectrum of the ions. An important feature of FTICR is that the ions are detected nondestructively and that longer acquisition times over a narrower $m/z$ range may be used to increase the measured mass resolution and the S/N.

FTICR instruments have a stringent requirement for a very low background pressure ($10^{-10}$ torr) to minimize ion–molecule reactions and for this reason most analytical experiments are accessed through a variety of external ion sources that are separated from the cell by several stages of differential pumping. This vacuum requirement and the cryogenic cooling needed to run the superconducting magnet make this form of MS very capital intensive and expensive to run. However, this is offset by the extraordinary mass accuracy (sub-ppm with internal calibration), mass resolution (>$10^6$ at 100 u), and sensitivity (able to detect a few hundred ions at a time) that may be achieved.[18] FTICR instruments can also serve as platforms for a variety of unique dissociation techniques (e.g., IRMPD, infrared multiphoton dissociation; ECD; EDD, electron detachment dissociation; see Section 9.10.3.2) and this

combined with their high mass accuracy and high mass resolution means they are ideally suited to identify and characterize large intact biomolecules – the 'top-down' approach.[81]

FTICR instruments that are designed to analyze low-molecular-weight molecules, such as VOCs, do not require superconducting cryogenic magnets and can be built using structured permanent magnets. Dehon *et al.*[43] built a dedicated PTR-FTICR (proton-transfer reaction Fourier transform ion cyclotron resonance) containing a cascade of three differentially pumped cells within the same magnetic field. The first cell is used as an ion source ($10^{-5}$ torr), from which the selected $H_3O^+$ ions are drifted via the second cell into the third cell where they react with the sample ($10^{-7}$–$10^{-5}$ torr). After the reaction, the ions are drifted back to the second cell for FTICR analysis. Although this instrumental approach is not as sensitive as in PTR-MS instruments (1 ppm compared with 0.1 ppb), the mass resolution and mass accuracy of the FTICR means that molecular formulas may be readily determined for the VOCs.

#### *9.10.2.3.9 Ion mobility spectrometry*

In drift tube ion mobility spectrometry (IMS), a packet of ions is drawn through an inert gas under the influence of a weak electric field. The extent of interaction with the inert gas and the rate of progress through the drift tube are dependent on the collisional cross section (shape and size) of the ion and on the number of charges carried by the ion. The requirement to gate the packets of ions entering the IMS and the need to wait for the ions to clear the drift tube result in a low duty cycle. If the sample is being supplied in a continuous flow, as in, for example, an ESI source, then much of the sample will be lost to the analysis. When this is combined with losses through radial diffusion, the overall sensitivity of the technique is poor. Nevertheless, the prospect of a technique to preprocess ions prior to MS analysis has proved attractive and in recent times two variations of this technique, circumventing these disadvantages, have been successfully developed for combination with MS.

In high-field asymmetric waveform ion mobility spectrometry (FAIMS), a continuous stream of ions is fed into the device inlet in a stream of dry carrier or bath gas.[82,83] The ions are then exposed to alternating strong and weak electric fields of opposite polarity across the carrier gas flow. The differential collisional interaction of ions with the carrier gas in the oscillating asymmetric fields results in different ions experiencing a net movement to one or the other wall electrode. If no other voltage is applied, the ions will eventually collide with one of the wall electrodes and be lost. However, if a low compensation voltage (CV) of correct magnitude and polarity is applied, then selected subsets of ions will be passed to the mass analyzer with a concomitant increase in their S/N and improved detection limits. For mixtures of ions, the CV can also be scanned. The ion separation achieved in the FAIMS device can also be refined by the use of different carrier gases.[82]

In the traveling wave IMS (TWIMS),[84] ions are initially accumulated in a trap ion guide and then released as an ion packet into the ion mobility ion guide. Here axial motion through the stack is generated by a repeating sequence of transient DC voltages providing a continuous series of 'traveling waves'. Ions are then separated as they are driven ahead of these potential hills through the stacked ring ion guides before transfer to the MS analyzer.

Although a relatively new adjunct to MS, IMS, whether the FAIMS or the TWIMS variety, has demonstrated a wide-ranging usefulness, particularly with respect to analyzing complex mixtures. It has been used, for example, to separate positional isomers of small molecules, to remove chemical noise and thereby improve detection limits and sensitivities of assays, and to examine conformational forms of multicharged protein ions. In proteomic experiments, IMS can be used to select out triply charged ions for ETD and doubly charged ions for CID, ignoring the single-charged peptides, solvent ion clusters, and other chemical noise (e.g., phthalate ions). Both FAIMS and TWIMS can be used with existing LC techniques to separate ions in a continuous stream and are in principle compatible with all types of ion sources and analyzers.

### 9.10.3 Tandem Mass Spectrometry

As you will see in the following section, it is quite common for an instrument to contain more than one analyzer. A shorthand nomenclature has been adopted to describe such instrumental configurations, using the analyzer abbreviations outlined above (Section 9.10.2.3), in which the order of the abbreviations represents the order of

the analyzers traversed by the ion beam. For example, QqQ designates the very common triple Q instrument with the two scanning Q's separated by an RF-only Q that acts as the collision chamber. Other examples will be discussed below.

The 'soft' ionization processes described above (Section 9.10.2.2) typically generate single- or multicharged molecular ions with little accompanying fragmentation. To obtain structurally informative fragments, these ions must be subject to a second round of mass spectral analysis. This is known as MS/MS or tandem MS. In the first MS stage, an ion is selected or isolated in the mass spectrometer, activated and fragmented, most commonly by CID, and the product ions mass analyzed in the second MS stage. Depending on the instrument being used, it is possible to perform multistage mass spectrometry ($MS^n$) and to construct ion fragmentation pathways as part of an exercise in structural elucidation. It is also possible to use tandem MS to add a large degree of selectivity and to improve sensitivity in an assay by removing background chemical noise (see discussion below, Sections 9.10.4.2.2 and 9.10.4.5.7). With the demand for the analysis of increasingly complex samples, often coupled with a 'soft' ionization process, tandem MS along with mass determination with high accuracy and resolution has become an essential feature of modern biological mass spectrometers.

### 9.10.3.1 Analyzers

#### *9.10.3.1.1 Tandem-in-space*

For the beam-type mass analyzers (sector, ToF, and Q), each stage of mass analysis is performed in discrete mass analyzers usually separated by a collision cell. This arrangement is called tandem-in-space. The use of multiple analyzers means that analyzers can be independently selected for the different stages of analysis based on the desired performance characteristics.

Two common instrumental configurations for tandem-in-space experiments are the so-called QqQs, which consist of two Q mass filters, $Q_1$ and $Q_3$, separated by an RF-only Q collision cell (q) (**Figure 7**), and the QqToF class of instruments, which use a ToF analyzer in place of the third Q. The QqQ analyzer arrangement has the advantages of cost and ease of operation associated with Qs but leaves the analyst with limited mass resolution and mass accuracy with which to select and analyze ions. The replacement of the third Q by a ToF analyzer, although representing an increase in cost, gives the operator access to high-resolution/high mass accuracy data, in addition to greatly improved full scan sensitivity.[85] Today's generation of collision cells use RF-only multipoles (hexapoles and octapoles) or ring guides, which have improved transmission characteristics over the RF-only Q, but these are still commonly denoted as 'q' in instrumental shorthand.

Recent developments in instrumentation have seen the commercial release of traps combined with ToF analyzers (QIT-ToF), quadrupoles with traps (QqLIT), and traps with traps (LIT-FTICR, LIT-ToF, and LIT-Orbitrap), all taking advantage of the $MS^n$ capabilities of the ion trap mass analyzers. The ability to select ions in a separate analyzer, prior to the final stage of MS analysis, serves to enhance the dynamic range and sensitivity of the final MS analysis. The development and characteristics of these hybrid combinations have been reviewed by Glish and Burinski[86] and Hagar.[87] The ToF–ToF combination with high mass accuracy and high mass resolution in both MS stages is also commercially available.[88]

#### *9.10.3.1.2 Tandem-in-time*

Tandem MS may also be performed intime using a trapping-type analyzer (e.g., LIT, QIT, and FT-ICR) (**Figure 6**). The experimental efficiency of this arrangement is usually higher than that of tandem-in-space instruments as ions do not have to be transferred between analyzers; however, experiments take longer to complete and sample presented to the mass analyzer from a continuous source while the trap is in the analysis mode will be lost. The different stages of the tandem-in-time experiment all take place in a temporal sequence within the same physical space. In these experiments, the selected precursor ion is retained in the trap and all other ions expelled. The selected ion is then activated and fragmented and the fragments analyzed to generate the MS/MS ($MS^2$) spectrum of the precursor ion. As long as there are sufficient ions still available in the trap, this process may be extended by selectively retaining one of the fragment ions and repeating the fragmentation process to generate the MS/MS/MS or $MS^3$ spectrum.

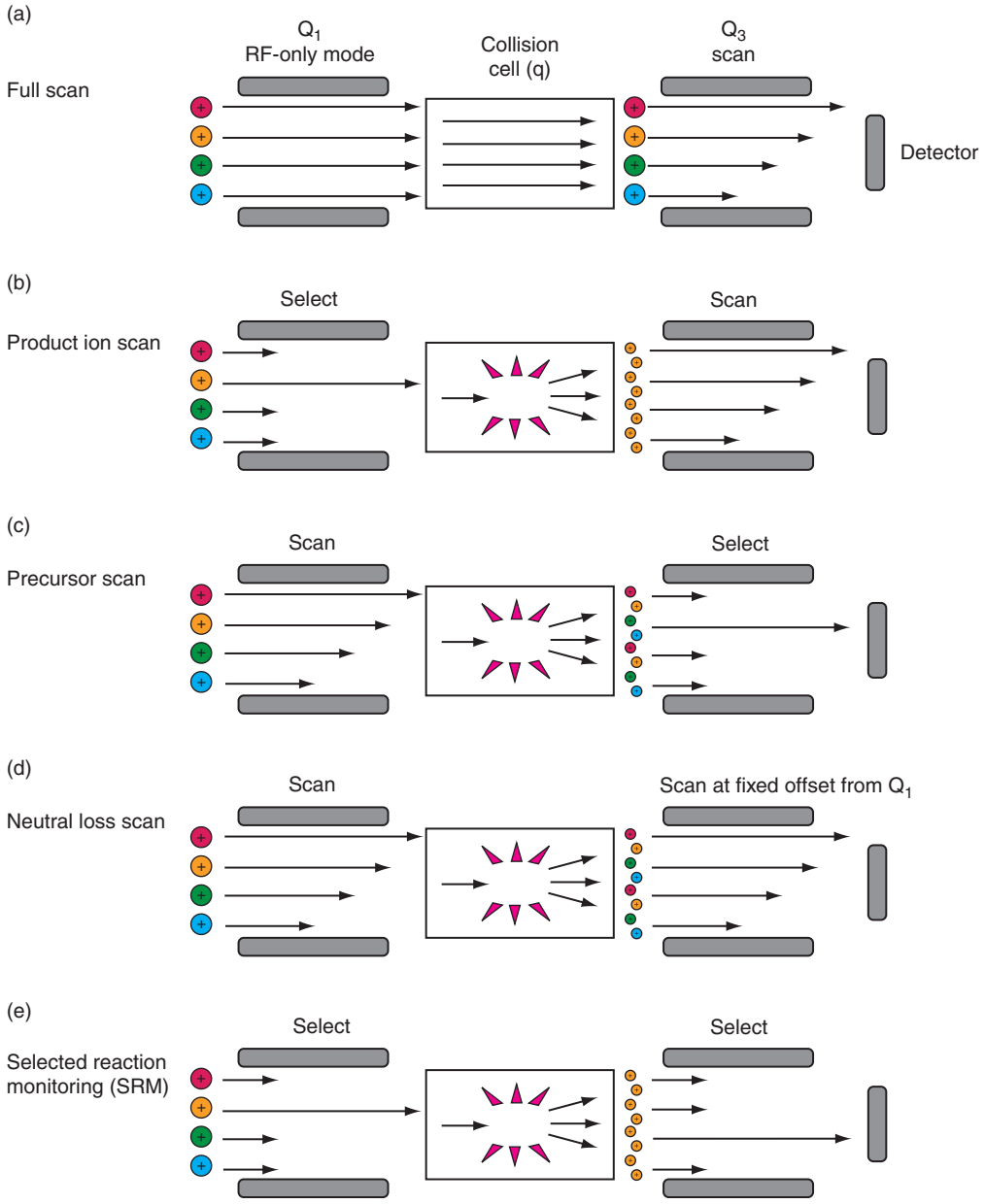


**Figure 7** Scan modes for a tandem-in-space instrument, the triple quadruple (QqQ). (a) Full scan: all source ions are passed through to $Q_3$ while $Q_1$ and q (collision cell) are set to the RF-only mode. (b) Production scan: $Q_1$ is set to pass a selected ion (precursor ion). This is fragmented in the collision cell and products are analyzed by scanning $Q_3$. (c) Precursor scan: $Q_1$ scans all the source ions into the collision cell for collision-induced dissociation (CID). $Q_3$ is set to pass a selected product ion. A signal recorded at $Q_3$ is correlated with the corresponding precursor ion passing through $Q_1$. (d) Neutral loss scan: $Q_1$ is set to scan ions into the collision cell for CID. The $Q_3$ scan is offset by a specified mass, equal to the mass of the neutral, relative to $Q_1$. (e) Selected reaction monitoring (SRM): an ion selected in $Q_1$ is fragmented and a specific fragment is then recorded after selection by $Q_3$. SRM is commonly used in quantitative work to improve assay selectivity and sensitivity.

### 9.10.3.2 Fragmentation

#### *9.10.3.2.1 Collision-induced dissociation*

Fragmentation of ions in tandem experiments requires an input of energy to break internal covalent bonds. This is most commonly achieved by converting the kinetic energy of a collision, between the selected ion and an

inert collision gas such as helium or argon, into vibrational energy. Fragmentation then occurs when the internal energy exceeds the activation energy required to cleave a particular bond. It is also important to note that bond cleavage may be preceded by an internal rearrangement, such as, for example, hydrogen scrambling or the McLafferty rearrangement.

For tandem-in-space experiments, CID occurs in a collision cell, physically located in the field-free region between the mass analyzers (**Figure 7**). The cell is differentially pumped and the flow of gas into the cell is carefully controlled. Increasing the collision gas pressure attenuates the main beam and, at the same time, the probability of ions undergoing single, double, triple, etc. collisions will increase, as will the scattering of the ion beam. Modern gas cells are usually either an RF-only multipole or a set of ring guides that are designed to contain and refocus, as much as possible, ions scattered from the direction of travel of the main beam. In high-energy collisions (KeV), the collision gas is usually helium as its high ionization energy reduces the risk of charge exchange. In low collision energy systems (1–200 eV), heavier gases such as argon or xenon have been used to improve the effectiveness of the CID process. The extent of fragmentation obtained from CID in tandem-in-space configurations is dependent on both the energy of the ions entering the collision cell and the pressure of the collision gas. Higher energy ions will be able to access fragmentations with higher activation energies and higher pressure of the collision gas will result in multiple collisions producing more extensive fragmentation, fragmenting fragments.

For small ions, a single collision may be sufficient to induce the dissociation of a covalent bond; however, as the size of an ion increases, so does the number of vibrational degrees of freedom over which the collisional energy may be distributed. Thus the effectiveness of CID decreases with mass. Nevertheless, CID is quite effective for relatively large, multicharged polypeptides (up to 5 kDa), where the bond cleavage may be assisted by the coulombic repulsion of the multiple charges.

The CID spectra generated in traps are qualitatively different from those generated by tandem-in-space experiments. In traps, only the selected ion is activated and once fragmentation of this ion has occurred, no further collisions can take place. Thus the fragment ion spectrum generated in a trap will be simpler and less informative than that from a tandem-in-space experiment. Where the precursor ion undergoes, for example, the simple loss of a neutral such as water, the product ion spectrum will be relatively uninformative, consisting mainly of $[MH - H_2O]^+$. However, this may be readily overcome by a broadband activation, which is applied to all ions in a range 20 $m/z$ below the precursor ion.

FTICR cells are typically operated under very high vacuum ($10^{-10}$ torr) and CID within the cell must be initiated by injecting a collision gas after an ion packet of a designated $m/z$ value has been selected by expulsion of all other ions from the cell. The selected ions are then activated by sustained off-resonance irradiation (SORI). This results in the ion orbit expanding and contracting with time and in the process the ions undergo multiple, low-energy collisions with the injected collision gas. The collision gas is then pumped away and the fragment ion spectrum measured. Alternatively, if the FTICR is part of a tandem-in-space instrument (e.g., QqFTICR or LIT-FTICR), then ions can be fragmented by CID outside of the cell, with the product ions presented to the FTICR for mass analysis. Fragmentation in the FTICR cell may also be accomplished by photon-induced dissociation (PID, Section 9.10.3.2.2), ECD (Section 9.10.3.2.3), and EDD (Section 9.10.3.2.4) (see also discussion in Section 9.10.3.2.6 on the use of CID/IRMPD and ECD/ETD for protein/peptide sequencing, and **Table 4**).

Finally, when using ESI or APCI, it is also possible to perform in-source CID at atmospheric pressure. This is sometimes referred to as 'pseudo-MS/MS'. By increasing the entrance cone voltage, newly formed ions can be accelerated toward the entrance cone, colliding with other molecules, mostly atmospheric nitrogen, and fragmenting. It is important to note that there is no mass selection for a precursor ion and that selection is entirely based on chromatographic separation.

#### *9.10.3.2.2 Photon-induced dissociation*

Gas-phase ions may be fragmented by photoexcitation (PID), particularly by IR photons tuned to the vibrational frequency of covalent bonds. The cross section of an ion for photon absorption is low compared with its collisional cross section, so PID is most commonly associated with the use of intense light sources (lasers) and FTICR where the period the ion is exposed to the photons can be lengthened to increase the

**Table 4** Comparison of CID/IRMPD with ECD/ETD for peptide sequencing

| CID/IRMPD | ECD/ETD |
|---|---|
| • Molecules are vibrationally excited by either physical collision with a neutral gas (CID) or by absorption of an IR photon (IRMPD). | • An electron is directly (ECD) or indirectly, via an anion ($M^{-\cdot}$ from fluoranthrene) (ETD), transferred to a cation (positively charged peptide). |
| • Vibrational energy can be distributed over whole molecule. | • Not applicable to singly charged ions. |
| • Larger analytes need more energy and efficiency drops off with increasing size. | • The electron is accepted by an amide-associated proton on the peptide backbone. This very unstable radical reacts very quickly to cleave the peptide bond at the site of reaction. |
| • The weakest, most labile bonds break first (loss of water, PTMs, etc). | • Rapid process does not allow time to distribute energy over whole molecule. |
| • In peptides, CID/IRMPD generates *y*- and *b*-series ions. | • Can be applied to whole proteins in 'top-down' proteomic analysis. |
| • Low-energy interactions do not allow isomeric Leu/Ile to be distinguished. | • Bonds cleaved are those that accept the electron, not simply the weakest bonds. |
| | • PTMs are preserved. |
| | • Can distinguish isomeric Leu/Ile via secondary fragmentation of radical $z^{\cdot}$ ions. |
| | • In peptides and proteins, ETD generates *c*- and *z*-series ions but some *y* ions may also be observed. |
| | • Masses of *c* and *z* ions may be 1 Da lighter or heavier, respectively, because of extensive hydrogen rearrangement. |

In modern instrumentation, these techniques may both be applied to the same peptide to generate complementary sequence data and PTM data (IRMPD and ECD in FTICR MS,[89] CID and ETD in QIT and LIT,[90] and CID and ETD in QToF[91]).

chance of absorption and subsequent dissociation. For IRMPD, these IR photons may be supplied by a laser (10.6 μm from a $CO_2$ laser) or they may be radiated from a heated blackbody (blackbody infrared dissociation, BIRD). IRMPD, BIRD, and CID all induce fragmentation by the addition of excess vibrational energy to covalent bonds and consequently yield very similar patterns of fragmentation. For example, when applied to protonated peptides and proteins, CID and IRMPD cleave the weakest bonds, the PTMs (e.g., phosphorylation, sulfation, γ-carboxylation, and N-and O-glycosylation) and the backbone peptide amide C–N bonds, to yield the characteristic series of N-terminal *b* ions and C-terminal *y* ions (**Figure 8**). The advantage of IRMPD and BIRD over CID is that no pump-down time is required to remove the collision gas and thus high-resolution detection can be effected immediately.

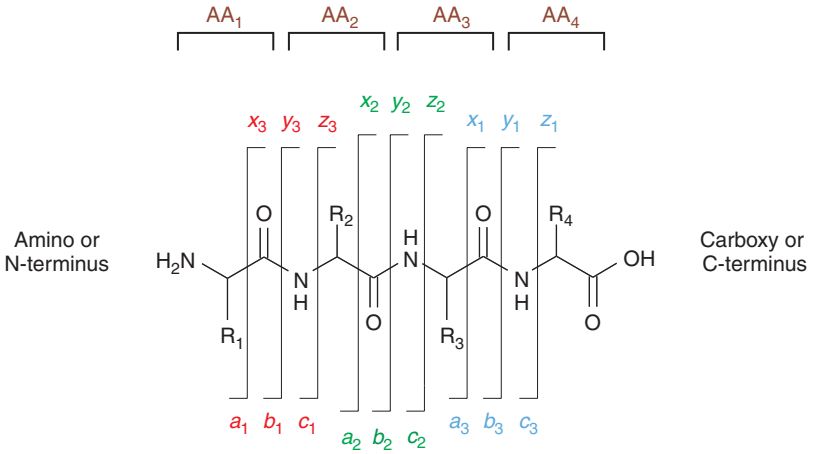


**Figure 8** Roepstorff and Fohlman[92] notation for peptide fragmentation. For the *x*-, *y*-, and *z*-ion series, charge is retained on the C-terminus fragment and for the *a*-, *b*-, and *c*-ion series, charge is retained on the N-terminus fragment. Cleavage of the $C_\alpha$–C bond gives rise to the *a* and *x* ions (e.g., by EDD); cleavage of the C–N amide bond, the *b* and *y* ions (e.g., CID); and cleavage of the N–$C_\alpha$ amine bond (e.g., by ECD or ETD), the *c* and *z* ions.

#### 9.10.3.2.3 Electron capture dissociation

An alternative method for achieving covalent bond cleavage in the FTICR cell, and one that has been mostly applied to sequencing peptides and proteins, is ECD.[93,94] The multicharged peptide and protein ions from ESI are an ideal target for ECD as the cross section for electron capture increases by approximately the square of the ionic charge. The capture of a thermal electron (~0 eV) is an exothermic reaction and in protonated peptides and proteins, results in cleavage of disulfide (S–S) bonds along with cleavage of the backbone N–$C_\alpha$ amine bond, yielding the characteristic complementary pairs of $c$ and $z^{\cdot}$ (~90%) or $a^{\cdot}$ and $y$ (~10%) fragment ions used for sequencing.

$$[\mathrm{M}+n\mathrm{H}]^{n+}+\mathrm{e}^{-}\rightarrow([\mathrm{M}+n\mathrm{H}]^{(n-1)+\cdot})_{\text{transient}}\rightarrow\text{fragments} \tag{48}$$

$$\mathrm{R_1-S-S-R_2}+\mathrm{e}^{-}\rightarrow\mathrm{R_1-SH}+^{\cdot}\mathrm{S-R_2} \tag{49}$$

A unique feature of ECD is that the N-terminal fragment ions, the $c$ ions, contain an extra hydrogen atom from the proton neutralized by the electron capture. The complementarity of the $c/z^{\cdot}$ pair can thus be confirmed by the fact that their mass sum is 1 u greater than the $M_r$ of the protein.

The ECD process, by its nature, is a very rapid process and bond dissociation occurs faster than the redistribution of intramolecular vibrational energy that occurs with CID. This explains the dissociation of the strong N–$C_\alpha$ amine bonds in the presence of the weaker C–N amide bonds in peptides and proteins.[93,94] Consequently, any labile PTMs (e.g., phosphorylation, sulfation, $\gamma$-carboxylation, N- and O-glycosylation) are preserved and may be unequivocally located in the peptide/protein sequence. See also discussion in Section 9.10.3.2.6 on the use of ECD/ETD and CID/IRMPD for protein/peptide sequencing, and **Table 4**.

Recently, it has been observed that ECD can also occur for electrons with energies in the range of 3–13 eV,[95] the so-called hot ECD (HECD), with the excess energy going into secondary fragmentation, including cleavage of the C–N amide bonds ($b$- and $y$-ion series) in multicharged peptides. Significantly, the isobaric isoleucine and leucine residues were reported as losing $^{\cdot}C_2H_5$ and $^{\cdot}C_3H_7$, respectively, allowing these isomeric amino acids to be distinguished.[96]

Unlike CID, where the applied intramolecular vibrational energy can be redistributed and dissipated across the whole molecule, so that the efficiency of CID is diminished with increasing analyte size, ECD can be used to sequence large, undigested proteins. This has enabled the development of the 'top-down' approach to proteomics, which has the advantage of directly sequencing a protein, along with its PTMs, rather than having to infer the sequence following an enzymic digestion (e.g., trypsin or Lys-C) and an *in silico* reassembly from the MS/MS data on the enzymic peptides. It has also been noted that there are a number of side chain losses in ECD that can aid, for example, in distinguishing the isobaric amino acid residues, leucine and isoleucine. However, the ECD technique is accessible only in the expensive FTICR instruments (see also discussion in Section 9.10.3.2.6 on the use of CID/IRMPD and ECD/ETD for protein/peptide sequencing, and **Table 4**).

#### 9.10.3.2.4 Electron detachment dissociation

EDD is a promising new FTICR technique, and is the negative ion complement to ECD. Both these electron-mediated techniques involve a radical ion intermediate, produced by either electron attachment to multiply charged cations (ECD) (Equations (48) and (49)) or electron removal from multiply charged anions (EDD) (Equation (50)).

$$[\mathrm{M}-n\mathrm{H}]^{n-}+\mathrm{e}^{-}_{\sim 20\ \mathrm{eV}}\rightarrow([\mathrm{M}-n\mathrm{H}]^{(n-1)-\cdot})_{\text{transient}}+2\mathrm{e}^{-}\rightarrow\text{fragments} \tag{50}$$

Many compounds such as glycosaminoglycans (GAGs), nucleic acids, acidic peptides, or peptides with acidic PTMs such as phosphorylation or sulfation do not readily form positive ions, especially in mixtures where ion formation is favored by the more basic mixture components. When positive ions can be formed, then the spectra are usually characterized by the abundant loss of the PTM (e.g., sulfate from GAG) or, in the case of oligonucleotides, a proton from the sugar–phosphate backbone.

However, these acidic compounds do readily form negative ions. Exposure of these anions to energetic electrons (~20 eV) is reported to produce a 'positive radical charge (hole)' which is exothermically neutralized by an electron.[97] For peptides, this results in $C_\alpha$–C bond cleavage, to form complementary $a^{\cdot}$ and $x$ fragment ions, with retention of the acidic PTM.[94,98] Thus like ECD, EDD can also cleave covalent bonds without affecting weaker noncovalent interactions. EDD has also been shown to preferentially cleave S–S and C–S bonds.[99] For GAGs, structurally informative glycosidic bond cleavages and cross ring cleavages can be generated without loss of the labile sulfate group.[100,101] and the glucuronic acid and iduronic acid epimers in heparan sulfate tetrasaccharides can also be distinguished.[102] EDD has also been used to partly characterize synthetic polyamidoamine dendrimers[103] and fragmentation was found to complement that obtained with CID. Complete sequences of short oligonucleotides of both DNA and RNA have been determined with EDD[104,105] and EDD may also be used to probe the tertiary structure of nucleic acid.[106]

#### 9.10.3.2.5 Electron transfer dissociation

With respect to peptide/protein sequencing, ECD has some very attractive features, producing random cleavages along the peptide backbone ($c$- and $z$-type ions) and at the same time preserving labile PTMs such as phosphorylation. Unfortunately, this technique is not readily transferable from FTICR instruments to the relatively low-cost and more common instruments that trap ions by RF electrostatic fields (QIT and LIT), where the bulk of this work is performed, as these analyzers are unable to trap the required dense cloud of thermal electrons. However, the Hunt group[107,108] have developed an alternative method of delivering electrons to multiply charged cations, using anion–cation interactions to effect ETD.

Radical cations ($M^{-\cdot}$) of a polyaromatic hydrocarbon, usually fluoranthrene, are generated by methane CI, externally to the trap.

$$C_{16}H_{10} + e^-_{\text{thermal}} \rightarrow C_{16}H_{10}{}^{-\cdot}\ (m/z\ 202) \tag{51}$$

These radical cations are then injected into the trap where they are mixed with the multiply charged peptide cations to which an electron is then transferred, leading to their direct dissociation into $c$- and $z$-type ions by the same mechanism responsible for ECD. The process is rapid (milliseconds) and quite compatible with the chromatographic timescale of LC–MS.

$$[M + 3H]^{3+} + C_{16}H_{10}{}^{-\cdot} \rightarrow [M + 3H]^{2+\cdot} + C_{16}H_{10} \tag{52}$$

$$[M + 3H]^{2+\cdot} \rightarrow [c + 2H]^{+} + [z + H]^{+\cdot} \tag{53}$$

ETD is also applicable to large intact proteins but the multiply charged fragments are difficult to interpret because of the limited resolving power of the Q traps. However, it is possible to deprotonate the multiply charged fragment ions and to reduce their charge by a further round of cation–anion interactions with even-electron benzoate anions.[108]

$$[M + 7H]^{7+} + 6C_6H_5COO^- \rightarrow [M + H]^{+} + 6C_6H_5COOH \tag{54}$$

More recently, it has been demonstrated that the reagent anions used for either ETD or proton transfer can be derived from the same neutral compound. The radical anions used for ETD, $[M]^{-\cdot}$, are converted into even-electron proton transfer reagent anions. $[M+H]^-$, by changing the potential on the methane CI source.[109] This voltage switch can be acheived in milliseconds allowing for rapid sequential ion–ion reactions and opens up the possibility of top-down sequencing of intact proteins in RF ion traps.

It is unusual for either CID or ETD to provide complete sequence information from any one peptide but the use of both techniques provides complementary information, which can greatly extend the sequence coverage (**Table 4**). In addition, because the energy from the ETD process is directed into cleaving the $C_\alpha$–N bond, the labile PTMs are preserved and their location in the peptide sequence can then be determined[90] (see also discussion in Section 9.10.3.2.6 on the use of CID/IRMPD and ECD/ETD for protein/peptide sequencing, and **Table 4**).

It should be noted that ETD is a relatively inefficient process for doubly protonated peptide precursors $[M + 2H]^{2+}$, which are the ions most commonly found in 'bottom-up' proteomics experiments. This situation may be retrieved, however, by using a supplemental low-energy CID method (ETciD) to target the nondissociated electron transfer (ET) product, $[M + 2H]^{2+\cdot}$. CID of the ET product then yields *c*- and *z*-type fragment ions. Swaney *et al.*[110] have reported that in a large-scale analysis of doubly charged tryptic peptides, the use of ETciD resulted in a median sequence coverage of 89% compared to 63 and 77% for ETD and CID, respectively.

#### 9.10.3.2.6 Combined use of dissociation techniques

In proteomics experiments, neither CID/IRMPD (*b*- and *y*-series ions) nor ECD/ETD (*c*- and *z*-series ions) fragmentation, when used on its own, is capable of generating a complete set of sequence ions from which an unambiguous primary structure of a peptide may be derived (IRMPD and ECD in FTICR MS,[86] CID and ETD in QIT and LIT,[90] CID and ETD in QToF[91]). Thus database searching, which is at the heart of MS/MS-based proteomics, is vulnerable to misidentification of peptides (false positives).[111] The respective characteristics of both these processes are summarized in **Table 4**.

In CID/IRMPD, the C–N bond is cleaved to generate the well-defined *b*- and *y*-series ions and, in ECD/ETD, the N–$C_\alpha$ bond is cleaved to generate the *c*- and *z*-series ions. However, the latter series is not so well defined as the masses of the *c* and *z* ions may be 1 Da lighter or heavier, respectively, due to hydrogen rearrangements.[112] The other important difference between these two processes is the retention of PTMs (phosphorylation of serine, threonine, and histidine, along with the N- and O-glycosylations) in ECD/ETD and the ability to distinguish the isomeric amino acids, leucine, and isoleucine.

On the basis of the complementarity of CID/IRMPD and ECD/ETD, Zubarev *et al.*[111] have concluded that *de novo* sequencing of peptides using these two fragmentation techniques in conjunction with high mass accuracy[113,114] can be achieved with >95% reliability. They have furthermore stated that it is

> . . . only de novo sequencing which can guarantee error-free sequence identification.

The complementarity of ECD/ETD has also been confirmed in a comprehensive comparison by Molina *et al.*[115] on some 19 000 peptides. They found that by combining the respective peptide fragmentation data they could achieve a 92% sequence coverage for an average tryptic peptide.

ECD may also be used in a complementary manner with the newly developed EDD technique. Although the fragmentation efficiency of EDD (average 3.6%) was low compared with ECD (average 15.7%), Kjeldsen *et al.*[116] have recently demonstrated that the combination of the two techniques could increase the overall amino acid sequence coverage of proteins and PTM characterization.

Further developments in the use of these complementary combinations of dissociation techniques will aid in generating a more comprehensive and reliable system of identifying and characterizing proteins and their PTMs. Such progress is likely to be based on a comprehensive understanding of gas-phase peptide chemistry and fragmentation.[117]

## 9.10.4 Experimental Use of Mass Spectrometry

Whether you are using MS for identification or quantification, it is important to first have as much information about the sample as possible, particularly the matrix, and whether the sample is a mixture or a pure compound, and to clearly identify the data that need to be obtained. This will influence decisions on

- type of instrument required (e.g., do you require exact mass data – high accuracy and resolution, or selected reaction monitoring (SRM) for a complex sample),
- method of presentation to the mass spectrometer (e.g., solids probe, GC, or LC),
- most appropriate method of ionization, and finally
- the scan mode to be used.

In this section, we will look briefly at factors to be considered in selecting an ionization method, the choice of a scan mode, how mass spectral data can be used to identify an unknown compound or a known compound, and the factors to be considered in setting up a quantitative mass spectral assay.

### 9.10.4.1 Spoilt for Choice – Which Ionization Method to Choose?

The general range of application for each of the ionization methods described above (Section 9.10.2.2) is illustrated in **Figure 9**. For low-molecular-weight samples (<∼1000 mass units) of moderate polarity, there will be several options. If analyte identification is required, then GC/MS will be a good option as the GC will permit high-resolution separation of mixture components and the use of EI will generate spectra that can be searched against large databases of EI spectra (e.g., NIST-Wiley). Also molecular weight can be confirmed by the use of CI. However, samples for GC/MS analysis will generally need to have polar functional groups (e.g., carboxylic acids, hydroxyls, amines) derivatized prior to analysis to improve volatility and thermal stability. There are a very large number of possibilities for derivatization and the reader is best referred to the very comprehensive literature that is available (e.g., Knapp,[21] Blau and Halket,[22] Halket and Zaikin,[23–27,118] Zaikin and Halket,[46,119]). Identification may be further aided by acquiring high-resolution, high mass accuracy data from which elemental formulas may be derived, particularly if constraints can be introduced with respect to the presence and number of particular elements (see Section 9.10.4.3.3).

If samples are to run without derivatization, then recourse may be had to the 'soft' liquid spray ionization processes, APCI, APPI, and ESI. ESI is the best choice for polar molecules (**Figure 9**) such as drugs and their metabolites and is by far the best choice of these three for peptides and proteins. At the relatively nonpolar end of the spectrum, APCI and APPI will be the preferred choice. However, APPI will have an advantage in terms of operability at low flow rates and its ready application to normal-phase chromatography and to lower polarity compounds than APCI. All three of these ionization methods produce molecular ions, and perhaps some adduct ions, yielding molecular weight information, but little fragmentation. In these cases, CID must be used in a tandem MS experiment to generate structurally informative fragmentation. Unfortunately, there is little in the

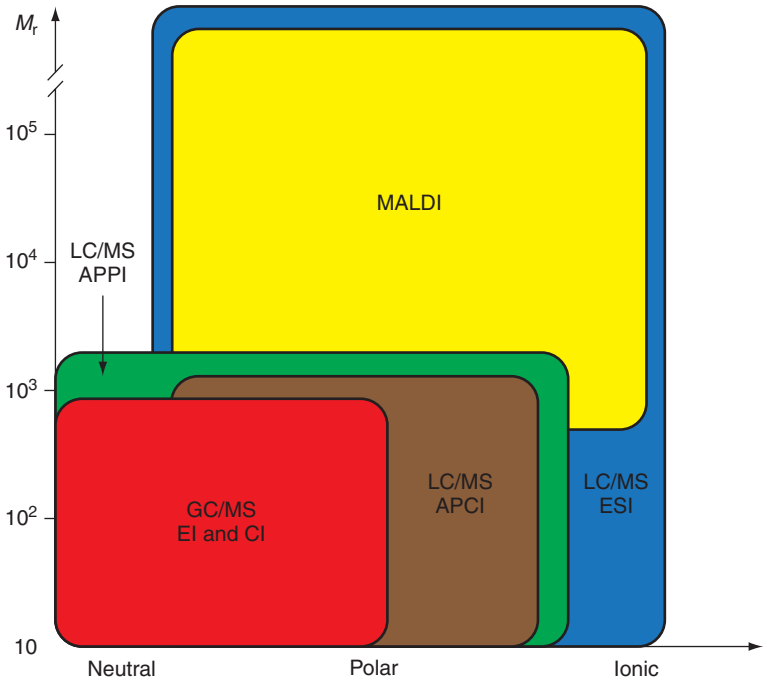


**Figure 9** Approximate ranges of analyte polarity and size that may be suited to different ionization techniques. With respect to the surface desorption techniques, DESI and DART, they are comparable in their range of application to ESI and APCI, respectively.

way of MS/MS libraries available for searching, and structural elucidation will have to rely on user-generated libraries and on an interpretation of the spectra from first principles.[5,31–33] Interpretation will be greatly assisted by the acquisition of high mass accuracy, high mass resolution data to generate elemental formulas (Section 9.10.4.3.3). It is worth noting that despite the very widespread use of tandem mass spectrometers, there are no standard conditions for the acquisition of MS/MS data (see Hopley *et al.*,[120] for a discussion on the attempts to develop tandem MS/MS libraries). This is because the amount of energy that can be put into the fragmentation process is dependent on both instrument design and the experimental conditions. For beam instruments (tandem-in-space), the variable experimental conditions will include the energy of the ions entering the collision cell, the collision gas (e.g., Ar, He, $N_2$), the pressure of the collision gas, and the dimensions of the collision cell. Similarly, for trap-type instruments, the extent of fragmentation will be dependent on the collision gas, energy of the ions, type of fragmentation (CID, PID, ECD, EDD, ETD), and duration of the process. This is in contrast to EI-generated spectra that are normally acquired with electrons of 70 eV energy. The induced EI fragmentation is readily reproduced across all brands of MS instruments with some variation in the intensity of fragment ions.

In summary, where samples require chromatography prior to MS, the separation technique as well as the size and polarity of the analyte will influence which ionization technique will be most appropriate. Thus GC/MS will use EI or CI and LC/MS will use ESI, APCI, APPI, or a combined source (e.g., APCI/APPI or ESI/APPI) to ionize the chromatographic eluant. In the case of LC/MS, the most effective form of ionization may not be easily predicted and some experimentation may be required.

For high-molecular-weight samples, most commonly proteins and peptides, but also polysaccharides and synthetic polymers, the choice of an ionization method will be limited to ESI (Section 9.10.2.2.4) and/or MALDI (Section 9.10.2.2.7) (see also **Table 5** for a comparison of ESI and MALDI). As mention above, MALDI is a solid-phase-based ionization technique and ESI is a flow-based liquid technique. Both readily generate

**Table 5** Comparison of ESI-MS with MALDI-MS

| Advantages of ESI-MS | Advantages of MALDI-MS |
|---|---|
| • Typical sensitivity in the range of femtomole to low picomole or attomole concentration. Best sensitivity combining capillary LC and nano-ESI.<br>• Can be readily interfaced to LC outlet, permitting multidimensional chromatography (MuDPIT analysis of whole proteomes).<br>• Desalting and sample cleanup can be performed online.<br>• Soft ionization with little fragmentation; however, labile posttranslational modifications such as phosphates are often lost.<br>• Soft ionization permits observation of noncovalently bound protein complexes.<br>• Multiple charging of proteins and peptides permits analysis of high-mass ions on low-mass range analyzers.<br>• Multicharged ions fragment more efficiently in CID than singly charged ions | • Typical sensitivity in the range of femtomole to low picomole or attomole concentration.<br>• Sample analysis is very rapid – a few seconds to analyze mixture of peptides.<br>• Sample can be stored and reanalyzed at leisure.<br>• Sample may be further purified *in situ* if required.<br>• Soft ionization with little fragmentation. Phosphate groups may be retained at very low laser power.<br>• Proteins and peptides usually ionized with a single charge simplifying interpretation.<br>• High practical mass limit but at low-resolution. |
| **Disadvantages of ESI-MS** | **Disadvantages of MALDI-MS** |
| • Sample injected onto LC column, or directly injected into source, is totally consumed.<br>• Multiple charging of proteins and peptides complicates interpretation of MS and MS/MS data.<br>• Mixture analysis requires use of LC interface to minimize problems of ion suppression.<br>• Gradient chromatography of a single sample can require 10 s or minutes to hours to complete. | • Intense matrix background below ~800 Da.<br>• Can only be interfaced with LC in an off-line mode.<br>• Cannot analyze noncovalently bound protein complexes.<br>• High-throughput productivity requires automation of sample preparation.<br>• Reflectron required for good mass resolution. |

These are complementary techniques and while many analytes, including proteins and peptides, may be equally well ionized by either method, some will only be ionizable by ESI and not MALDI and *vice versa*.

gas-phase ions, with MALDI-generated ions being singly charged and ESI-generated ions carrying multiple charges. Samples for ESI are readily, and conveniently, analyzed in an online mode accepting the separated analytes from an interfaced LC column. However, this means that the MS analysis must be completed in the time it takes to elute each individual component. In very complex samples, where separation is incomplete, analysis must be completed very quickly and it is possible that minor components, or poorly ionized components, may not be analyzed at all. It should be noted that capillary LC while yielding enhanced chromatographic separation also results in narrower chromatographic peaks and a requirement for even faster MS analysis particularly where quantification is desired. MALDI, on the other hand, is not readily interfaced with chromatography and is usually performed off-line in conjunction with an automated plate spotter, yielding highly reproducible mixtures of sample and matrix and consequently very consistent high-quality MALDI spectra. However, the size of the fractions collected compromises, to some extent, the chromatographic separation but this disadvantage is offset by the ability to archive the samples stored on the MALDI target so that the MS analysis can be repeated at leisure. When coupled with an automated off-line plate spotter, MALDI is faster than ESI and is often used for high-throughout proteomic analysis.

Spectra generated by ESI are more complex than MALDI because of the multicharging phenomena. However, multiply charged ions are more amenable to CID because the coulombic repulsion of like charges aids the fragmentation process. CID of MALDI-generated singly charged ions lack this advantage. As the size of the analyte ions increases, the efficiency of CID diminishes, as there is a corresponding greater capacity for the ion to absorb and redistribute the impact energy. Nevertheless, this has proven to be a very effective method of amino acid sequencing for 'bottom-up' proteomics on peptides (typically 800–5000 Da) from trypsin digests.

In general, MALDI and ESI are of comparable sensitivity (femtomolar to low picomolar levels of peptides/proteins); however, it is impossible to make definitive comparisons for two reasons. First, there have been, and continue to be, technological advances improving the sensitivity of both techniques whereby, for example, the use of special hydrophobic surfaces on MALDI targets has been matched by the development of nano-ESI. Second, it has been observed that in complex proteomic analyses, perhaps only 30–50% of all proteins are adequately ionized by both ESI and MALDI, with the remainder being best ionized by either ESI or MALDI alone. Thus there is a good case to be made for the use of both techniques in a comprehensive proteomic analysis (**Table 5**).

### 9.10.4.2 MS Scan Modes

#### *9.10.4.2.1 Single MS analyzer (nontrapping) scan modes*

In the case of beam-type mass analyzers (B, BE, Q, ToF, and hybrids), the analyzer is commonly operated to scan over a defined mass range, generating a mass spectrum of all ions generated in the ion source. This is often referred to as a full scan (**Figure 10(a)**). Alternatively, the Q, B, or BE analyzers can be set to pass a selected ion or a selected series of ions (**Figure 10(b)**). This is known as SIM. This scan mode is commonly used for single Q analyzers (Section 9.10.2.3.3) because they can be rapidly switched between different ions over a large mass range.

The SIM mode is designed to enhance the sensitivity of an assay by concentrating the analyzer time onto only the ions of interest. For example, if instead of scanning a mass range of 500, the analyzer is set to monitor just 5 $m/z$ values, then the number of ions counted in each of those channels will be 100 times that observed in the scanning mode. This improvement in ion statistics translates directly into improved sensitivity; however, this must be offset against the loss of a great deal of analytical information. It should also be noted that SIM is inappropriate for ToF analyzers because instead of scanning, they sample the entire mass range at any one time (Section 9.10.2.3.7). However, postacquisition processing of ToF data can be used to extract the time-based intensity trace for any of the ions in the mass range monitored. SIM is also problematic for B analyzers except over a narrow mass range; however, a double-focusing instrument (BE or EB) (Section 9.10.2.3.2) does have the possibility to further enhance selectivity by performing SIM with high mass resolution, as does the more common ToF analyzer.

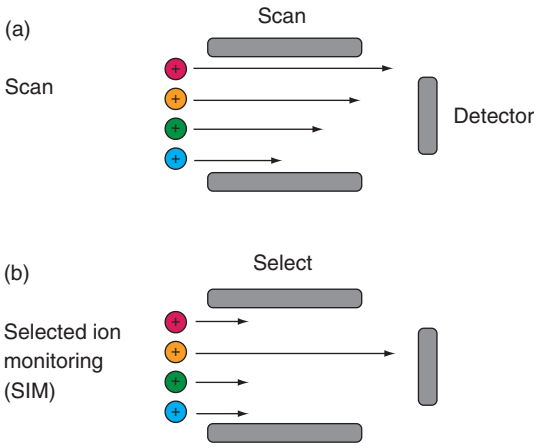


**Figure 10** Scan modes for a single beam-type analyzer (e.g., Q, B, E). (a) Full scan. (b) Selected ion monitoring scan, commonly used in quantitative work to improve assay sensitivity.

#### *9.10.4.2.2 Tandem MS scan modes*

There are five main scan modes possible using MS/MS and these will be described and illustrated using the QqQ as an example (**Figures 7(a)–7(e)**). Double-focusing BE or EB instruments are also capable of tandem MS using linked scans to monitor ion transitions; however, they suffer from the disadvantage of having to either select ions with low mass resolution or detect ions with low mass resolution. Consequently, these instruments are rarely used today for tandem MS (see Gross,[33] for further discussion).

The first scan type to consider is the full scan of all the ions generated in the ion source using no mass selection. This is done by setting both $Q_1$ and $Q_2$ to pass all ions (RF-only mode) through to $Q_3$, which is then scanned in the normal way (**Figure 7(a)**) to generate a spectrum of ions present in the source.

The product ion scan entails the mass selection of a precursor ion in the first stage ($Q_1$), fragmentation (CID or ETD) in the collision cell, and then mass analysis of all resultant fragment masses in the second stage of mass analysis ($Q_3$) (**Figure 7(b)**). This experiment can be performed by beam (tandem-in-space) or trap (tandem-in-time) instruments. It is commonly performed to identify transitions used for quantification by tandem MS or as part of an exercise in structural elucidation.

In the precursor ion scan, the first mass analyzer ($Q_1$) sequentially scans all precursor ions into the collision cell (**Figure 7(c)**) for fragmentation. The second analyzer ($Q_3$) is then set to transmit a single specified ion product. The resulting mass spectrum is then a record of all the precursor ions that give rise to the specified common product ion, such as, for example, the metabolites of a particular drug, or class of compounds, which can be fragmented to a common structural moiety. The precursor ion scan can be carried out only with tandem-in-space instruments.

For the neutral loss scan, the first mass analyzer ($Q_1$) scans all the masses (**Figure 7(d)**). The second mass analyzer ($Q_3$) also scans, but at a fixed offset from the first mass analyzer. This offset corresponds to a neutral loss that is commonly observed for a particular class of compounds; for example, the loss of 44 u ($CO_2$) from $[M-H]^-$ ions will be indicative of carboxylic acids. Alkyl loss ($C_nH_{2n+1}$) will be seen in the loss of 15, 29, or 43, etc. and the loss of 18 u ($H_2O$) will be indicative of a primary alcohol. A comprehensive table of common neutral fragments may be found in McLafferty and Tureček.[32] The mass spectrum is then a record of all precursor ions that lose the specified neutral fragment. Again, neutral loss scans cannot be performed with trap-type MS instruments or with ToF analyzers. However, postacquisition analysis software can be used to search for the specified neutral loss.

SRM is a version of the product ion scan and is used in experiments designed to identify and quantify targeted analytes (**Figure 7(e)**). Both mass analyzers, $Q_1$ and $Q_3$, are set to pass predetermined masses. These correspond, first, to a specific precursor ion ($Q_1$) and, second, to a fragmentation or transition ($Q_3$) that is characteristic of the selected analyte. Typically, the MS will be rapidly switched between several sets of such transitions representing different analytes, internal standards (ISs), or possibly an alternative confirmatory

transition. Thus SRM adds a considerable degree of selectivity to an assay in that the fragmentation monitored is specific to the target analyte and is unlikely to also occur with any background chemical noise that is also selected by $Q_1$. If the first mass analyzer can be operated with high mass accuracy and high mass resolution, this will further enhance selectivity. Sensitivity in SRM is also concomitantly improved, because by removing all the background chemical noise, the S/N of the monitored ion is improved. SRM may be performed by both tandem-in-space and trap-type instruments.

### 9.10.4.3 Identification – Unknown Small Molecules

Identification or structural elucidation of an unknown compound is one of the most challenging tasks that can be undertaken by an analytical chemist. Where the analyst has milligram or more amounts of the unknown, MS is often used in conjunction with other techniques such as nuclear magnetic resonance (NMR) and IR spectroscopy. However, when there are only limited quantities of sample, the sensitivity of MS makes this the technique of choice for assembling structural information and, where no definitive conclusion can be reached on the mass spectral data alone, serves to limit the search to a particular class of chemicals or set of isomers.

#### *9.10.4.3.1 An LC/MS approach*

A useful first step is to analyze the sample using LC interfaced to ESI or APCI on a tandem mass spectrometer capable of accurate mass measurement at high resolution. The LC will serve to separate the unknown away from the matrix components and will reduce the potential for ion suppression. A short linear gradient of acetonitrile against 0.05 mol $l^{-1}$ ammonium acetate on a reverse-phase C-18 column represents a good starting point (see, e.g., Eckers *et al.*,[121] Arthur *et al.*,[122] Tozuka *et al.*,[123] and Wolff *et al.*[124]).

Spectra obtained from ESI or APCI will generally yield molecular ions of the type $[M+H]^+$ and little, if any, fragmentation. However, fragmentation can be induced by CID (Section 9.10.3.2.1) followed by an MS/MS analysis of the product ions (Section 9.10.4.2.2). High mass accuracy/high mass resolution measurement of the molecular ion can, with appropriate constraints, generate an elemental formula (see discussion in Section 9.10.4.3.3).

The MS/MS analysis of the molecular ion will also yield a structurally informative set of fragment ions. Again, if exact mass data can be obtained for these, a further set of elemental formulas may be obtained. Unfortunately, because there are only limited collections of library spectra generated by MS/MS (see Section 9.10.3.2), the experimenter will generally have to resort directly to a first-principles interpretation.

Considerable structural information is to be found in the fragmentation patterns of gas-phase ions. Although this discussion is often held in the context of EI-generated spectra, it is important to remember that the reactions of gas-phase ions are not dependent on their method of formation but rather on their intrinsic structural properties and their internal energy. Thus structural information can be obtained from fragmentation that is induced by a high-energy ionization process, such as EI, as well as from collisionally induced fragmentation of a $[M+H]^+$ ion that may have been generated by a 'soft' ionization process. Instructive examples of structural elucidation of drug metabolites using $MS^n$ fragmentation trees and exact mass data are described by Eckers *et al.*,[121] Arthur *et al.*,[122] Tozuka *et al.*,[123] and Wolff *et al.*[124] and of complex lipids are described by Hsu and Turk.[125,126] In brief, the drugs and their metabolites are exhaustively fragmented and the fragments compared to locate the biologically induced structural changes – for example, oxidations, cleavages, alkylations, and conjugations. The relationship between the product ions and the precursor ions, and their elemental composition are key elements in assembling the structural features of the unknowns. One must also be aware of the possibility of isomers and the use of an appropriate separation technique may be required in addition to the MS and $MS^n$ data.

#### *9.10.4.3.2 GC/MS approach*

If the unknown is sufficiently volatile or can be made volatile by derivatization, then the LC/MS approach can be complemented by the use of GC/MS. A useful starting point in this regard is to make a trimethylsilyl derivative. Silylation is applicable to a wide range of nonsterically hindered functional groups, including alcohols, phenols, thiols, amines, oximes, and carboxylic acids (**Table 6**).[22,127] The dried sample (1 μg

**Table 6** Trimethylsilylation reagents

| *Silylation reagent* | *Abbreviation* |
|---|---|
| *Strong silyl donors* | |
| *N*,*O*-Bis(trimethylsilyl)acetamide | BSA |
| *N*,*O*-Bis(trimethylsilyl)trifluoroacetamide | BSTFA |
| *N*-Methyl-*N*-trimethylsilyltrifluoroacetamide | MSTFA |
| *Moderate strength silyl donors* | |
| Trimethylsilyldiethylamine | TMSDEA |
| *Weak selective donors* | |
| Trimethylimidazole (hydroxyl groups) | TMSIM |
| Hexamethyldisilazane (hydroxyl groups) | HMDS |
| Trimethylchlorosilane (hydroxyl groups) | TMCS |

A range of reagents, with differing degrees of reactivity, are commonly available to make trimethylsilyl (TMS) derivatives. The silylating potential can be increased by the choice of an appropriate solvent (e.g., pyridine, DMF, acetonitrile) or by the addition of a catalyst (e.g., 1–20% TMCS).[22,127]

maximum) is dissolved in pyridine (10 µl) to which is added an equal volume of a strong silylation reagent such as *N*,*O*-bis(trimethylsilyl)trifluoroacetamide (BSTFA) plus 1% trimethylchlorosilane (TMCS) or *N*-methyl-*N*-trimethylsilyltrifluoracetamide (MSTFA). It is important that the silylation reagent is present in an excess of at least 2:1 molar ratio to active hydrogens and that the sample is dry. Unhindered moieties will be quickly silylated but derivatization times and the need for heat vary widely depending on the degree of steric hindrance but unless determined otherwise, heating at 70 °C for 20–30 min will ensure the reaction is driven to completion for most active hydrogens. A variation on this approach, widely used in metabolomics experiments where a large range of chemical classes need to be derivatized, is to initially protect any carbonyl moieties by methyloximation (10 µl of a 20 mg ml$^{-1}$ solution of methoxyamine HCl in pyridine at 40 °C for 90 min) (see, e.g., Fiehn[128]). The silylation reagent can then be directly added at the end of the methoximation reaction. After silylation, the sample may be injected onto a general purpose capillary column such as one coated with 5% phenyl-95% methylpolysiloxane. The column temperature is then increased to drive off the less volatile components. Although silylation is a good general derivatization reaction, it should be remembered that there are many other possibilities available, especially if a particular class of analyte is being assayed (e.g., Knapp,[21] Blau and Halket,[22] Halket and Zaikin,[23–37] Zaikin and Halket[46,119]). If assay sensitivity is important then derivatization with electron-capturing groups for ECI should be considered (Section 9.10.2.2.2).

The advantage of GC/MS over LC/MS is that extensive libraries of EI data are available for searching (see Section 9.10.4.3.4). Where necessary, this can be complemented by molecular weight data from CI. Library identification then requires confirmation by comparing the column retention time and MS and MS$^n$ data with that of a standard. If no library match is found, then a similar process of determining elemental formulas (see Section 9.10.4.3.3) and interpretation of the fragmentation data from first principles must be followed (see Section 9.10.4.3.4).

A more sophisticated method of comparing retention times, and one that is applicable across different column phases and temperature programs, is by way of retention time indices or Kovát's indices (KIs).[129] The KI for a particular analyte is calculated against a homologous series of *n*-alkanes, coinjected with the sample.

$$\mathrm{KI} = 100n + \frac{100(t_x - t_n)}{(t_{n+1} - t_n)} \tag{55}$$

where $n$ is the number of carbon atoms in the *n*-alkane standard that elutes immediately prior to the analyte of interest, $t_x$ is the retention time of the analyte, $t_n$ is the retention time of the *n*-alkane standard that elutes immediately prior to the analyte of interest, and $t_{n+1}$ is the retention time of the *n*-alkane standard that elutes immediately after the analyte of interest.

Thus in metabolomic experiments, the KI for individual metabolites is an important piece of confirmatory information where the mass spectral differences between isomers are minimal or nonexistent (**Figure 11**). Unfortunately, no such comparative set of indices are available for LC.

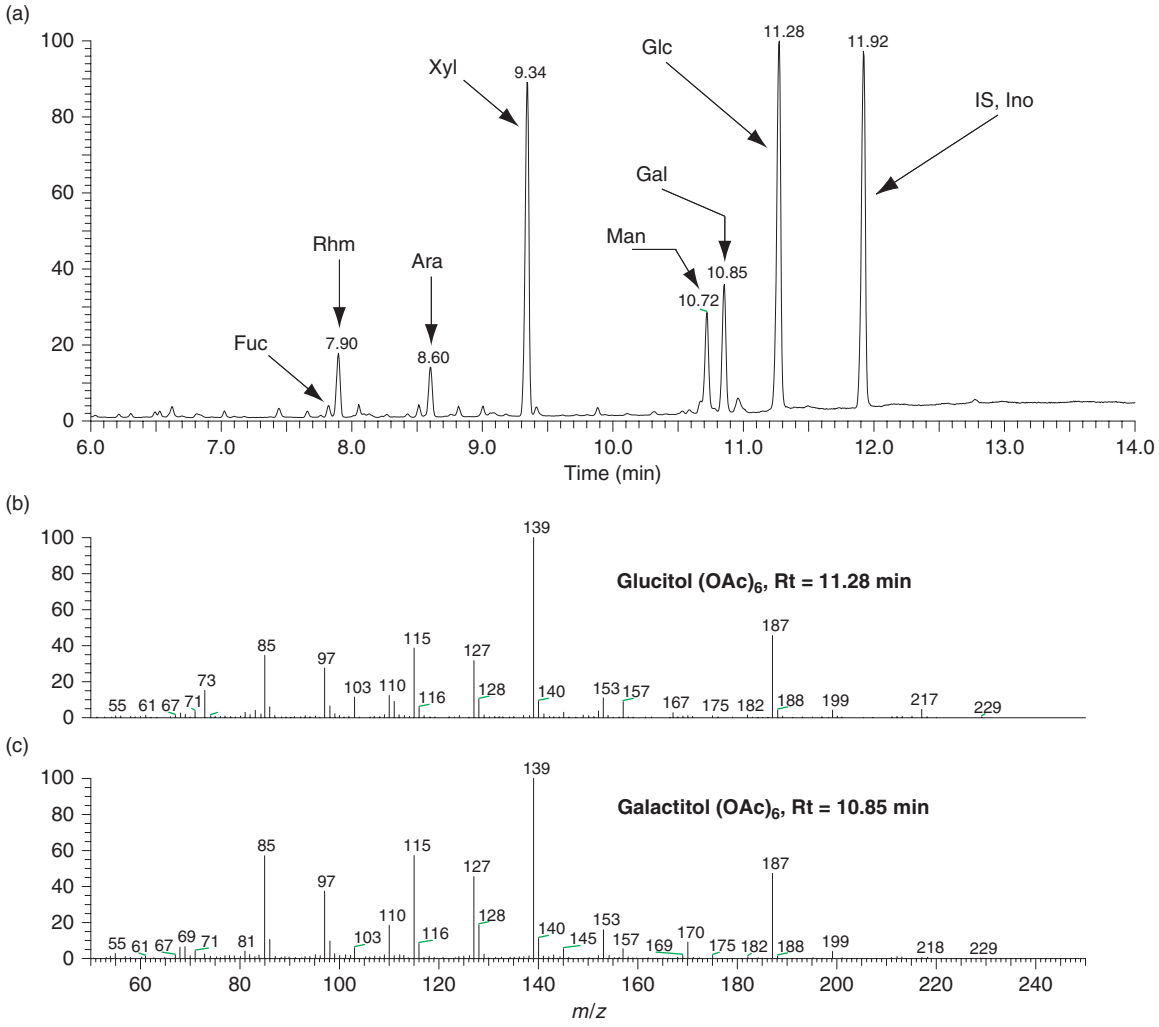


**Figure 11** GC/MS assay of alditol hexa-acetates quantified against inositol internal standard (IS). (a) In the chromatogram shown here the monosaccharides making up a plant cell wall are being quantified as their alditol acetates, using inositol (Ino) as the (IS). The GC separation of these reduced sugars is essential for their identification. The mass spectra of the alditol acetates of the hexoses, glucose (Glc) (b), galactose (Gal) (c), and mannose (Man), are essentially identical, as are the mass spectra of the alditol acetates of the pentoses, xylose (Xyl) and arabinose (Ara), and the deoxysugars, rhamnose (Rhm) and fucose (Fuc).

### *9.10.4.3.3 Determination of elemental formula*

Accurate mass data can be a significant aid in identifying compounds as it can yield the elemental composition of the molecular ion and the associated fragment ions.[130] The theoretical mass of a compound can be readily calculated from tables of elemental masses (**Table 7**) and there are software packages to automate this procedure. Although it is possible to accurately measure mass at low-resolution, the analyst runs the risk of including extraneous isobaric ions in the measurement. This will result in the mass measurement being skewed or shifted by the interfering ion(s) producing an erroneous elemental formula.[131] Note that as higher mass ions are analyzed, the number of possible elemental formula consistent with the measured mass also increases along with the requirement to resolve away isobaric ions. This situation is nicely summarized by the editor of the *JASMS*[132] in the journal's guidance on the use of accurate mass data:

> When valence rules and candidate compositions encompassing $C_{0\text{-}100}$, $H_{3\text{-}74}$, $O_{0\text{-}4}$, and $N_{0\text{-}4}$ are considered at nominal parent mass 118, there are no candidate formulae closer together than 34 ppm. At nominal parent mass 500, there are

**Table 7** Stable isotopic masses and abundances[a]

| *Isotope* | *Mass (u)* | *Natural abundance (%)* |
|---|---|---|
| $^{1}H$ | 1.007 825 031 9(6)[b] | 99.988 5(70)[b] |
| $^{2}H$ | 2.014 101 777 9(6) | 0.011 5(70) |
| $^{12}C$ | 12 (exactly, by definition)[c] | 98.93(8) |
| $^{13}C$ | 13.003 354 838(5) | 1.07(8) |
| $^{14}N$ | 14.003 074 007 4(18) | 99.636(20) |
| $^{15}N$ | 15.000 108 973(12) | 0.364(20) |
| $^{16}O$ | 15.994 914 622 3(25) | 99.757(16) |
| $^{17}O$ | 16.999 131 50(22) | 0.038(1) |
| $^{18}O$ | 17.999 160 4(9) | 0.205(14) |
| $^{19}F$ | 18.998 403 20(7) | 100 |
| $^{23}Na$ | 22.989 769 66(26) | 100 |
| $^{28}Si$ | 27.976 926 49(22) | 92.223(19) |
| $^{29}Si$ | 28.976 494 68(22) | 4.685(8) |
| $^{30}Si$ | 29.973 770 18(22) | 3.092(11) |
| $^{31}P$ | 30.973 761 49(27) | 100 |
| $^{32}S$ | 31.972 070 73(15) | 94.99(26) |
| $^{33}S$ | 32.971 458 54(15) | 0.75(2) |
| $^{34}S$ | 33.967 866 87(14) | 4.25(24) |
| $^{36}S$ | 35.967 080 88(25) | 0.01(1) |
| $^{35}Cl$ | 34.968 852 71(4) | 75.76(10) |
| $^{37}Cl$ | 36.965 902 60(5) | 24.24(10) |
| $^{39}K$ | 38.963 7069(3) | 93.258 1(44) |
| $^{40}K$ | 39.963 998 67(29) | 0.011 7(1) |
| $^{41}K$ | 40.961 825 97(28) | 6.730 2(44) |
| $^{79}Br$ | 78.918 337 9(20) | 50.69(7) |
| $^{81}Br$ | 80.916 291(3) | 49.31(7) |
| Electron ($e^{-}$)[d] | $5.485\,799\,09(27) \times 10^{-4}$ | – |
| Proton ($H^{+}$)[d] | 1.007 276 452 | – |

[a] Data are derived from an IUPAC Technical Report by deLaeter *et al*.[133]
[b] The (±) uncertainty of the measurement is indicated in parentheseis.
[c] In mass spectrometry, the unit of measurement is the unified atomic mass unit (u), which is defined as 1/12 the mass of a $^{12}C$ atom ($1\ u = 1.660\,540\,29 \times 10^{-27}$ kg).
[d] The very high mass resolution and accuracy that are available from BE, EB, FTICR, Orbitraps, and ToF analyzers mean that calculations of exact masses need to also account for electrons in the analyte ion.[134,135] Thus, for example, an electron is lost in the formation of a radical cation ($M^{+\cdot}$) and a protonated molecule ($[M+H]^{+}$) gains a proton not a hydrogen atom ($\Delta m = 1\ e^{-}$). An electron is gained in the formation of a radical anion ($M^{-\cdot}$) and a deprotonated molecule ($[M-H]^{-}$) loses a proton not a hydrogen atom. While this error will be insignificant for large molecules such as proteins, for small molecules, the error can be as large as several ppm. For example, ignoring the mass of three electrons in triply charged GluFib, $[M+3H]^{3+}$, leads to an error of 1 ppm in the exact mass calculation.[134]

These are the isotopes most commonly encountered in natural product chemistry. Silica is encountered as a generic derivative for GC (e.g., trimethylsilyl and *tert*-butyldimethylsilyl derivatives).

five compositions that have a neighbouring candidate less than 5 ppm away. Using $C_{0\text{-}100}$, $H_{25\text{-}110}$, $O_{0\text{-}15}$, and $N_{0\text{-}15}$ at mass 750.4, there are 626 candidate formulae that have a neighbouring possibility less than 5 ppm away. Thus, for a measurement at $m/z$ 118, an error of only 34 ppm uniquely defines a particular formula. At $m/z$ 750.4 an error of 0.018 ppm would be required to eliminate all extraneous possibilities.

In practice, it is important to be able to restrict the type and number of elements in any possible formula so as to improve the degree of confidence in selecting the most appropriate formula and to eliminate impossible or unlikely combinations of elements. Further information to help with this may be gleaned from an examination of the isotope pattern of the molecular ion. Most of the elements present in organic compounds (C, H, N, O, P, and S; Si must obviously be included if silyl derivatives were used for GC/MS) have two or more stable isotopes (**Table 7**). This information can be used, for example, to estimate the number of carbons present in an

unknown from knowing that the $^{13}C$ isotope has an abundance equal to 1.1% that of the $^{12}C$ isotope. Thus an ion containing 10 carbons will have a $^{13}C$ abundance ratio of 11% and by extension an ion containing 20 carbons will have a $^{13}C$ abundance ratio of 22%. A number of other elements such as chlorine ($^{35}Cl$:$^{37}Cl$, 1:3), bromine ($^{79}Br$:$^{81}Br$, 1:1), sulfur ($^{32}S$:$^{33}S$:$^{34}S$: 100:1:5), and silicon ($^{28}Si$:$^{29}Si$:$^{30}Si$, 100:5:3) also have distinctive isotope patterns, recognition of which will aid in restricting the possible elemental formula of the unknown (for further discussion, see McLafferty and Tureček,[32] Gross,[33] and Watson and Sparkman[5]). Algorithms such as that described by Pickup and McPherson[136] and Hsu[137] can be used to model isotope distributions in elemental formulas and the comparison between the experimental and theoretical isotopic distribution can be assigned a goodness-of-fit score.

Further constraints may be identified by application of the nitrogen rule,[5,32,33] which states that a compound containing the common elements, C, H, O, S, Si, P, and the halogens, will have an odd nominal molecular weight if it contains an odd number of nitrogens. A compound with zero or an even number of nitrogen atoms will have an even nominal molecular weight. This is because every element with an odd mass has an odd valence and every element with an even mass has an even valence, with nitrogen being an exception, having an odd valence and an even mass.

In addition, a consideration of the valency of the constituent elements leads to the derivation of a general algorithm for the number of rings and double bonds (R + DB) present in an ion.[32,33,138] Thus, for the elemental formula $C_cH_hN_nO_o$

$$(R + DB) = c - 0.5h + 0.5n + 1 \tag{56}$$

Other monovalent elements (F, Cl, Br, and I) are counted as hydrogens, trivalent elements (P) are counted as nitrogen, and tetravalent elements (Si) are included with carbon. For chemically possible formulae, $r + db > -1.5$. Odd-electron ions ($M^{+\cdot}$) will have an integer value and even-electron ions will have 0.5 $r + db$ more than expected, so round up to next lowest integer.[32,33] By way of example, Kind and Fiehn[139] have described an integrated application of accurate mass data to metabolite identification, constrained by isotope abundance information and valence rules, in addition to the KI (Section 9.10.4.3.2).

In the ideal case, the high mass accuracy and high mass resolution determination of the molecular ion will yield an unambiguous formula but this says nothing about the connectivity of the constituent atoms. For the trivial case of $C_2H_6O$, the exact mass is 46.041 864 8 but this does not distinguish ethanol ($CH_3CH_2OH$) from dimethyl ether ($CH_3OCH_3$). However, fragmentation occurs in a mostly predictable fashion and an examination of the molecular ion fragments will often reveal a distinctive 'fingerprint' including structurally diagnostic ions ($m/z$ 31 for ethanol and $m/z$ 29 for dimethyl ether).

#### 9.10.4.3.4 Database searching and interpretation of fragmentation from first principles

For the EI spectra of unknowns, a very valuable first step toward identification is to perform a simple spectral comparison with an EI library. As noted above, EI spectra (Section 9.10.2.2.1) are highly reproducible and are not instrument dependent. The widely available NIST-Wiley Library, for example, contains several hundred thousand spectra. A satisfactory match of the unknown and reference spectra can be confirmed experimentally against a reference standard. However, it should be noted that the EI mass spectra of stereoisomers and geometric isomers are often very similar, exhibiting the same fragmentation pattern and similar abundances of fragments. This can be seen, for example, in the spectra of glucitol hexaacetate and galactitol hexaacetate (**Figures 11(b) and (c)**). In these cases, the ambiguity of the MS identification can be overcome by a comparison of the GC retention times (Rt) (**Figure 11(a)**) (the use of KIs is described in Section 9.10.4.3.2). Judicious selection of the phase coating the inside of the capillary column (a wide range of different chemistries and polarities are available) that is interfaced with the MS instrument will permit the separation of many of these stereoisomers and geometric isomers. An alternative approach is to make a chemical derivative that the MS can distinguish. For example, mass spectra of fatty acid methyl esters (FAMEs) containing two double bonds are essentially identical regardless of the location of the double bond; however, if instead a dimethyloxazoline derivative is made, the location of the double bond can be readily determined (**Figure 12**).

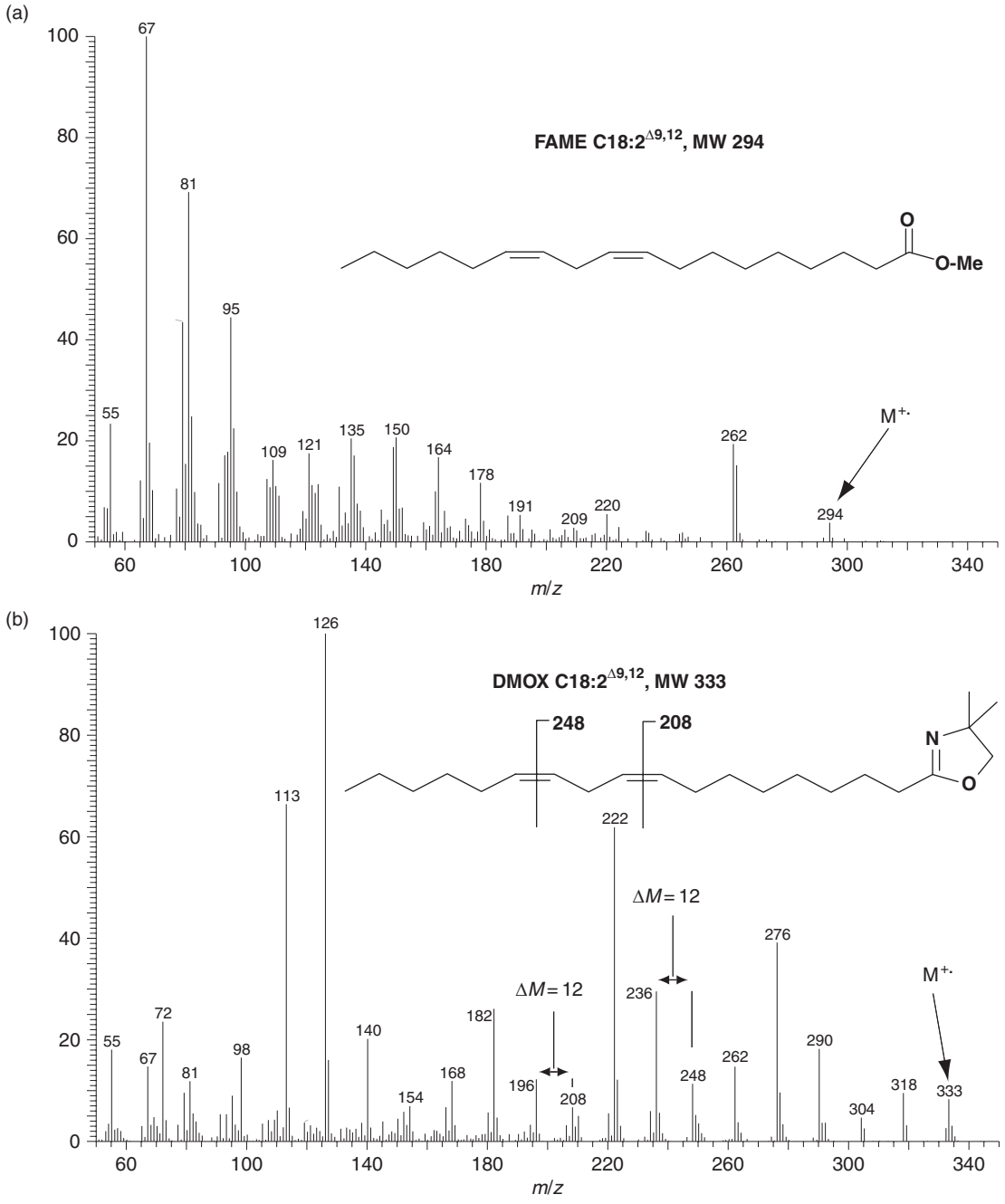


**Figure 12** The mass spectrum of the fatty acid methyl ester (FAME) of linolenic acid (C18:2$^{\Delta 9,12}$) contains no readily discernable structural information beyond the molecular ion (a). However, the dimethyloxazoline (DMOX) derivative, in which the charge is retained by the heterocyclic ring, can undergo charge remote fragmentation yielding a mass spectrum from which the location of the double bonds, but not their geometry (*cis* versus *trans*), can be readily determined (b). The latter stereochemistry can usually be distinguished by the GC retention time on an appropriate column.

Where no satisfactory comparable spectra can be found by a database search, the more laborious process of interpreting the spectra from first principles must be attempted. As mention before, this process will be considerably aided if elemental compositions of the molecular ion and the EI fragments are available.

Much effort has been expended on providing rational mechanisms for fragmentation and these are well summarized by, for example, Budzikiewicz *et al.*,[31] McLafferty and Tureček,[32] Gross,[33] de Hoffmann and Stroobant[34], and Watson and Sparkman.[5] In EI, an odd-electron ion ($M^{+\cdot}$) is generated and the subsequent bond cleavages that follow result in the formation of the most stable cation with paired electrons (even-electron ion). The soft ionization techniques such as CI, ESI, APCI, and MALDI produce molecular species by the addition or abstraction of a proton, yielding an ion with an even number of electrons (e.g., $[M+H]^+$). These ions are more stable than radical cations and their fragmentation is more likely to reflect steric effects, so isomers with essentially identical EI spectra often give rise to different soft ionization spectra and may fragment differently following CID.[32]

A comprehensive description of these processes is beyond the scope of this chapter and the reader is referred to one of many texts on the interpretation of fragmentation and to tables of common neutral losses and of common ion series for particular classes of compounds (see, e.g., Budzikiewicz *et al.*,[31] McLafferty and Tureček,[32] Gross,[33] de Hoffmann and Stroobant,[34] Dass,[140] and Watson and Sparkman[5]).

As mentioned above, mass spectral interpretation will be greatly aided if high mass accuracy data at high mass resolution are available to determine the elemental formula of the unknown and its fragments. Also there is increasing use of gas-phase ion/molecule reactions that can be exploited for class and functional group identification.[141]

### 9.10.4.4 Criteria for Identification of a Known Compound

Forensic laboratories and regulatory authorities responsible for the quality of food, drugs, and environmental pollution are major users, directly and indirectly, of MS for the purpose of identification and quantification. The major question they face is: How much information is required to support their claim, within the specified confidence limits, for the presence of known specified compounds in their samples? This is not an easy question to answer and is usually dealt with by defining the core analytical technology and a set of minimal performance criteria for acceptable identification and by reserving the right to assess methods on a case-by-case basis. While there may be a general consensus on the broad issues of what is required for confirmation of identity, there is no general agreement on specifics and a number of different approaches and specific requirements are used around the world. By way of example, we will look at the requirements of two such regulatory authorities, the US Food and Drug Administration (FDA) and the European Union (EU), with respect to residues of banned substances, mostly veterinary drugs, in animal products. The identification criteria set by both these regulatory authorities are quite stringent and similar types of criteria are also required for other regulatory authorities and also by editors of research journals.

In addition to the mass spectral aspects of these assays, which are outlined below, there may also be extensive requirements to be met by the analyst with respect to compliance with good laboratory practice, which governs the operations of analytical laboratories and includes sampling regimes, assay validation procedures (e.g., limits of detection, limits of quantification, accuracy, reproducibility, and ruggedness), and laboratory accreditation (e.g., staff training, laboratory equipment, documentation, quality assurance, and quality control).[142–145]

#### *9.10.4.4.1 FDA Guidance for Industry 118*

In its Guidance for Industry 118,[144] the FDA requires that methods for confirmation of identity include the use of a

- comparison standard,
- chromatography interfaced to MS (GC/MS or LC/MS), and
- mass spectral matching.

The use of a standard is a fairly obvious requirement but where matrix effects alter either the chromatography or the spectrum, the authority will allow the use of a control extract spiked with the standard instead of using a pure standard. However, the analyst must then be able to demonstrate the absence of interference in a control extract containing no standard.

The FDA asks that the use of MS be combined with chromatography but specifications are only listed for GC/MS and LC/MS. The omission of interfaces such as CE/MS SFC/MS is a reflection of the conservative

**Table 8** FDA criteria for mass spectral matching

| *MS scan* | *Requirements* |
|---|---|
| Full scan | |
| | • At least three structurally specific ions that completely define the molecule are present above a specified level. |
| | • General correspondence between relative abundance of sample and standard ions (within the range of ±20%). |
| | • Prominent ions, not from analyte, can be explained. |
| SIM | |
| | • Relative abundance of three structurally specific ions of sample and standard should be within ±10%. |
| | • Relative abundance of four or more structurally specific ions of sample and standard should be within ±15%. |
| $MS^n$ full scan | |
| | • All structurally specific ions present in standard spectra should be present in sample spectra. |
| | • General correspondence between relative abundance of sample and standard ions (within the range of ±20%). |
| | • Prominent ions, not from analyte, can be explained. |
| $MS^n$ SRM | |
| | • If precursor ion is completely dissociated and only two structurally specific ions are monitored, the relative abundance of sample and standard ions should match within ±10%). |
| | • If three or more structurally specific ions are monitored, the relative abundance of sample and standard ions should match within ±20%). |

Summary of FDA requirements for identifying animal drug residues.[144]

nature of regulatory authorities with respect to the unproven reliability of these techniques to robustly deliver reproducible chromatograms, not only on a day-to-day basis but also over an extended period of time. There is, however, flexibility in the type of chromatogram that may be used: total ion currents (TICs), reconstructed ion currents (RICs), SIM, and SRM are all acceptable with the provision that the retention times for the standard and the analyte should be within 2% for GC/MS and 5% for LC/MS.

With respect to mass spectral matching, the criteria for identification vary depending on the technique used for mass spectral data acquisition (see summary of requirements in **Table 8**). It is interesting to note that while the FDA does not rule out the use of exact mass measurements, it views these data as problematical as there are no generally accepted specific standards for their use. The problem here is that it is difficult to be definitive about the resolving power required, particularly, when analytes have masses greater than $m/z$ 500. Clearly the resolving power and accuracy must be sufficient to exclude all reasonable alternative elemental compositions and they recommend that if exact mass measurements are to be used then multiple structurally specific ions should be measured.

#### *9.10.4.4.2 EU performance of analytical methods*

The EU takes a slightly different approach to the FDA in setting the criteria for identification (**Tables 9–11**) but agrees with the FDA in accepting only GC/MS and LC/MS methods and in their requirement for an analyte standard.[145] The EU tolerance for chromatographic performance is more stringent than the FDA, requiring GC and LC retention times for standards and samples to be within ±0.05 and ±2.5%, respectively. In addition to outlining a set of performance criteria for the different types of MS data (**Tables 9 and 10**), the EU uses a system of identification points to score the MS data (**Table 11**). Identification under this system is acceptable only if a certain number of identification points have been accumulated. So, for example, identification using $GC/MS^2$ for one precursor ion and two product ions will earn four identity points, and identification using GC/MS and LC/MS, monitoring two ions with each technique, will also accrue four identity points. This level of identification is deemed sufficient for identification of their Group A banned substances (veterinary drug residues in meat for human consumption). It is interesting to note that the EU has set no qualifications around the acceptability of exact mass data, save that resolution should be greater than 10 000 (10% valley) for the entire mass

**Table 9** EU criteria for mass spectral matching

| *MS scan* | *Requirements* |
|---|---|
| Full scan | • A minimum of four diagnostic ions (molecular ion, adducts, fragments, and isotope ions) with an intensity >10% in the standard must be observed in the sample.<br>• The molecular ion must be included if the relative intensity is ≥10% of the base peak.<br>• The relative intensities of the sample diagnostic ions are required to match those of the standard, within specified tolerances (**Table 10**). |
| SIM | • The molecular ion shall be one of the selected diagnostic ions.<br>• The S/N for each diagnostic ion shall be ≥3:1.<br>• A minimum of four identity points (Group A, banned substances) (**Table 11**) must be accumulated and these must be derived from at least one ion ratio measurement, meet the specified intensity tolerances (**Table 10**), and no more than three techniques can be used to achieve the minimum number of identity points. |

Summary of EU requirements for identifying animal drug residues.[145]

**Table 10** EU maximum permitted tolerances for relative ion intensities

| *Relative intensity (% base peak)* | *GC–EI–MS (%)* | *GC/CI-MS, GC/MS$^n$, LC/MS, LC/MS$^n$ (%)* |
|---|---|---|
| >50 | ±10 | ±20 |
| >20–50 | ±15 | ±25 |
| >10–20 | ±20 | ±30 |
| ≤10 | ±50 | ±50 |

**Table 11** EU identification points earned

| *MS technique* | *Identity points/ion* |
|---|---|
| Low-resolution (LR)-MS | 1.0 |
| LR-MS$^n$precursor ion | 1.0 |
| LR-MS$^n$product ions | 1.5 |
| High-resolution (HR)-MS | 2.0 |
| HR-MS$^n$precursor ion | 2.0 |
| HR-MS$^n$product ions | 2.5 |

A minimum of four identity points are required to confirm the presence of a Group A substance (banned veterinary products).

range and indeed it assigns two identity points for each measured ion (**Table 11**). This lack of qualification ignores the fact that the number of candidate elemental compositions increases markedly with mass (Section 9.10.4.3.3). This point is well illustrated by Nielen *et al.*,[146] who using the anabolic steroid, stanozolol, and the $\beta$-agonist Clenbuterol-R, as models, demonstrate the current EU mass accuracy criteria can yield false negative results.

### 9.10.4.5 Quantification

As noted by the Reverend Stephen Hales as long ago as 1727, scientific insight into the processes of nature can be obtained only through the discipline of measurement.

> Since we are assured that the all-wise Creator has observed the most exact proportions, of number, weight and measure, in the make of all things, the most likely way therefore, to get any insight into the nature of those parts of the creation, which come within our observation, must in all reason be to number, weigh and measure.
>
> *Vegetable Staticks*, Stephen Hales 1977–1761

It should be no surprise therefore that mass spectrometers are most commonly used for quantification. In addition to quantitative applications by regulatory authorities and industry (e.g., petrochemical, pharmaceutical, food, forensic, and environmental areas), the postgenomic era has witnessed an explosion in the use of mass spectrometers to determine and quantify gene function as exhibited in the gene products – proteins and metabolites. This has given rise to two new and unique areas of endeavor, proteomics and metabolomics. Both of these aim to analyze the complete respective sets of proteins or metabolites, present in a cell, tissue or organism at any one time point. The importance of these analyses lies in the fact that they provide information that is not directly attainable from the genomic sequence, including, for example, insight into developmental processes and responses to environmental stimuli and pathogens, at the cellular level. These data can then be linked to genomic and transcriptomic data to present the scientist with a holistic or systems biology view of an organism (see, e.g., Weckwerth *et al.*[147] and Trauger *et al.*[148]).

The challenge of proteiomic and metabolomic analysis lies in the complexity (e.g., PTMs of proteins and the array of different chemical classes of metabolites), and the large range of concentrations, of the components present in the sample and in the need for high-throughput and reproducible methodologies for their identification and quantification. A detailed discussion of protein and peptide analysis by MS may be found elsewhere in this volume (see Chapter 9.12).

#### *9.10.4.5.1 Components of an MS-based metabolite assay*

Although techniques such as NMR and IR spectroscopy have found some utility in metabolite analysis, the most common approach has been to draw upon the versatility, speed, and high degree of specificity and sensitivity inherent in tandem MS.[149] In the case of complex samples, this specificity and sensitivity can be enhanced by interfacing the mass spectrometer to some form of high-resolution chromatography such as GC, nano-LC, or CE.

Using MS for quantification is no different in principle to using any other detector, and generally encompasses sample quenching, homogenization to break down tissue and cell structure, extraction, separation, sample analysis, calibration standard analysis, and finally data processing (**Figure 13**).[143] Also included will be assay validation–determining the limits of quantitation, selectivity, accuracy, precision, and linear dynamic range of the assay (see FDA Guidance for Industry,[144] Bioanalytical Method Validation,[150] Pritchard and Barwick,[151] and Boyd *et al.*,[143] for a detailed discussion on validation and quality assurance in analytical chemistry). In addition, a mass spectral assay will include specific consideration of the following items:

- Optimizing the quenching, extraction, and purification processes, being cognisant of reagents that may be incompatible with MS (e.g., nonvolatile salts and detergents; see also discussion on chemical noise and contamination in Section 9.10.4.5.8).[152]
- Selecting the method of sample introduction to the MS, for example, GC/MS (need to consider analyte derivatization; Section 9.10.4.3.2) or LC/MS.[152]
- Choosing the best ionization method (Section 9.10.4.1). For a metabolomics experiment, the most complete metabolite coverage may require analysis with multiple ionization methods.[153]
- Choice of quantitative standard – IS (isotopically labeled of not), external standard, or standard addition.[154]
- Selecting the most appropriate method of ion analysis – full scan, SIR, SRM.

It is important to remember, however, that in any quantitative assay, MS is just one part of a closely integrated overall procedure and that failure and compromise in any one step will invalidate the entire procedure. Some of the above points are illustrated in the development of a mass spectral assay for salicylic acid in tomato (**Figures 14–17**).

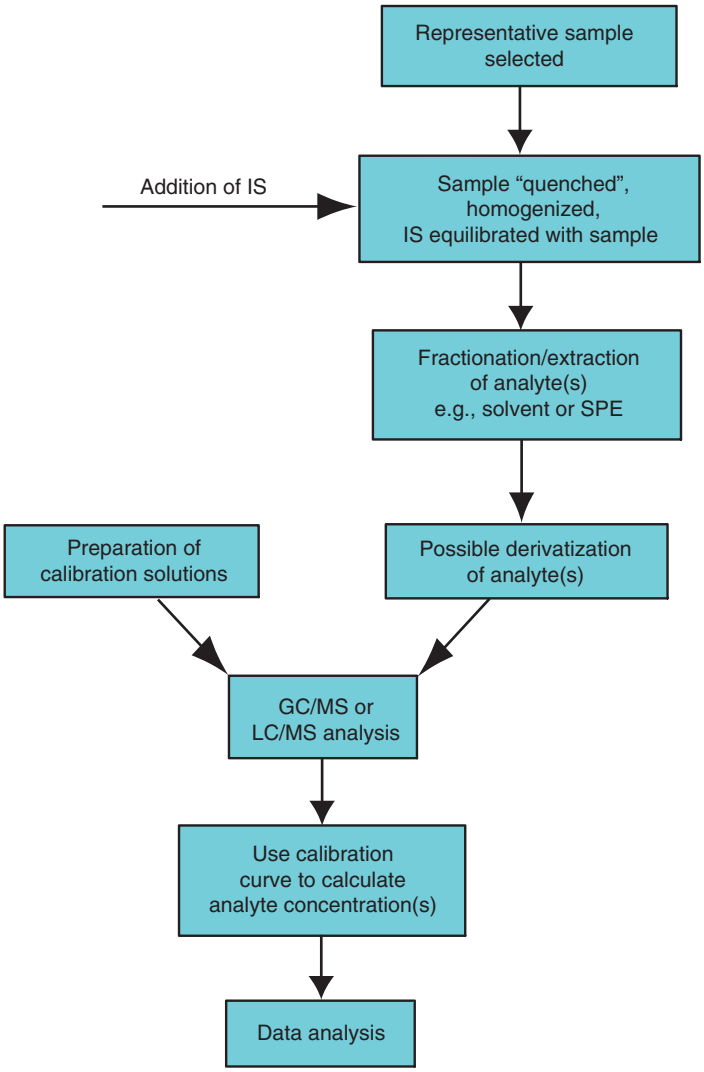


**Figure 13** Flow chart for a quantitative assay using an internal standard. The most critical steps are the selection of a representative sample, the accurate preparation of the standards, and finally the addition of the standard to the sample – planning, weighing, making up to volume, and pipetting. It is sobering to remember that failure in any one of these will invalidate the entire assay no matter how sophisticated the instrumentation or how powerful the statistics applied to data analysis.

#### *9.10.4.5.2 Sample preparation*

Cellular processes are dynamic and the level of a particular metabolite at any one time will represent the balance of biosynthesis, biochemical transformation into other metabolites, degradation, transportation into and out of the cell, and sequestration into and out of storage forms. Depending on the rates of these respective processes, the level of a metabolite can be subject to large and rapid change during quenching. Similarly, subtle changes introduced by developmental processes or genetic manipulation can also induce large changes in the level of metabolites (see, e.g., Schwab[155]). In any metabolite analysis, it is important that the analytical sample accurately represents the cellular or tissue status at the time the sample is taken. This means that quenching must very rapidly terminate all biological processes and that chemical degradation is minimized.[13,152,156] Typically, quenching is achieved by extremes of temperature (<20 or >80 °C) or acidity (pH < 2 or >10), possibly in the presence of an organic solvent, and/or an antioxidant, and in conjunction with homogenization. If the analysis is directed at a particular metabolite or class of metabolites (targeted analysis), the optimization

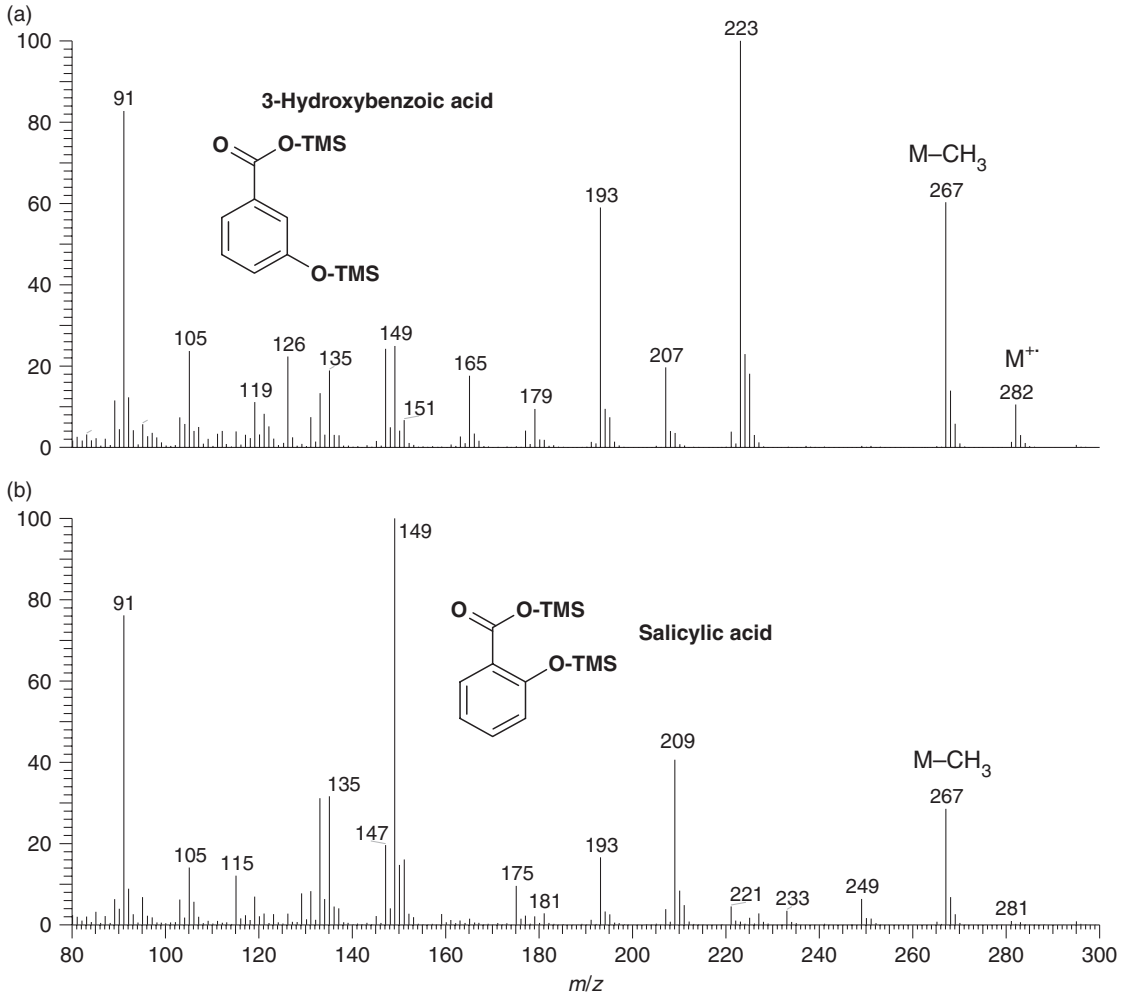


**Figure 14** Quantifying salicylic acid in tomato. Full-scan mass spectra of the per-trimethylsilyl derivatives of 3-hydroxybenzoic acid internal standard (IS) (a) and salicylic acid (b). In both cases, the $[M - CH_3]^+$ ion (*m/z* 267), a structurally significant ion, was chosen for selected reaction monitoring.

of quenching is readily monitored. However, if, as in a metabolomic analysis, the objective is to analyze as many metabolites as possible, then it is inevitable that some compromise will have to be made, in which case reproducibility of the process becomes very important (see the review by Villas-Bôas,[157] and two case studies of optimizing metabolomic assays in blood plasma,[158] and plant tissue.[159]

### *9.10.4.5.3 Fractionation and extraction of sample*

For a targeted assay, considerable effort is typically devoted to extracting the analyte or analyte class away from the sample matrix. Depending on the matrix, this may be as simple as a liquid–liquid extraction, selecting appropriate solid-phase extraction (SPE) chemistry (e.g., C-18 or ion exchange), or using affinity chromatography (specific lectins or antibodies bound to an inert matrix).[13,152,156] This step is designed to, first, reduce the possibility of interference by isobaric ions and, second, to reduce the possibility of ion suppression in the ionization process (ESI and APCI). This sample purification step may then be complemented by a high-resolution chromatographic separation interfaced to the MS source (e.g., nano-LC or GC).

ESI suppression has been correlated with high concentrations of nonvolatile matrix materials present in the spray and it is thought that this acts by inhibiting the formation of smaller droplets. Salts (e.g., phosphates and

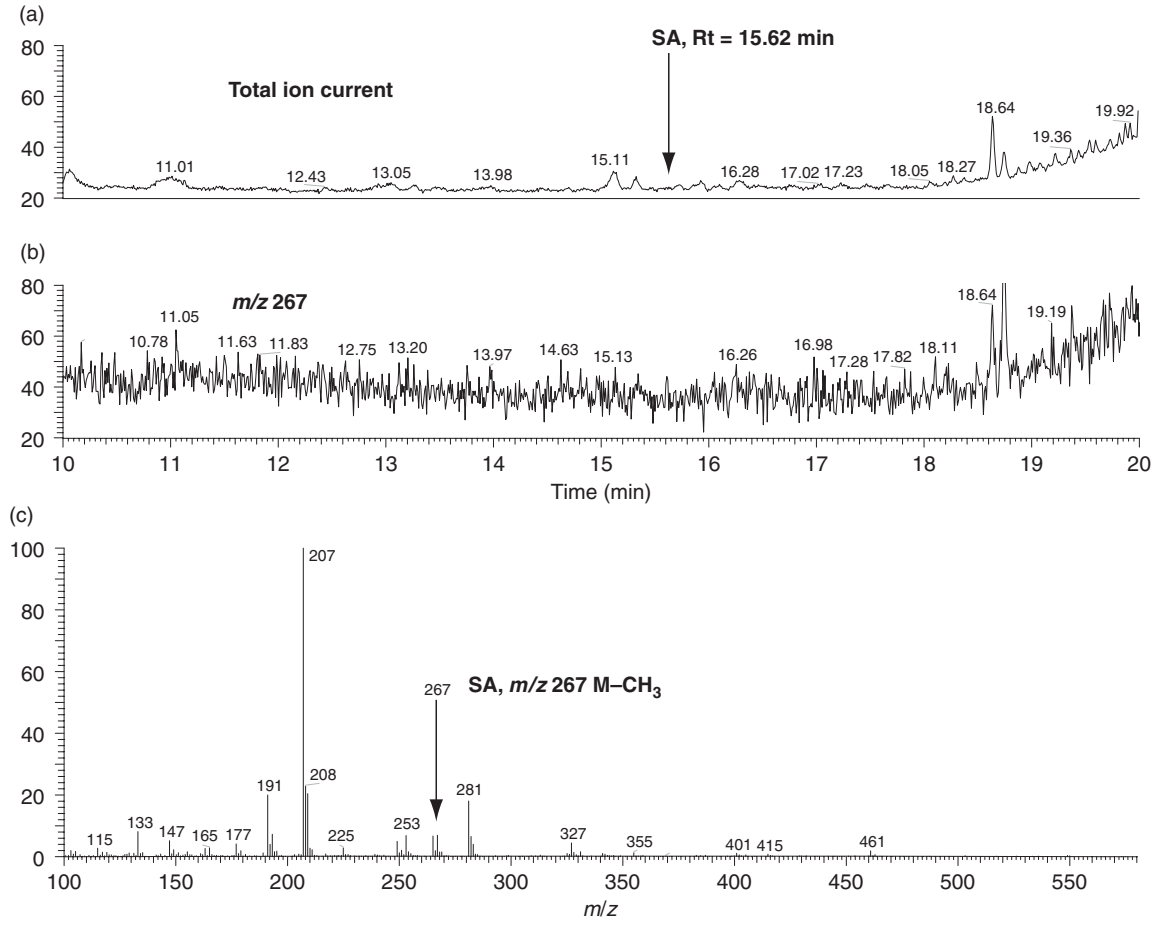


**Figure 15** Quantifying salicylic acid in tomato. The full-scan mass spectra of the trimethylsilylated tomato extract contains too much background chemical noise for the salicylic acid to be satisfactorily assayed. Neither the total ion current chromatogram (a) nor the extracted ion chromatogram of *m/z* 276 (b) contains a discrete peak for salicylic acid, although *m/z* 276 is observable in the mass spectra corresponding to the retention time of the analyte (c).

sulfates) and ion-pairing reagents (e.g., trifluoroacetic acid) are also implicated in ion suppression.[160] Matrix effects may also be minimized by a simple process of sample dilution.[161]

As mentioned above, in a competitive ionization process, molecules with the lowest ionization potentials will be preferentially ionized and it is quite possible that this competition, in addition to matrix suppression, will result in the relative abundance of sample metabolites not being reflected in the MS data. Any reduction in the number of analyte ions available for analysis will have an impact on the assay with loss of sensitivity (higher limits of detection and quantitation).

In the case of an untargeted metabolomic experiment, the issue of sample cleanup is complicated by the need to retain as many of the metabolites as possible, and avoiding bias against any particular group or class of components. This is often resolved by fractionation into a number of subsamples, for example, by retention and analysis of the remaining aqueous phase after solvent extraction or fractionation by mixed mode SPE. The trade-off here is that more analytes are potentially available for assay but at the expense of time devoted to running many more analyses on the different sample fractions.[157,162]

### *9.10.4.5.4 Internal standards*

In any analytical procedure, it is inevitable that there will be variations in instrumental parameters and in compliance with analytical protocols. It is also important to remember that in a mass spectrometer equimolar

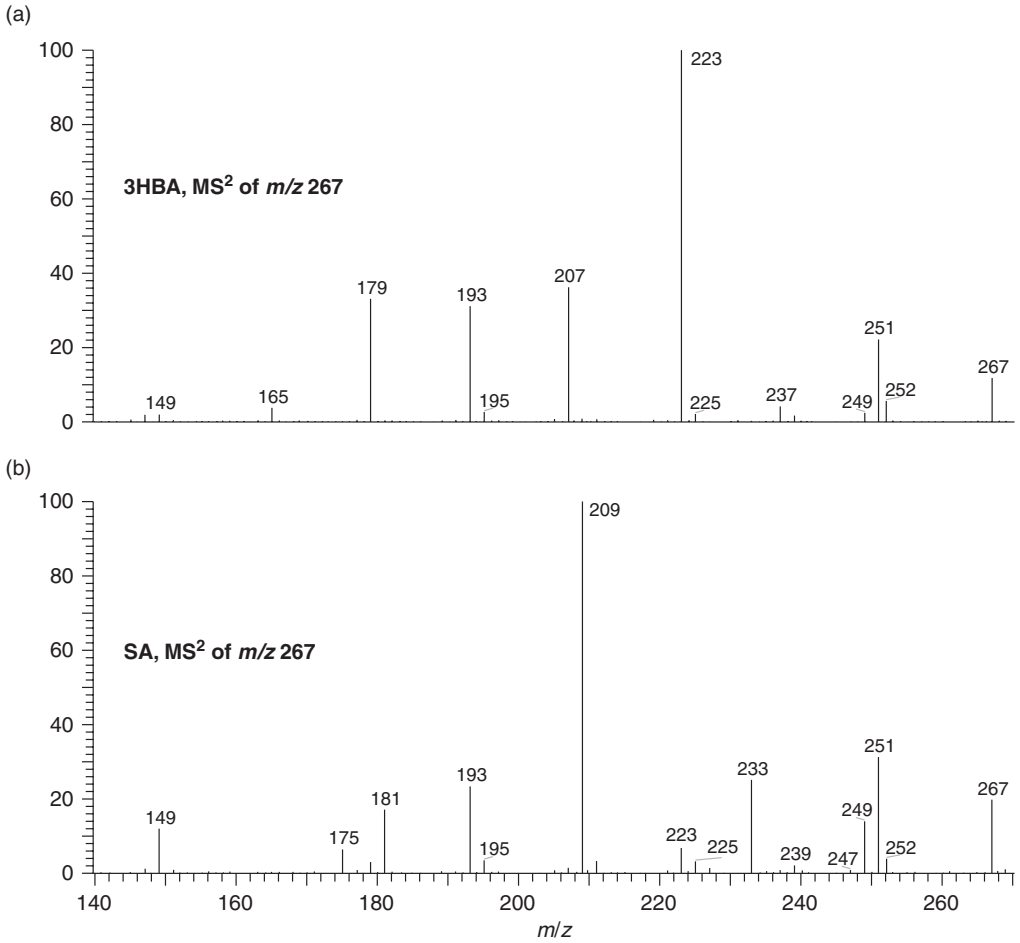


**Figure 16** Quantifying salicylic acid in tomato. $MS^2$ of *m/z* 267 for both 3-hydroxybenzoic acid (a) and salicylic acid (b). The salicylic acid ion at *m/z* 209 was chosen for quantification against the *m/z* 223 ion from the internal standard, 3-hydroxybenzoic acid.

amounts of different compounds do not give an equal response because of variation in the ionization efficiency, which is in part dependent on the molecular structure and in part the result of competition (ion suppression) from other analytes present in the source. These procedural and instrumental variations will affect the accuracy and precision of the assay; however, they may be compensated for by the inclusion of a standard in the assay. There are four possible ways in which a standard may be incorporated into an MS-based assay.

The first is the use of a stable isotope-labeled standard (isotopomer) of the target analyte. The most common isotopes available for use include deuterium ($^2$H), $^{13}$C, $^{15}$N, and $^{18}$O. The advantage of this approach is that the labeled standard will have identical chemical properties to the analyte and will be partitioned with the analyte throughout the analytical procedure, eliminating extraction and instrument bias and compensating for any ionization suppression by matching the ionization properties of the analyte. Thus the ratio of the amount of IS to analyte will remain constant up to the point of analysis. The mass spectrometer will then be able to independently detect the isotopically labeled standard by virtue of the heavier mass of its parent ion and fragment ions containing the labeled moiety. Quantification is then achieved by measuring the ratio of ions from the analyte and the IS, rather than an absolute value as in the use of an external standard. Then knowing the amount of standard added, the amount of the analyte present in the sample can be calculated from a comparison of the determined ion ratios (**Figure 18**).

Some caution needs to be exercised in using such a standard; the label should ideally be nonexchangeable and the number of incorporated isotopes must be sufficient so that there is minimal cross talk from the naturally

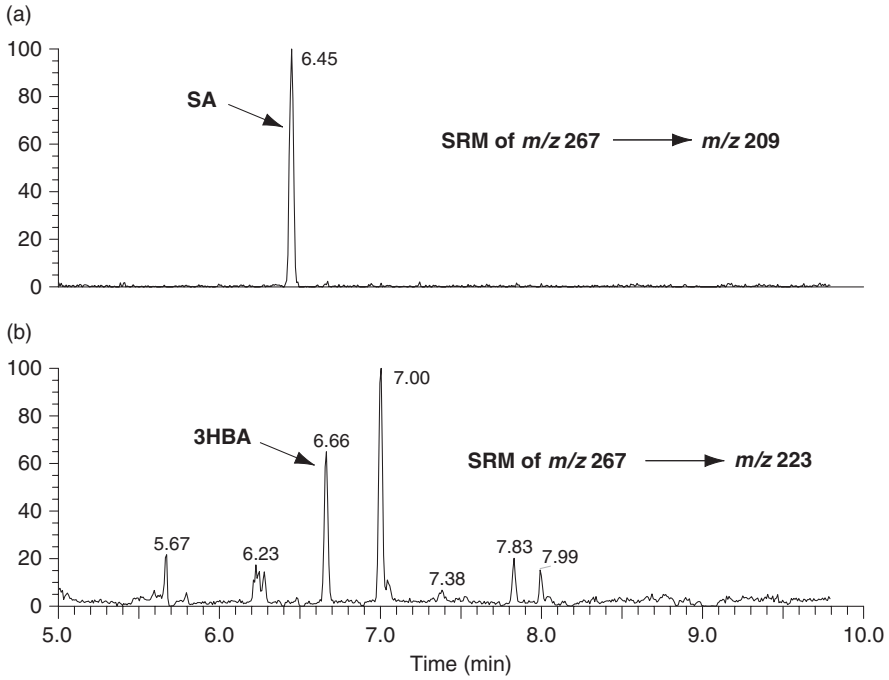


**Figure 17** Quantifying salicylic acid in tomato. Selected reaction monitoring of the transition from *m/z* 267 to *m/z* 209 and from *m/z* 267 to *m/z* 223 from a tomato extract. Salicylic acid (Rt 6.45 min) (a) and 3-hydroxybenzoic acid (Rt 6.66 min) (b) can be observed at an S/N of 222 and 95, respectively.

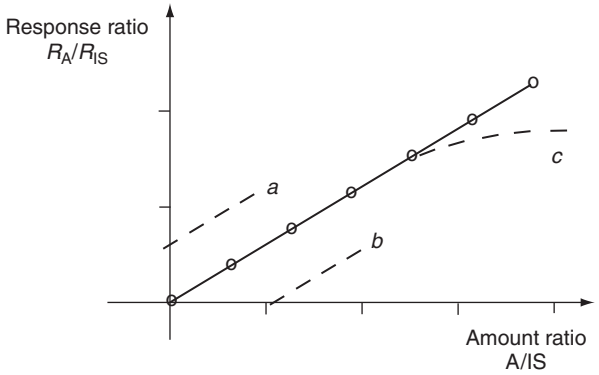


**Figure 18** Calibration curves using an internal standard (IS). Analytes are quantified against an IS that has been added as early as possible in the analytical procedure. The ratios of detector responses for the analyte ($R_A$) and IS ($R_{IS}$) are plotted against the ratio of known amounts of analyte (A) and IS. When a sample is analyzed, the ratio $R_A/R_{IS}$ is measured. Then knowing the amount of IS added into the sample, the amount of analyte present in the sample can be estimated. Curves that do not pass through the origin of the graph or which are nonlinear are diagnostic of (a) chemical interference or sample carryover, (b) sample loss during the assay due to adsorption, and (c) saturation or cross-contribution between the IS and the analyte.

occurring levels of $^{13}C$ and from isotopes of chlorine, bromine, and sulfur, when present. This also means that the highest degree of isotopic incorporation should be sought. Any large degree of cross talk will pose a limitation on the ultimate sensitivity of the assay. Nevertheless, isotopically labeled standards are usually regarded as approaching ideal although they are costly and of limited availability.

Where a stable isotope-labeled standard is unavailable, the analyst can use either a chemically similar homologue (e.g., incorporating an additional methylene; different $m/z$ values to monitor) or a chemically similar analogue (e.g., geometric isomer; same $m/z$ values to monitor) that will need to be chromatographically separated

from the analyte. Obviously, it is also important that this chosen standard is not present in the sample (see, e.g., the use of 3-hydroxybenzoic acid as an IS for the quantification of salicylic acid in tomato in **Figures 11–17**).

In metabolomic experiments, where hundreds of analytes are to be quantified, a number of ISs representing different chemical classes of analytes are generally used (see, e.g., Jiye *et al.*[158] and Gullberg *et al.*[159]). These experiments are primarily comparative in nature as the experimenter is seeking to identify relative changes in metabolite levels and relative changes in metabolite fluxes as they occur in different experimental states.

#### *9.10.4.5.5 Standard addition*

Where there is no appropriate standard for an analyte, quantification can be made by standard addition (spiking). In this procedure, the sample is divided into several aliquots of equal volume and a series of known but increasing amounts of the analyte standard are then added to each aliquot. The samples are then diluted to the same volume yielding a series of solutions with equal concentrations of matrix but increasing concentrations of analyte. These samples are then analyzed individually for the analyte of interest and the concentration of the unknown can then be calculated from where the regression curve of the responses versus the standard additions intercepts the abscissa ($y = 0$) (**Figure 19**). The advantage of this method is the elimination of any chemical or physical bias between the standards and samples but this is achieved at the cost of a six- or sevenfold increase in the number of determinations required for each sample.

#### *9.10.4.5.6 External standards*

External standards, so named because they are not added to the sample, are also occasionally used but are generally only applicable to samples requiring limited preparation and for which a consistent high degree of reproducibility and good recovery can be attained. Experiments should also be completed as quickly as possible to minimize instrumental variations (e.g., ion source contamination). In brief, instrument response is plotted against the concentration (or amount) of standard analyzed and this response curve is then used to calculate analyte concentration (or amount). However, unless the matrix is well characterized, this method can be subject to matrix effects (ion suppression) and to interference from isobaric matrix components.

#### *9.10.4.5.7 Optimization of the MS assay*

In quantitative mass spectrometric assays, sources of error can be reduced to those associated with sample handling and processing, and to instrumental variation, for example, source contamination and stability of mass calibration. In general, the largest component of error is associated with sample handling and processing.[163] To a large degree, variations in protocols for purification and derivatization, poor technique, and even gross spillage of sample can be

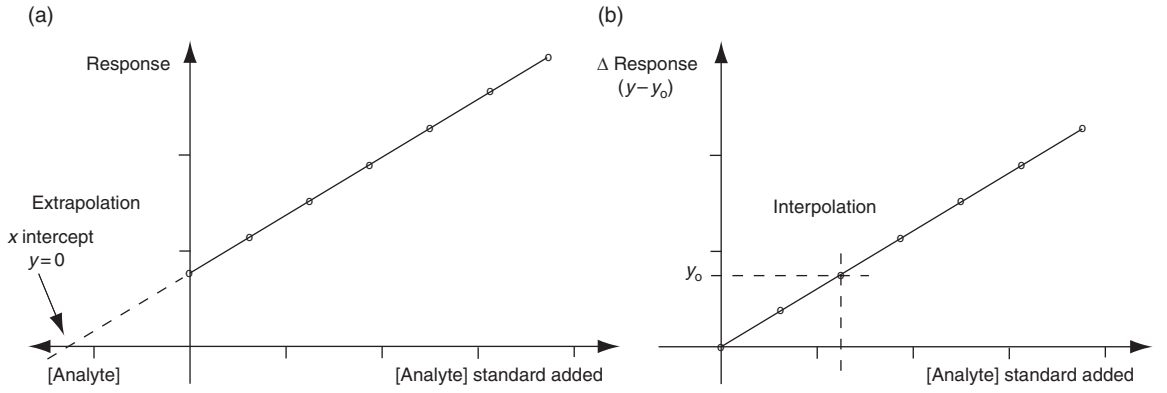


**Figure 19** Standard addition calibration curves. Equal volumes of solvent containing varying amounts of standard are added (spiked) into the sample. The samples are analyzed and the analyzer response (e.g., area under the TIC or selected ion chromatogram) is plotted against the amount of standard added. The analyte concentration is estimated by extrapolating a linear least-squares regression to $y = 0$ (a). An alternative approach is to plot the difference between the spiked samples and the unspiked sample. The same calibration curve now passes through the origin and the sample analyte concentration can now be determined by interpolation with improved confidence limits[164] (b).

obviated by the use of an IS, as outlined above. Once the ratio of internal standard to analyte has been established, it will remain unchanged as long as the standard and the analyte have the same chemical properties. The integrity of the assay then depends almost entirely on the analyst's ability to accurately weigh, dissolve, dilute, and dispense the IS into the sample as required. Any errors associated with the IS will be propagated throughout the entire assay. This equates to the analyst having a basic knowledge and understanding of the analytical capabilities of balances (milligram quantities measured on analytical balance), volumetric flasks (clean and temperature equilibrated), and pipettes (calibrated, serviced, and used appropriately).[143]

It is thus critical that the IS be added to the sample at the earliest possible stage of the assay, usually the quenching or homogenization steps, and that it be allowed to equilibrate with the analyte in the sample matrix over some defined period of time (**Figure 13**). This is particularly important where there is nonspecific binding of the analyte to proteins or other cellular debris and where complete (100%) recovery cannot be achieved. The equilibration time can be established by a time-course study.[163]

Adding too much or too little IS can also limit the dynamic range of the assay, as the comparison of very large ion currents (detector saturation) with very small ion currents (poor ion statistics) will greatly increase the variance of the assay. A good guide is a threefold excess of the IS over the analyte but this may take a few trials to establish.

Other errors may be introduced into an MS assay by interference from isobaric ions. There are a number of possible remedies for this, including revising the sample preparation, changing the GC or LC column to separate away the interference, selecting an alternative structurally specific ion for the assay, and increasing the assay specificity by increasing mass resolution to monitor ions of selected elemental compositions. It is important to remember that the analyte spectrum should not be examined in isolation when choosing a set of ions for quantification but should include an appreciation of the 'background' ions that are also likely to be present, for example, ions from GC column bleed or solvent/reagent adduct ions from ESI (see Section 9.10.4.5.8). Any change in retention time and/or the shape of the chromatographic peak is likely to be indicative of interference, which is to say a lack of assay specificity.

Selected ions should be structurally specific to the analyte and should be abundant in order to maximize the assay sensitivity. In the example of the assay for salicylic acid in tomato (**Figure 14**), the ion selected for $MS^2$ was the structurally specific $[M - CH_3]^{+\cdot}$ ion for both the analyte and the IS. The ion at $m/z$ 91, although intense, is a tropylium ion ($C_7H_7^{+\cdot}$) and would be an inappropriate selection as it would be present in most analytes containing a benzyl moiety. The ions at $m/z$ 223 and $m/z$ 209 in the product spectra (**Figure 16**) were chosen for the quantification because they were the most intense.

For assays based on a full-scan MS, the specificity and sensitivity can be increased by

- Careful selection of ions for quantification. In general, higher $m/z$ values are less subject to interference. Using a different analyte derivative might assist in this. It must be borne in mind, however, that regulatory authorities will require these to be structurally specific ions.[144,145] Note that moving to SIM will not improve selectivity over that of a full scan but will improve sensitivity.
- Moving to high-resolution SIM and targeting a specific elemental composition may remove interference except when the interfering compound has the same elemental composition as the analyte. In this case, one should suspect an analyte isomer and change the sample chromatography accordingly.
- Using SRM. It is unlikely that the interfering ion will fragment in the same way as the analyte and the elimination of background chemical 'noise' by SRM will also improve sensitivity. Again, the ions selected should be structurally specific.[144,145] See, for example, the S/Ns in the TIC for the salicylate assay (**Figure 15**) and compare them with those realized in the SRM traces (**Figure 17**).
- Using high-resolution SRM and targeting specific elemental compositions in the precursor and product ions.

A comprehensive discussion of trace quantitation using MS, including error calculations, confidence limits, limits of detection (LoD), limits of quantitation (LoQ), and method validation may be found in Boyd *et al.*,[143] but also see a more general discussion of these issues as they pertain to analytical chemistry by Pritchard and Barwick.[151]

An example of a method validated according to the FDA and EU guidelines is described by Hermo *et al.*[165] These authors used LC–ToF MS to determine the levels of multiresidue antibiotic quinolines in pig livers below the maximum residue limits. They describe the optimization of their method, which is then

comprehensively characterized by the determination of the linearity, the decision limit, LoD, LoQ, the precision, the accuracy, and finally the recoveries for the different residues.

#### *9.10.4.5.8 Chemical noise and contamination*

As the sensitivity of mass spectral-based assays has improved and the interest in quantifying trace analytes has increased, the problems associated with chemical noise and sample contamination have also increased. Chemical noise and contamination in an assay have the effect of reducing the S/N of the analyte signal. This places an immediate restriction on achieving the full potential of the instrumental sensitivity with the assay LoD and LoQ set higher than they might otherwise have been. While it is unlikely that chemical noise and contamination can ever be completely eliminated, they can be minimized if care is taken to avoid known sources of contamination when the assay protocols are being planned (see reviews by Ende and Spiteller[166] and Keller *et al.*,[167] on mass spectral contaminants and their origins; the supplementary data in the latter review includes a literature compilation of contaminants in an Excel spreadsheet). In general, sample contamination can be sourced to almost every part of the assay, including

- the person of the analyst (e.g., keratin proteins, fatty acids, amino acids, and cosmetic residues from hair and skin),
- solvents (e.g., degradation products, antioxidants, and stabilizers),
- reagents used in sample preparation (e.g., proteins, detergents, antioxidants, chemical bleed from 'dip sticks'),
- laboratory ware (e.g., detergent residues, plasticizers, lubricants),
- chromatography (GC or LC column degradation or bleed, and late eluting components of previous samples),
- ionization process (matrix clusters from MALDI and solvent clusters from ESI, APCI, APPI, and DESI; clusters may also include common alkali metal cations, $Na^+$ and $K^+$, in addition to other cations from the assay reagents), and
- sample carryover and cross-contamination (inadequate washing of components that are reused for each batch of samples, e.g., pipettors, recycled sample vials, GC and LC autosamplers).

Some of the precautions that can be exercised should be a normal part of good laboratory practice, and include the appropriate use of personal protection. Covering the hair and using gloves will minimize the possibility of contamination from skin and hair-derived keratin proteins, as well as amino acids, fatty acids, and cosmetic residues from the skin surface.

It is also obvious that, unless determined otherwise, the highest quality solvents should be used. This is particularly so in the case of water, which, as the initial solvent in reverse-phase chromatography, can concentrate impurities at the head of the column. It is worth remembering that with laboratory-prepared water, the outlet conductivity meter provides an estimation of residual ions in the water and does not provide a measure of any neutral organic contaminants, should they be present. Again good laboratory practice, as exemplified by the recommended periodic changes of the purification cartridges, is the best way to prevent this water becoming a source of contamination.

Other potential contaminants are, however, less obvious and these include lubricants (e.g., silicone grease), plasticizers (e.g., phthalates, phenyl phosphates, sebacates, and bisphenol A), slip agents (e.g., oleamide, erucamide, and stearamide), biocides (e.g., quarternary ammonium compounds) and polymers extracted from laboratory consumables (e.g., silicones from laboratory tubing) and membrane filters (e.g., cyclic oligomers and Nylon 66).[168,169]

Contaminants can also be sourced to reagents used in sample protocols. For example, in the extraction and purification of proteins, it is common to use detergents, which, unless they are removed from the sample that is presented for MS analysis, can represent a very persistent form of contamination that is not readily removed except by long periods of washing or by replacement of the LC column and other associated components. Detergents can also be inadvertently introduced from laboratory glassware or sample vials that have been inadequately rinsed after washing.

In addition to analyst-derived keratins, proteins/peptides can also be introduced, for example, in 'bottom-up' proteomics where the sample is digested by a proteolytic enzyme (most commonly trypsin).

This will give rise to a set of autolysis peptides from the self-digestion of the enzyme. These autolysis peptides are impossible to eliminate but can be minimized by using the highest quality autolysis-resistant enzyme. Other proteins such as bovine serum albumin (BSA) may be used in the immunopurification of specific proteins. Again, if this is an unavoidable part of the protocol, then the analyst should expect to observe peptide ions derived from these proteins.

Chromatographic materials (e.g., solid-phase extraction tubes, LC and GC columns, TLC plates) including single-use materials must be thoroughly, and appropriately, washed or conditioned to remove contaminants originating from the manufacturing process or those that may have been acquired by exposure to packing materials or to the laboratory atmosphere. In some cases, contamination is unavoidable and it is important for the analyst to be able to recognize this and to plan accordingly. For example, all GC columns and septa continuously shed volatile siloxanes, a process known as 'bleeding', as the temperature is raised. The amount of bleed is proportional to the temperature and to the amount of phase on the column. Thus columns with thicker phase coatings generally bleed more, and especially so at higher temperatures. Although modern column phase chemistry is extremely robust, columns are inevitably degraded over time with a concomitant increase in bleed. This phase degradation is accelerated by trace levels of oxygen in the carrier gas at high temperatures, so it is important to ensure that a functional oxygen trap is part of the in-line gas purification process and that column temperature limits are not exceeded.

LC columns can also bleed in the presence of the eluting solvent but for modern columns operated within their pH range this problem is generally minimal but will be exacerbated when chromatographing at high temperatures. Of greater concern is the solvent and adduct clusters generated by the atmospheric pressure ionization (ESI, APCI, APPI, and DESI).[170] The many combinations and permutations of solvent clusters, complicated by the inclusion of solvent modifiers such as acetic acid, formic acid, or triethylamine, along with the ever-present sodium and potassium cations, form a very complex chemical background against which analyses must be performed. Moreover, in the case of a solvent gradient, this chemical noise will be changing, over time, in accord with the gradient. In addition to solvent clusters, clusters also form around the eluting analytes and any contaminants picked up during the assay. A number of hardware approaches have been used to minimize the impact of this chemical noise, including orthogonal and '*z*' geometries for the spray outlet and MS inlet, the use of nebulizing and curtain gases, and ion mobility interfaces (FAIMS and TWIMS in Section 9.10.2.3.9). Tandem MS (Section 9.10.3) can be used to remove much of the remaining chemical noise and this approach can be enhanced by the use of curved collision cells to eliminate the transmission of fast neutrals to subsequent stages of tandem MS.

A considerable amount of chemical noise (mostly $< m/z$ 1000) in the form of matrix clusters is also generated by MALDI and this has generally precluded MALDI from being used to analyze small molecules. Some reduction in the occurrence and intensity of matrix clusters can be obtained by minimizing salt contamination by on-target washing and/or by sample purification (e.g., use of Zip-Tips)[167] but this must be offset against potential loss of hydrophilic analytes. Various attempts have been made to find a substitute for the MALDI matrix but to date these have lacked universal acceptance, often related to the cost, difficulty of preparation, ease of contamination, or lack of long-term stability of the alternative target surfaces (e.g., porous silica, sol gels, graphite, carbon nanotubes, fullerenes, and polymers[171]).

Finally, contamination of sample spectra can also occur by cross-contamination during sample preparation and by carryover of residual analyte from a sample analyzed earlier in the run.[172,173] Essentially, any component of the assay that is reused for each sample or batch of samples can be a source of cross-contamination or carryover. These include, for example, evaporators, pipettors, automated liquid handlers, recycled sample vials, and LC and GC autosamplers. Care needs to be taken in the selection of appropriate wash solvents that will readily solubilize the sample and analytes. This will usually be a combination of high percentage of organic solvents that may include a volatile acidic or basic modifier (e.g., formic acid or aqueous ammonia). Failure to properly wash all sample components from a chromatographic column can result in late eluting components appearing in the next, or later, analytical runs.

Unless care is exercised by the analyst, both these forms of contamination can go unnoticed and erroneous results may be reported for individual samples. Problems with cross-contamination should normally be identified during the validation phase of method development by the judicious use of blanks to test for problems with general laboratory contamination, sample preparation, and the autosampler. Carryover is

assessed by injecting one or more blanks after a high concentration sample, normally at the upper limit of quantitation. If the carryover is less than 20% of the lower limit of quantitation, then this is normally deemed to be acceptable. If possible, the analyst should order the analysis from low-concentration samples to high, with high-concentration samples followed by a blank and/or additional cycles of sample syringe washing.

Trace analysis and the move to the use of smaller sample sizes represent particular challenges in that the ratio of surface area exposure to sample volume, or quantity of analyte, is increased, multiplying the possible effect and level of contamination. While mass spectral identification of contaminants will aid in identifying their source (see the literature-derived Excel database of contaminant mass spectra in the supplementary data of Keller *et al.*[172]), this is not essential. The key tool to their elimination is the appropriate use of sample blanks at each step of the analytical protocol during method development and validation.

### 9.10.4.6 MS Imaging

Traditional histological studies of tissue sections have been limited to either light or electron microscopy. Both these techniques have been used to obtain limited amounts of chemical information from the examined tissue. For the most part, this has been achieved through the use of a small number of specific chemical, radiographic, autoradiographic, and immunological stains. More recently, organisms have been genetically engineered to incorporate fluorescent tags into proteins (e.g., green fluorescent protein, GFP); however, these can potentially interfere with the normal functioning of the tagged protein. In general, although microscopy can yield excellent images at high resolution, there is little direct chemical information on the imaged components of the tissue surface.

Since the original idea to generate chemical images of tissue sections using MALDI-MS (Section 9.10.2.2.7),[174–177] two additional ionization techniques, SIMS (Section 9.10.2.2.8)[11,60,178] and DESI (Section 9.10.2.2.9),[179] have been added to the imaging repertoire but these have yet to gain the relative popularity of MALDI imaging. Unlike the traditional histological stains, these three MS imaging techniques require no prior assumptions about chemical identity and they are capable of sensitively visualizing a large range of small (e.g., metabolites) and large molecules (e.g., proteins) provided that they are ionizable for subsequent MS analysis, including direct molecular identification using tandem spectrometry ($MS^n$).

The great challenge in preparing a tissue sample for MALDI-MS imaging is that two contradictory processes must occur.[176,180] First, tissue sections are frozen in liquid nitrogen to avoid delocalization and degradation of the peptide and protein analytes. Sections are then prepared by cryosectioning and these are then mounted on a cold MALDI target. Next, matrix, either sinapinic acid for high-molecular-weight proteins or $\alpha$-cyano-4-hydroxycinnamic acid for low-molecular-weight peptides and proteins ($<\sim$3 kDa), is applied. For best image resolution and reproducibility, the matrix is usually uniformly sprayed directly onto the tissue surface. At this stage, it is important for the matrix solution to be able to solubilize, extract, and cocrystallize with the protein and peptide analytes while minimizing their delocalization. Several coatings of matrix are usually applied with a short interval between applications for the solvent to dry. This avoids the problem of large quantities of solvent potentially mobilizing the surface analytes with concomitant loss of image resolution. Images are then obtained by rastering a laser across the tissue surface, desorbing and ionizing the analytes, and generating spectra from specific locations (pixels). Virtual images based on the location of specific ions can then be generated and matched to the images of other specific ions and to light microscope images of the section. The intrinsic value of these MALDI images can be greatly enhanced if they can be precisely aligned with the image generated by traditional histopathological stains. Several approaches to this goal have been investigated and include rinsing the matrix from the tissue surface before applying the histological stain, staining the consecutive section,[181] and the use of MALDI-compatible stains.[182]

Most recently, Caprioli's group[183] have reported a novel method of dry coating tissue sections with MALDI matrix, thus minimizing the problem of the matrix solvent mobilizing the surface analytes. The dry coating procedure proved to be simple and rapid and yielded high-quality images of phospholipids.

Where it may not be convenient, or possible, to immediately flash freeze a tissue sample, ethanol-preserved paraffin-embedded specimens may also be used for MALDI imaging.[184] Thinner microtome sections can be cut from the frozen tissue following this treatment and this is an advantage where comparisons need to be made with traditional histological stains for light microscopy.

Neither DESI nor SIMS requires any special treatment of the sample surface and images are generated by rastering a microprobe spray of solvent (DESI) or a beam of energetic ions (SIMS) over the tissue section. Virtual images of desorbed secondary ions are then generated as for MALDI imaging. SIMS and MALDI imaging must both be carried out in a high vacuum. They are also complementary techniques in that SIMS is applicable to small molecules ($<\sim 500\ m/z$) and MALDI to large molecules ($>\sim 800\ m/z$ to avoid matrix cluster ions) with the SIMS analysis being performed prior to the application of matrix.[59] SIMS imaging has been reported as being able to achieve lateral resolutions down to 50 nm[11] and MALDI imaging has achieved resolutions down to 10–25 μm.

Unlike MALDI ($> \sim 800$ Da) and SIMS ($< \sim 500$ Da), the new DESI technique can usefully image both small metabolite molecules and large proteins but the spatial resolution is limited to only slightly better than 400 μm[179] when sampling from tissue sections. The image resolution that DESI can achieve is determined by the cross-sectional area of the applied solvent spray as it strikes the target and this in turn is determined by solvent flow rate, solvent composition, applied voltage, and size of spray orifice. The height of the spray orifice above the surface, the angle of the incident spray (~55°), and the angle at which the desorbed and ionized analytes are sampled (0–20°) are also critical. When sampling from printed patterns on paper and thin-layer chromatography plates, image resolutions of ~40 μm have been reported.[185] Although DESI imaging will require further development before it can compete with the resolution achieved to date by SIMS and MALDI, it does offer the advantage of being applicable to surfaces and samples not readily brought within the vacuum system of the mass spectrometer.

With the release of the first generation of commercial MS imaging instruments, MS imaging is being actively applied to problems in biology and human health. If the availability of chemical images, particularly if they can be correlated with the images from the traditional histopathology stains, proves useful, this will feedback to promote further technical developments of the technique. However, future developments in a clinical or diagnostic setting will have to meet the challenge of quality assurance and information validation.[186]

### 9.10.4.7 Future Prospects

Over the past 100 years, MS has moved from the exclusive domain of physics to chemistry, and is now an essential tool for biologists in creating holistic approaches to studying biology. Thus, for example, developments in mass spectrometric-based proteomic and metabolomic studies directly complement high-throughput chip-based transcriptomics and the large number of genomes – bacterial, plant, and animal – that have been completely sequenced.

The increasing utility of mass spectrometers can be directly attributed to the development of new ionization methods. This is particularly exemplified in the development of ESI and MALDI, which have allowed the routine ionization of large, labile, and polar molecules. This initiated an exponential growth in the sale of mass spectrometers, which is now sustained by demands from biology and the health sciences for increasing sensitivity, resolution, and accuracy, all at a cheaper cost. As a result, the performance of mass analyzers and peripheral instrumentation has improved, size and cost have decreased, new analyzers invented (e.g., Orbitrap), old ones improved (e.g., ToF), new configurations assembled (e.g., QIT-ToF and LIT-Orbitrap), and more sophisticated computer algorithms developed to increase sample throughput and to improve the ease of operation for the nonspecialist. The improved availability of mass spectrometers has also seen their application to new areas of endeavor such as PTR-MS for environmental monitoring and MALDI-MS for microscopy, providing a new chemical dimension to the imaging of tissue sections. There are also active programs of miniaturization in progress and the prospect of handheld mass spectrometers with the new ambient ionization techniques of DESI and DART is very real.[187]

Forecasting the future is always fraught with difficulties; however, extrapolating from the immediate past, the future of MS looks to be very bright as the need to identify and quantify with increasing sensitivity and reliability is one that is not going to diminish whether it be for the purposes of research, regulation, or law enforcement.

## Acknowledgments

I thank my colleagues, Sharyn Wragg for Figure 1, and Carolyn McKinlay who kept the MS lab operating during my periodic absences and who provided the myoglobin spectra.

## Abbreviations

| | |
|---|---|
| **2D** | two-dimensional linear ion trap |
| **3D** | three-dimensional quadrupole ion trap |
| **APCI** | atmospheric pressure chemical ionization |
| **APPI** | atmospheric pressure photoionization |
| **BIRD** | blackbody infrared dissociation |
| **BSA** | bovine serum albumin |
| **BSTFA** | *N*, *O*-bis(trimethylsilyl)trifluoroacetamide |
| **CE** | capillary electrophoresis |
| **CI** | chemical ionization |
| **CID** | collision-induced dissociation |
| **CV** | compensation voltage |
| **DART** | direct analysis in real time |
| **DESI** | desorption electrospray ionization |
| **DMOX** | dimethyloxazoline |
| **ECD** | electron capture dissociation |
| **ECI** | electron capture ionization |
| **EDD** | electron detachment dissociation |
| **EI** | electron ionization |
| **ESI** | electrospray ionization |
| **ET** | electron transfer |
| **ETciD** | supplemental low-energy CID method |
| **ETD** | electron transfer dissociation |
| **EU** | European Union |
| **FAIMS** | field asymmetric waveform ion mobility spectrometry |
| **FAME** | fatty acid methyl ester |
| **FDA** | Food and Drug Administration |
| **FTICR MS** | Fourier transform ion cyclotron resonance MS |
| **FWHM** | full-width at half-maximum height |
| **GAG** | glycosaminoglycans |
| **GC** | gas chromatography |
| **HECD** | hot ECD |
| **HR** | high-resolution |
| **ICR** | ion cyclotron resonance |
| **IMS** | ion mobility spectrometry |
| **IR** | infrared |
| **IRMPD** | infrared multiphoton dissociation |
| **IS** | internal standard |
| **KI** | Kovat's indices |
| **LC** | liquid chromatography |
| **LIT** | linear ion trap |
| **LMIG** | liquid metal ions gun |
| **LoD** | limits of detection |
| **LoQ** | limits of quantitation |
| **LR** | low-resolution |

| | |
|---|---|
| ***m/z*** | mass to charge |
| **MALDI** | matrix-assisted laser desorption ionization |
| **MS** | mass spectrometry |
| **$MS^n$** | multistage mass spectrometry |
| **MSTFA** | *N*-methyl-*N*-trimethylsilyltrifluoracetamide |
| **MuDPIT** | multidimensional protein identification technology |
| **NICI** | negative ion chemical ionization |
| **NMR** | nuclear magnetic resonance |
| **PICI** | positive ion chemical ionization |
| **PID** | photon-induced dissociation |
| **PPINICI** | pulsed positive ion/negative ion CI |
| **PTM** | posttranslational modification |
| **PTR-FTICR** | proton-transfer reaction Fourier transform ion cyclotron resonance |
| **PTR-MS** | proton-transfer reaction mass spectrometry |
| **Q** | quadrupole |
| **QIT** | quadrupole ion trap |
| **RF** | radio frequency |
| **RIC** | reconstructed ion current |
| **S/N** | signal-to-noise ratio |
| **SIFT-MS** | selected ion flow tube mass spectrometry |
| **SIM** | selected ion monitoring |
| **SIMS** | secondary-ion mass spectrometry |
| **SORI** | sustained off-resonance irradiation |
| **SPE** | solid-phase extraction |
| **SRM** | selected reaction monitoring |
| **TIC** | total ion current |
| **ToF** | time-of-flight |
| **TMCS** | trimethylchlorosilane |
| **TWIMS** | traveling wave IMS |
| **VOC** | volatile organic compound |

## Nomenclature

| | |
|---|---|
| ***B*** | magnetic field or magnetic sector analyzer |
| **BE** | double-focusing mass spectrometer using a magnetic sector analyzer linked to an electrostatic analyzer – reverse geometry |
| **CE/MS** | instrument in which capillary electrophoresis is directly interfaced with a mass spectrometer |
| **Da** | dalton, an atomic mass unit, commonly used in biochemistry for the mass of ions and molecules |
| **E** | electrostatic analyzer |
| **EB** | double-focusing mass spectrometer using an electrostatic analyzer linked to a magnetic sector analyzer – forward geometry |
| **$E_k$** | kinetic energy |
| **ETciD** | ETD combined with a supplemental low-energy CID of a peptide electron transfer product |
| **GC/MS** | instrument in which gas chromatography is directly interfaced to a mass spectrometer |
| **LC/MS** | instrument in which liquid chromatography is directly interfaced to a mass spectrometer |
| ***m*** | mass of an ion |
| **metabolome** | the complete set of all metabolites present in a cell at any one time. These are usually arbitrarily defined as having a molecular weight of less than 1000 Da. |

| | |
|---|---|
| **mmu** | millimass units ($10^{-3}$ u) |
| $M_r$ | molecular weight |
| **MS** | commonly used with respect to mass spectrometer instruments, the data they generate (the mass spectrum), and the technique mass spectrometry |
| $MS^n$ | tandem mass spectrometry of *n* stages; $MS^2$ may be written as MS/MS |
| *m/z* | mass to charge ratio |
| **ppb** | parts per billion |
| **ppm** | parts per million |
| **proteome** | the complete set of all proteins present in a cell at any one time |
| **q** | collision cell contained within an RF-only quadrupole or multipole |
| *R* | mass resolution |
| **u** | unified atomic mass unit, one-twelfth the mass of the most abundant naturally occurring isotope of carbon, $^{12}C$ |
| *z* | number of charges on an ion |

## References


1. B. Bothner; G. Siuzdak, *ChemBioChem* **2004**, *5*, 258–260.
2. J. J. Thompson, *Rays of Positive Electricity and Their Application to Chemical Analysis*; Longmans: London, UK, 1913.
3. M. A. Grayson, Ed., *Measuring Mass: From Positive Rays to Proteins*; Chemical Heritage Press: Philadelphia, USA, 2002.
4. J. Griffiths, *Anal. Chem.* **2008**, *80*, 5678–5683.
5. J. T. Watson; O. D. Sparkman, *Introduction to Mass Spectrometry: Instrumentation, Applications and Strategies for Data Interpretation*, 4th ed.; John Wiley and Sons: Chichester, UK, 2007.
6. G. J. Trout; R. Kazlauskas, *Chem. Soc. Rev.* **2004**, *33*, 1–13.
7. M. Thevis; W. Schänzer, *Curr. Org. Chem.* **2005**, *9*, 825–848.
8. P. Hemmersbach, *J. Mass Spectrom.* **2008**, *43*, 839–853.
9. C. Fenselau; R. Caprioli, *J. Mass Spectrom.* **2003**, *38*, 1–10.
10. J. R. de Laeter, *Mass Spectrom. Rev.* **1998**, *17*, 97–125.
11. L. A. McDonnell; R. M. A. Heeren, *Mass Spectrom. Rev.* **2007**, *26*, 606–643.
12. Y. Hayasaka; G. A. Baldock; A. P. Pollnitz, *Aust. J. Grape Wine Res.* **2005**, *11*, 188–204.
13. K. Dettmer; P. A. Aronov; B. D. Hammock, *Mass Spectrom. Rev.* **2007**, *26*, 51–78.
14. E. J. Want; A. Nordström; H. Morita; G. Siuzdak, *J. Proteome Res.* **2007**, *6*, 459–468.
15. R. Aebersold; D. R. Goodlet, *Chem. Rev.* **2001**, *101*, 269–295.
16. J. C. Smith; J.-P. Lambert; F. Elisma; D. Figeys, *Anal. Chem.* **2007**, *79*, 4325–4344.
17. R. J. Simpson, *Proteins and Proteomics: A Laboratory Manual*; Cold Spring Harbour Laboratory Press: New York, USA, 2003.
18. A. G. Marshall; C. L. Hendrickson; G. S. Jackson, *Mass Spectrom. Rev.* **1998**, *17*, 1–35.
19. M. L. Vestal, *Chem. Rev.* **2001**, *101*, 361–375.
20. K. B. Tomer, *Chem. Revi.* **2001**, *101*, 297–328.
21. D. R. Knapp, *Handbook of Analytical Derivatization Reactions*; Wiley-Interscience Publication, John Wiley & Sons, Inc.: New York, USA, 1979.
22. K. Blau, J. Halket, Eds., *Handbook of Derivatives for Chromatography*, 2nd ed., John Wiley & Sons, Inc.: Chichester, UK, 1993.
23. J. M. Halket; V. G. Zaikin, *Eur. J. Mass Spectrom.* **2003**, *9*, 1–21.
24. J. M. Halket; V. G. Zaikin, *Eur. J. Mass Spectrom.* **2003**, *9*, 421–434.
25. J. M. Halket; V. G. Zaikin, *Eur. J. Mass Spectrom.* **2004**, *10*, 1–19.
26. J. M. Halket; V. G. Zaikin, *Eur. J. Mass Spectrom.* **2004**, *10*, 555–568.
27. J. M. Halket; V. G. Zaikin, *Eur. J. Mass Spectrom.* **2005**, *11*, 127–160.
28. A. J. Dempster, *Philos. Mag.* **1916**, *31*, 438–443.
29. C. J. W. Brooks, *Philos. Trans. R. Soc. London Ser. A* **1979**, *293*, 53–67.
30. S. G. Wyllie; B. A. Amos; L. Tökés, *J. Org. Chem.* **1977**, *42*, 725–732.
31. H. Budzikiewicz; C. Djerrassi; D. H. Williams, *Mass Spectrometry of Organic Compounds*; Holden-Day, Inc.: San Francisco, USA, 1967.
32. F. W. McLafferty; F. Tureček, *Interpretation of Mass Spectra*, 4th ed.; University Science Books: Sausalito, CA, USA, 1993.
33. J. H. Gross, *Mass Spectrometry. A Textbook*; Springer-Verlag: Heidelberg, Germany, 2004.
34. E. de Hoffmann; V. Stroobant, *Mass Spectrometry: Principles and Applications*, 3rd ed.; John Wiley and Sons: Chichester, UK.
35. A. A. Solovev; V. I. Kadentsev; O. S. Chizhov, *Russian. Chem. Rev.* **1979**, *48*, 631–644.
36. B. Munson; F. H. Field, *J. Am. Chem. Soc.* **1966**, *88*, 2621–2630.
37. B. Munson, *Anal. Chem.* **1977**, *49*, 772A–778A.
38. A. G. Harrison, *Chemical Ionization Mass Spectrometry*, 2nd ed.; CRC Press: Boca Raton, FL, USA, 1992.
39. K. Bieman; J. A. McCloskey, *J. Am. Chem. Soc.* **1962**, *84*, 3192–3193.

40. G. Junk; H. Svec, *J. Am. Chem. Soc.* **1962**, *85*, 839–845.
41. G. W. A. Milne; T. Axenrod; H. M. Fales, *J. Am. Chem. Soc.* **1970**, *92*, 5170–5175.
42. W. Lindinger; A. Hansel; A. Jordan, *Chem. Soc. Rev.* **1998**, *27*, 347–354.
43. C. Dehon; E. Gaüzère; J. Vaussier; M. Heninger; A. Tchapla; J. Bleton; H. Mestdagh, *Int. J. Mass Spectrom.* **2008**, *272*, 29–37.
44. D. Smith; P. Španěl, *Mass Spectrom. Rev.* **2004**, *24*, 661–700.
45. C. K. Meng; M. Mann; J. B. Fenn, *Phys. D* **1988**, *10*, 361–368.
46. V. G. Zaikin; J. M. Halket, *Eur. J. Mass Spectrom.* **2006**, *12*, 79–115.
47. E. C. Horning; M. G. Horning; D. I. Carroll; I. Dzidic; R. N. Stillwell, *Anal. Chem.* **1973**, *45*, 936–943.
48. K. A. Hanold; S. M. Fischer; P. H. Cormia; C. E. Miller; J. A. Synge, *Anal. Chem.* **2004**, *76*, 2842–2851.
49. S.-S. Cai; K. A. Hanald; J. A. Syage, *Anal. Chem.* **2007**, *79*, 2491–2498.
50. A. Bagag; A. Giuliani; O. Laprévote, *Int. J. Mass Spectrom.* **2007**, *264*, 1–9.
51. D. B. Robb; M. W. Blades, *Anal. Chim. Acta* **2008**, *627*, 34–49.
52. D. Debois; A. Giuliani; O. Laprévote, *J. Mass Spectrom.* **2006**, *41*, 1554–1560.
53. F. Hillenkamp, J. Peter-Katalinić, Eds., *MALDI MS: A Practical Guide to Instrumentation, Methods and Applications*; Wiley-VCH Verlag GmbH & Co. KGaA: Weinheim, Germany, 2007.
54. M. Karas; D. Bachmann; F. Hillenkamp, *Int. J. Mass Spectrom. Ion Processes* **1987**, *78*, 53–68.
55. M. Karas; D. Bachmann; U. Bahr; F. Hillenkamp, Matrix-Assisted UV Laser Desorption of Non-volatile Compounds. In *Advances in Mass Spectrometry*; J. F. J. Todd, Ed.; Wiley: Chichester, 1987; Vol. 10B, p 969.
56. M. Karas; U. Bahr; U. Giessmann, *Mass Spectrom. Rev.* **1991**, *10*, 335–357.
57. F. Hillenkamp; M. Karas; R. C. Beavis; B. T. Chait, *Anal. Chem.* **1991**, *63*, 1193A–2003A.
58. S. C. C. Wong; R. Hill; P. Blenkinsop; N. P. Lockyer; D. E. Weibel; J. C. Vickerman, *Appl. Surf. Sci.* **2003**, *203*, 219–222.
59. A. Brunelle; D. Touboul; O. Laprévote, *J. Mass Spectrom.* **2005**, *40*, 985–999.
60. R. M. A. Heeren; L. A. McDonnell; E. Amstalden; S. L. Luxembourg; A. F. M. Altelaar; S. R. Piersma, *Appl. Surf. Sci.* **2006**, *252*, 6827–6835.
61. R. G. Cooks; Z. Ouyang; Z. Takáts; J. M. Wiseman, *Science* **2006**, *311*, 1566–1570.
62. Z. Takáts; J. M. Wiseman; B. Gologan; R. G. Cooks, *Science* **2004**, *306*, 471–473.
63. R. B. Cody; J. A. Larameé; H. D. Durst, *Anal. Chem.* **2005**, *77*, 2297–2302.
64. I. Cotte-Rodriguez; C. C. Mulligan; R. G. Cooks, *Anal. Chem.* **2007**, *79*, 7069–7077.
65. S. A. McLuckey; J. M. Wells, *Chem. Rev.* **2001**, *101*, 571–606.
66. N. I. Tarantin, *Phys. Part. Nucl.* **1999**, *30*, 167–194.
67. H. Wollnik, *J. Mass Spectrom.* **1999**, *34*, 991–1006.
68. A. A. Makarov, *Anal. Chem.* **2000**, *72*, 1156–1162.
69. R. E. March; J. F. J. Todd, *Quadrupole Ion Trap Mass Spectrometry*, 2nd ed.; John Wiley and Sons: Hoboken, NJ, USA, 2005.
70. J. C. Schwartz; M. W. Senko; J. E. P. Syka, *J. Am. Soc. Mass Spectrom.* **2002**, *13*, 659–669.
71. J. W. Hagar, *Rapid Commun. Mass Spectrom.* **2002**, *16*, 512–526.
72. M. Hardman; A. A. Makarov, *Anal. Chem.* **2003**, *72*, 1156–1162.
73. Q. Hu; R. J. Noll; H. Li; A. Makarov; M. Hardman; R. G. Cooks, *J. Mass Spectrom.* **2005**, *40*, 430–443.
74. M. W. Senko; J. D. Canterbury; S. Guan; A. G. Marshall, *Rapid Commun. Mass Spectrom.* **1996**, *10*, 1839–1844.
75. H.-K. Lim; J. Chen; C. Sensenhauser; K. Cook; V. Subrahmanyam, *Rapid Commun. Mass Spectrom.* **2007**, *21*, 1821–1832.
76. J. V. Olsen; L. M. F. de Godoy; G. Li; B. Macek; P. Mortensen; R. Pesch; A. Makarov; O. Lange; S. Horning; M. Mann, *Mol. Cell. Proteomics* **2005**, *4*, 2010–2021.
77. J. V. Olsen; B. Macek; O. Lange; A. Makarov; S. Horning; M. Mann, *Nat. Methods* **2007**, *4*, 709–712.
78. M. Guilhaus; D. Selby; V. Mlynski, *Mass Spectrom. Rev.* **2000**, *19*, 65–107.
79. N. Mirsaleh-Kohan; W. D. Robertson; R. N. Compton, *Mass Spectrom. Rev.* **2008**, *27*, 237–285.
80. M. P. Barrow; W. I. Burkitt; P. J. Derrick, *Analyst* **2005**, *130*, 18–28.
81. K. Breuker; M. Jin; X. Han; H. Jiang; F. W. McLafferty, *J. Am. Soc. Mass Spectrom.* **2008**, *19*, 1045–1053.
82. R. Guevremont, *J. Chromatogr. A* **2004**, *1058*, 3–19.
83. B. M. Kolakowski; Z. Mester, *Analyst* **2007**, *132*, 842–864.
84. S. D. Pringle; K. Giles; J. L. Wildgoose; J. P. Williams; S. E. Slade; K. Thalassionos; R. H. Bateman; M. T. Bowers; J. H. Scrivens, *Int. J. Mass Spectrom.* **2007**, *261*, 1–12.
85. I. V. Chernushevich; A. V. Loboda; B. A. Thompson, *J. Mass Spectrom.* **2001**, *36*, 849–865.
86. G. L. Glish; D. J. Burinski, *J. Am. Soc. Mass Spectrom.* **2008**, *19*, 161–172.
87. J. W. Hagar, *Anal. Bioanal. Chem.* **2004**, *378*, 845–850.
88. R. J. Cotter; W. Griffith; C. Jelinek, *J. Chromatogr. B* **2007**, *855*, 2–13.
89. R. Mihalca; Y. E. M. van der Burgt; L. A. McDonnell; M. Duursma; I. Cerjak; A. J. R. Heck; R. M. A. Heeren, *Rapid Commun. Mass Spectrom.* **2006**, *20*, 1838–1844.
90. L. M. Mikesh; B. Ueberheide; A. Chi; J. J. Coon; J. E. P. Syka; J. Shabanowitz; D. F. Hunt, *Biochim. Biophys. Acta* **2006**, *1764*, 1811–1822.
91. H. Han; Y. Xia; M. Yang; S. A. McLuckey, *Anal. Chem.* **2008**, *80*, 3492–3497.
92. P. Roepstorff; J. Fohlman, *Biomed. Mass Spectrom.* **1984**, *11*, 601.
93. R. A. Zubarev; K. F. Haaselmann; B. Budnik; F. Kjeldsen; F. Jensen, *Eur. J. Mass Spectrom.* **2002**, *8*, 337–349.
94. R. A. Zubarev, *Mass Spectrom. Rev.* **2003**, *22*, 57–77.
95. F. Kjeldsen; K. F. Haselmann; B. A. Budnik; F. Jensen; R. A. Zubarev, *Chem. Phys. Lett.* **2002**, *356*, 201–206.
96. M. M. Savitski; F. Kjeldsen; M. L. Nielsen; R. A. Zubarev, *J. Am. Soc. Mass Spectrom.* **2007**, *18*, 113–120.
97. B. A. Budnik; K. F. Haselmann; R. A. Zubarev, *Chem. Phys. Lett.* **2001**, *342*, 299–302.
98. F. Kjeldsen; O. A. Silivra; I. A. Ivonin; K. F. Haselmann; M. Gorshkov; R. A. Zubarev, *Chem. Eur. J.* **2005**, *11*, 1803–1812.
99. A. Kalli; K. Håkansson, *Int. J. Mass Spectrom.* **2007**, *263*, 71–81.
100. J. J. Wolff; I. J. Amster; L. Chi; R. J. Linhardt, *J. Am. Soci. Mass Spectrom.* **2006**, *18*, 234–244.
101. J. J. Wolff; T. N. Laremore; A. M. Busch; R. J. Linhardt; I. J. Amster, *J. Am. Soci. Mass Spectrom.* **2008**, *19*, 790–798.

102. J. J. Wolff; L. Chi; R. J. Linhardt; I. J. Amster, *Anal. Chem.* **2007**, *79*, 2015–2022.
103. M. Kaczorowska; H. J. Cooper, *J. Am. Soc. Mass Spectrom.* **2008**, *19*, 1312–1319.
104. J. Yang; J. Mo; J. T. Adamson; K. Håkansson, *Anal. Chem.* **2005**, *77*, 1876–1882.
105. J. Yang; K. Håkansson, *J. Am. Soc. Mass Spectrom.* **2006**, *17*, 1369–1375.
106. J. Mo; K. Håkansson, *Anal. Bioanal. Chem.* **2006**, *386*, 675–681.
107. J. E. P. Syka; J. J. Coon; M. J. Schroeder; J. Shabanowitz; D. F. Hunt, *Proc. Natl. Acad. Sci. U.S.A.* **2004**, *101*, 9528–9533.
108. A. Chi; D. L. Bai; Y. L. Geer; J. Shabanowitz; D. F. Hunt, *Int. J. Mass Spectrom.* **2007**, *259*, 197–203.
109. R. Hartmer; D. A. Kaplan; C. R. Gebhardt; T. Ledertheil; A. Brekenfeld, *Int. J. Mass Spectrom.* **2008**, *276*, 82–90.
110. D. L. Swaney; G. C. McAlister; M. Wirtala; J. C. Schwartz; J. E. P. Syka; J. J. Coon, *Anal. Chem.* **2007**, *79*, 477–485.
111. R. A. Zubarev; A. R. Zubarev; M. M. Savitski, *J. Am. Soc. Mass Spectrom.* **2008**, *19*, 753–761.
112. M. M. Savitski; M. L. Nielsen; R. A. Zubarev, *Anal. Chem.* **2007**, *79*, 2296–2302.
113. A. Scherl; S. A. Shaffer; G. K. Taylor; P. Hernandez; R. D. Appel; P.-A. Binz; D. R. Goodlett, *J. Am. Soc. Mass Spectrom.* **2008**, *19*, 891–901.
114. M. Mann; N. L. Kelleher, *Proc. Natl. Acad. Sci. U.S.A.* **2008**, *105*, 18132–18138.
115. H. Molina; R. Matthiesen; K. Kandasamy; A. Pandey, *Anal. Chem.* **2008**, *80*, 4825–4835.
116. F. Kjeldsen; O. B. Horning; S. S. Jensen; A. M. B. Giessing; O. N. Jensen, *J. Am. Chem. Soc.* **2008**, *19*, 1156–1162.
117. C. K. Barlow; R. A. O'Hair, *J. Mass Spectrom.* **2008**, *43*, 1301–1319.
118. J. M. Halket; V. G. Zaikin, *Eur. J. Mass Spectrom.* **2006**, *12*, 1–13.
119. V. G. Zaikin; J. M. Halket, *Eur. J. Mass Spectrom.* **2005**, *11*, 611–636.
120. C. Hopley; T. Bristow; A. Lubben; A. Simpson; E. Bull; K. Klagkou; J. Herniman; J. Langley, *Rapid Commun. Mass Spectrom.* **2008**, *22*, 1779–1786.
121. C. Eckers; J. J. Monaghan; J.-C. Wolff, *Eur. J. Mass Spectrom.* **2005**, *11*, 73–82.
122. K. E. Arthur; J.-C. Wolff; D. J. Carrier, *Rapid Commun. Mass Spectrom.* **2004**, *18*, 678–684.
123. Z. Tozuka; H. Kaneko; T. Shiraga; Y. Mitani; M. Beppu; S. Terashita; A. Kawamura; A. Kagayama, *J. Mass Spectrom.* **2003**, *38*, 793–808.
124. J.-C. Wolff; L. A. Thompson; C. Eckers, *Rapid Commun. Mass Spectrom.* **2003**, *17*, 215–221.
125. F.-F. Hsu; J. Turk, *J. Am. Soc. Mass Spectrom.* **2005**, *68*, 1510–1522.
126. F.-F. Hsu; J. Turk, *J. Am. Soc. Mass Spectrom.* **2007**, *18*, 2065–2073.
127. J. Heberle; G. Simchen, *Silylating Agents*, 2nd ed.; Fluka Chemie AG: Buchs, Switzerland, 1995.
128. O. Fiehn, *Phytochemistry* **2003**, *62*, 875–886.
129. H. Van den Dool; P. D. Kratz, *Chromatogr.* **1963**, *11*, 41 463–471.
130. J. H. Beynon, *Nature* **1954**, *174*, 735–737.
131. A. W. T. Bristow, *Mass Spectrom. Rev.* **2005**, *25*, 99–111.
132. M. L. Gross, *J. Am. Soc. Mass Spectrom.* **1994**, *5*, 57.
133. R. J. DeLaeter; J. K. Böhlke; P. De Brièvre; H. Hidaka; H. S. Peiser; K. J. R. Rosman; P. D. P. Taylor, *Pure Appl. Chem.* **2003**, *75*, 683–800.
134. O. A. Mamer; A. Lesimple, *J. Am. Soc. Mass Spectrom.* **2004**, *15*, 626.
135. I. Ferrer; E. M. Thurman, *Rapid Commun. Mass Spectrom.* **2007**, *21*, 2538–2539.
136. J. F. Pickup; K. McPherson, *Anal. Chem.* **1976**, *48*, 1885–1890.
137. C. S. Hsu, *Anal. Chem.* **1984**, *56*, 1356–1361.
138. V. Pellegrin, *J. Chem. Educ.* **1983**, *60*, 626–632.
139. T. Kind; O. Fiehn, *BMC Bioinf.* **2006**, *7*, 234–243.
140. C. Dass, *Fundamentals of Contemporary Mass Spectrometry*; John Wiley and Sons: Hoboken, NJ, USA, 2007.
141. M. N. Eberlin, *J. Mass Spectrom.* **2006**, *41*, 141–156.
142. R. K. Boyd; J. D. Henion; M. Alexander; W. L. Budde; J. D. Gilbert; S. M. Musser; C. Palmer; E. K. Zurek, *J. Am. Soc. Mass Spectrom.* **1996**, *7*, 211–218.
143. R. K. Boyd; C. Basic; R. A. Bethem, *Trace Quantitative Analysis by Mass Spectrometry*; John Wiley and Sons: Chichester, UK, 2008.
144. FDA Guidance for Industry 118, Mass spectrometry for confirmation of the identity of animal drug residues, US Department of Health and Human Services, Food and Drug Administration, May 2003. http://www.fda.gov/ (accessed April 2009).
145. European Union COMMISSION DECISION 2002/657/EC of 12 August 2002, *Official J. Eur. Union* **2002**, *L 221*, 8–36.
146. M. W. F. Nielen; M. C. van Engelen; R. Zuiderent; R. Ramaker, *Anal. Chim. Acta* **2007**, *586*, 122–129.
147. W. Weckwerth; K. Wenzel; O. Fiehn, *Proteomics* **2004**, *4*, 78–83.
148. S. A. Trauger; E. Kalisak; J. Kalisiak; H. Morita; M. V. Weinberg; A. L. Menon; F. L. Poole, II; M. W. W. Adams; G. Siuzdak, *J. Proteome Res.* **2008**, *7*, 1027–1035.
149. G. G. Harrigan, R. Goodacre, Eds., *Metabolic Profiling: Its Role in Biomarker Discovery and Gene Function Analysis*; Kluwer Academic Publishers: Dordrecht, The Netherlands, 2003.
150. FDA Guidance for Industry, Bioanalytical Method Validation, US Department of Health and Human Services, Food and Drug Administration, May 2001. http://www.fda.gov/ (accessed April 2009).
151. E. Pritchard; V. Barwick, *Quality Assurance in Analytical Chemistry*; John Wiley and Sons: Chichester, UK, 2007.
152. S. G. Villas-Bôas; S. Mas; M. Åkesson; J. Smedsgaard; J. Nielsen, *Mass Spectrom. Rev.* **2005**, *24*, 613–646.
153. A. Nordström; E. Want; T. Northen; J. Lehtiö; G. Siuzdak, *Anal. Chem.* **2008**, *80*, 421–429.
154. L. Cuadros-Rodríguez; M. G. Bagur-González; M. Sánchez-Viñas; A. González-Casado; A. M. Gómez-Sáez, *J. Chromatogr. A* **2007**, *1158*, 33–46.
155. W. Schwab, *Phytochemistry* **2003**, *62*, 837–849.
156. D. E. Raynie, *Anal. Chem.* **2004**, *76*, 4659–4664.
157. S. G. Villas-Bôas, Sampling and Sample Preparation. In *Metabolome Analysis: An Introduction*; S. G. Villas-Bôas, U. Roessner, M. A. E. Hansen, J. Smedsgaard, J. Nielsen, Eds.; John Wiley and Sons: Hoboken, NJ, USA, 2007.
158. A. Jiye; J. Trygg; J. Gullberg; A. I. Johansson; P. Jonsson; H. Antti; S. L. Marklund; T. Moritz, *Anal. Chem.* **2005**, *77*, 8086–8094.

159. J. Gullberg; P. Jonsson; A. Nordström; M. Sjöström; T. Moritz, *Anal. Biochem.* **2004**, *331*, 283–295.
160. R. King; R. Bonfiglio; C. Fernandez-Metzler; C. Miller-Stein; T. Olah, *J. Am. Chem. Soc.* **2000**, *11*, 942–950.
161. J. Schuhmacher; D. Zimmer; F. Tesche; V. Pickard, *Rapid Commun. Mass Spectrom.* **2003**, *17*, 1950–1957.
162. W. Weckwerth, Ed., *Metabolomics: Methods and Protocols*; Humana Press: Totowa, NJ, USA, 2007.
163. B. J. Millard, *Quantitative Mass Spectrometry*; Heydon and Sons Ltd.: London, UK, 1978.
164. P. C. Meier; R. E. Zünd, *Statistical Methods in Analytical Chemistry*; John Wiley and Sons: New York, NY, USA, 1993.
165. M. P. Hermo; D. Barrón; J. Barbosa, *J. Chromatogr. A* **2008**, *1201*, 1–14.
166. M. Ende; G. Spiteller, *Mass Spectrom. Rev.* **1982**, *1*, 29–62.
167. B. O. Keller; J. Sui; A. B. Young; R. M. Whittal, *Anal. Chim. Acta* **2008**, *627*, 71–81.
168. Q&A News Article, *Nature* **2008**, *453*, 964.
169. G. R. McDonald; A. L. Hudson; S. M. J. Dunn; H. You; G. B. Baker; R. M. Whittal; J. W. Martin; A. Jha; D. E. Edmondson; A. Holt, *Science* **2008**, *322*, 917.
170. X. Guo; A. P. Bruins; T. R. Covey, *Rapid Commun. Mass Spectrom.* **2006**, *20*, 3145–3150.
171. M. Najam-ul-Haq; M. Rainer; C. W. Huck; P. Hausberger; H. Kraushaar; G. K. Bonn, *Anal. Chem.* **2008**, *80*, 7467–7472.
172. N. C. Hughes; E. Y. K. Wong; J. Fan; N. Bajaj, *AAPS J.* **2007**, *9*, E353–E360.
173. J. W. Dolan, *LCGC North Am.* **2006**, *24*, 754–760.
174. M. Stoeckli; P. Chaurand; D. E. Hallahan; R. M. Caprioli, *Nat. Med.* **2001**, *7*, 493–496.
175. R. M. Caprioli; T. B. Farmer; J. Gile, *Anal. Chem.* **1997**, *69*, 4751–4760.
176. B. Spengler, Microprobing and Imaging MALDI for Biomarker Detection. In *MALDI MS: A Practical Guide to Instrumentation, Methods and Applications*; F. Hillenkamp, J. Peter-Katalinic, Eds.; Wiley-VCH Verlag GmbH and Co.KGaA: Weinheim, Germany, 2007.
177. W. M. Hardesty; R. M. Caprioli, *Anal. Bioanal. Chem.* **2008**, *391*, 899–903.
178. J. S. Fletcher; N. P. Lockyer; S. Vaidyanathan; J. C. Vickerman, *Anal. Chem.* **2007**, *79*, 2199–2206.
179. D. R. Ifa; J. M. Wiseman; Q. Song; R. G. Cooks, *Int. J. Mass Spectrom.* **2007**, *259*, 8–15.
180. R. L. Caldwell; R. M. Caprioli, *Mol. Cell. Proteomics* **2005**, *4*, 394–401.
181. D. S. Cornett; J. A. Mobley; E. C. Dias; M. Anderson; C. L. Arteaga; M. E. Sanders; R. M. Caprioli, *Mol. Cell. Proteomics* **2006**, *5*, 1975–1983.
182. P. Chaurand; S. A. Schwartz; D. Billheimer; B. J. Xu; A. Crecelius; R. M. Caprioli, *Anal. Chem.* **2004**, *76*, 1145–1155.
183. S. M. Puolitaival; K. E. Burnum; D. S. Cornett; R. M. Caprioli, *J. Am. Soc. Mass Spectrom.* **2008**, *19*, 882–886.
184. P. Chaurand; J. C. Latham; K. B. Lane; J. A. Mobley; V. V. Polosukhin; P. S. Wirth; L. B. Nanney; R. M. Caprioli, *J. Proteome Res.* **2008**, *7*, 3543–3555.
185. V. Kertesz; G. J. Van Berkel, *Rapid Communi. Mass Spectrom.* **2008**, *22*, 2639–2644.
186. G. Maddalo; F. Petrucci; M. Iezzi; T. Pannellini; P. Del Boccio; D. Ciavardelli; A. Biroccio; F. Forli; C. Di Ilio; E. Ballone; A. Urbani; G. Federici, *Clin. Chim. Acta* **2005**, *357*, 210–218.
187. Z. Ouyang; L. Gao; M. Fico; W. J. Chappell; R. J. Noll; R. G. Cooks, *Eur. J. Mass Spectrom.* **2007**, *13*, 13–18.

## Biographical Sketch

Charles H. Hocart, descendent of Guernsey and Yorkshire stock, completed a B.Sc. (Hon) degree (Chemistry, 1977) and an M.Sc. (Clinical Biochemistry, 1979) at the University of Western Australia, where his long-term interest in the use of mass spectrometry to solve biological problems was aroused. His Ph.D. studies with Professor Berthold Halpern (Wollongong) using GC/MS to look for markers of metabolic diseases were unfortunately curtailed by Halpern's premature death. He then moved to Canberra to study the cytokinin family of plant hormones under the supervision of Professor Stuart Letham (Australian National University, 1981–85). Two postdoctoral fellowships then followed with Professor Jim McCloskey (Utah, 1986–87) and Professor Urs Schlunegger (Bern, 1988–99) for identifying modified nucleotides from Archaebacteria, and for studying the negative ion mass

spectrometry of cytokinins, respectively, before he again started to work with Letham, courtesy of a National Research Fellowship (ANU, 1989–93). A 3-year period as an analyst and evaluator at the Therapeutic Drug Administration then led to his current appointment managing the RSBS Mass Spectrometry Facility (ANU, 1996–present). Research collaborations have included the archaeology of betel nut and kava in the Pacific islands (Dr. Barry Fankhauser); the identification and quantification of cell wall polysaccharides in cellulose-deficient *Arabidopsis thaliana* mutants (Professor Richard Williamson); the chemical signals regulating the interaction of rice with *Rhizobium* isolates from the Nile Delta (Professor Barry Rolfe); and most recently, the generation of biodiesel from the native leguminous tree, *Pongamia pinnata*, and from microalgae (Professor Peter Gresshoff and Dr. Michael Djordjevic).